let. - vol. 48 (2002) št. - no. 9

STROJNIŠKI VESTNIK 9

JOURNAL OF MECHANICAL ENGINEERING

strani - pages 471 - 518

ISSN 0039-2480 . Stroj V . STJVAX

cena 800 SIT

9 770039 248001

© Strojniški vestnik 48(2002)9,471
Mesečnik
ISSN 0039-2480

© Journal of Mechanical Engineering 48(2002)9,471
Published monthly
ISSN 0039-2480

Vsebina
Contents

Strojniški vestnik - Journal of Mechanical Engineering
letnik - volume 48, (2002), številka - number 9

© Strojniški vestnik 48(2002)9,472-481
ISSN 0039-2480
UDK 004.94:536.2:621.762.5
Izvirni znanstveni članek (1.01)

© Journal of Mechanical Engineering 48(2002)9,472-481
ISSN 0039-2480
UDC 004.94:536.2:621.762.5
Original scientific paper (1.01)

Analiza prenosa toplote v postopku sintranja feritov

A Heat-Transfer Analysis of the Ferrite Sintering Process

Zlatko Rek - Matjaž Perpar - Iztok Žun

Obravnavana je analiza prenosa toplote v postopku sintranja feritov v komorni peči. Izvedeni sta bili meritev in numerično simuliranje časovnega razvoja temperaturnega polja. Zaradi zahtevnosti problema je simuliranje potekalo v dveh delih. V prvem delu je obravnavana celotna peč, v drugem delu pa je analiziran samo pladenj s feriti. V prispevku je opisan postopek meritve temperature, numerični model (enačbe prenosa toplote) in generacija mrežastega modela peči za izbrano računsko območje, t.j. notranjost peči z grelniki, pladnji, feriti, nosilci in podstavki. Narejena je analiza rezultatov numerične simulacije in njihova primerjava z izmerjenimi vrednostmi. Ujemanje numerične rešitve in izmerjenih vrednosti je dobro.

(Ključne besede: sintranje feritov, prenos toplote, simuliranje numerično, modeli sevanja)

The paper deals with a heat-transfer analysis of the process of sintering ferrites in a furnace. Experimental measurements and a numerical simulation of the time development of the temperature field were performed. Due to the complexity of the problem the simulation had to be performed in two steps. The first step takes into consideration the whole furnace, while in the second step only a single ferrite plate is analyzed. The experiment, the numerical model (the heat-transfer equations) and the generation of the discretized model of the furnace for the chosen computational domain, e.g. furnaces with heaters, plates, ferrites, bearers and supports, are described. The results of the numerical simulation are analyzed and compared with experimental data. The agreement between the numerical results and the experimental data was good.

(Keywords: ferrite sintering, heat transfer, numerical simulations, radiation models)

0 UVOD

Prispevek predstavlja opravljeno delo v okviru raziskovalnega projekta L2-0784: Izboljšave postopkov pri sintranju feritov v peči, pri katerem sta sodelovala Fakulteta za strojnišvo - Laboratorij za dinamiko fluidov in termodinamiko, Ljubljana in Iskra Feriti, Podjetje za proizvodnjo feritov in navitih komponent, d.o.o., Ljubljana.

V postopku sintranja feritov je natančen časovni potek temperature, poleg drugih parametrov, ključnega pomena za kakovost izdelka, to je njegove elektromagnetne in reološke lastnosti. Da bi bolje razumeli dogajanje pri prenosu toplote v postopku sintranja, skušamo narediti numerični model peči ([1] in [2]). Tako lahko proučujemo vpliv posameznih parametrov na kakovost izdelka.

Ker je treba numerični model preveriti, smo v prvi fazi izvedli meritve temperatur [3]. Namen je bil dvojen:

0 INTRODUCTION

This paper presents work done in the framework of research project L2-0784 – Improvement of ferrite sintering in furnaces – in collaboration of the Faculty of Mechanical Engineering, Laboratory for Fluid Dynamics and Thermodynamics, Ljubljana with Iskra Feriti, Company of ferrite materials and wound components production Ltd., Ljubljana.

In the process of ferrite sintering, an accurate time-dependent temperature distribution (among other parameters) is of key importance for achieving a high-quality product, i.e. a material with good electromagnetic and rheological properties. To understand better the heat transfer during the sintering process a numerical model of the furnace has to be made ([1] and [2]). In this way the influence of the process parameters on the quality of the product can be studied.

Because the numerical model has to be verified, in the first step the temperature measurements [3] are performed. The purpose is twofold:

1. Izmeriti časovni potek temperatur na notranji steni peči in na grelnikih, ki jih potrebujemo za robne pogoje pri numeričnem simuliranju.
2. Izmeriti časovni potek temperatur ob feritih, v feritih na robu pladnja in v feritih na sredini pladnja. Te izmerjene vrednosti so namenjene za primerjavo oz. overitev numeričnega modela.

1 MERITEV TEMPERATUR

V komornih pečeh je sintranje pod nadzorom računalnika, ki vodi postopek glede na vstavljen program obratovalnih parametrov. Za (iz)gradnjo ter testiranje modela prenosa toplote je poleg vstopnih parametrov potrebno poznavanje temperatur znotraj peči, še posebej ob samem sintrancu. Izmerjen je bil časovni potek temperatur na različnih mestih v peči, na zunanji steni peči in v okolici. Temperature v snovi so bile izmerjene s termopari tipa S in K, na zunanji steni peči pa z merilnikom temperature na infrardeče zaznavalo.

1.1 Izvedba meritev

Za merjenje temperatur v peči so bili uporabljeni termopari tipa S (Pt-10%Rh/Pt) in K (Ni-Cr/Ni-Al). Tip S so bili iz neoplaščenih žic debeline 0,5 mm, vodenih skozi keramične cevi, tip K pa so bili iz žic debeline 0,8 mm, oplaščenih s temperaturno odporno tkanino. Termopar S je omogočal meritve temperatur do 1700 °C, termopar K pa meritve do 1200 °C stalno ter do 1400 °C kratkotrajno. Pripravljena je bila merska veriga termopar - podaljševalni vod - referenčna točka hladnega spoja (0 °C) - priključni kabel - preklopno stikalo - digitalni voltmeter. Temperatura zunanje stene peči je bila izmerjena z infrardečim digitalnim merilnikom.

Temperatura ob zunanji steni (25 mm od stene) in temperatura okolice sta bili izmerjeni z digitalnima termometroma z zaznavali tipa K. Izmerjene vrednosti so bile zapisane v računalnik. Merska veriga je bila umerjena za vsak tip termoparov. Termopar tipa S je bil umerjen v območju 170,0 °C do 1123,2 °C, največja vrednost poprave je bila -2,6 °C. Termopar tipa K je bil umerjen v območju 170,0 °C do 1086,0 °C, največja vrednost poprave je bila -2,4 °C. Relativna napaka kazanja merila (razmerje med vsoto absolutnih vrednosti poprave in merilne negotovosti ter dogovorno pravo vrednostjo temperature) za temperature, večje od 170 °C ni presegla 0,5%. Ocenjeno je bilo, da je bila točnost merske verige zadostna, torej poprava izmerjenih temperatur ni bila potrebna. Vrednosti temperatur, ki so bile izmerjene z digitalnim voltmetrom, so bile izračunane z znižanima polinomoma po ameriškem standardu NBS (9. stopnje za tip S in 8. stopnje za tip K). Za testiranje izračuna so bili uporabljeni rezultati kalibracijske meritve. Razlike med

1. To determine the time-dependent temperature of the furnace's internal wall, which is used as a boundary condition for the numerical simulation.
2. To measure the time-dependent temperature profile near the ferrites, in the ferrites at the edge, and in the plate centre.

1 TEMPERATURE MEASUREMENTS

The process of sintering in the furnace is controlled by computer with an operation schedule. Besides input parameters, the development and testing of the heat-transfer model requires temperatures inside the furnace, especially near the ferrite. A time history of the temperatures at different locations in the furnace, on the outer wall, and in the surroundings was measured. Thermocouples (types S and K) and an infrared (IR) thermometer were used for the medium and outer-wall temperatures, respectively.

1.1 Obtaining the measurements

The temperatures in the furnace were measured by types S (Pt-10%Rh/Pt) and K (Ni-Cr/Ni-Al) thermocouples. The S type thermocouple was made of uncoated 0.5-mm-thick wire led through a ceramic tube. The type K wire was 0.8-mm thick and shielded with a high-temperature-resistant textile. Thermocouple S was suitable for measurements up to 1700 °C, while thermocouple K was suitable for permanent measurements up to 1200 °C, and for a short duration up to 1400 °C. The composition of the measuring chain was: thermocouple – extension wire – cold reference point (0 °C) – connecting cable – switch contact – digital voltmeter. The temperature of the outer furnace wall was measured with a IR digital thermometer.

The temperature near the outer wall (25 mm from the wall) and the temperature of the surroundings were measured by digital thermometers with type K sensors. The measured values were recorded with a computer. The measuring range was calibrated for each thermocouple. The type S thermocouple was calibrated in the range 170.0 °C to 1123.2 °C, the highest correction was -2.6 °C. The type K thermocouple was calibrated in the range 170.0 °C to 1086.0 °C, the highest correction was -2.4 °C. The relative error of the instrument readouts (the proportion between the sum of the absolute correction values and of the measurement uncertainty and the conventional true value of the temperature) for temperatures higher than 170 °C did not exceed 0.5%. The accuracy of the measuring chain was estimated to be sufficient, therefore, a correction of the measured temperatures was not necessary. Temperature values measured with a digital voltmeter were calculated using polynomial regression following the NBS standard (9th order for type S and 8th order for type K). The results of the calibration measurement

dogovornimi pravimi in izračunanimi vrednostmi so bile istega reda velikosti kot vrednosti poprav pri kalibraciji, zato smo menili, da so bile temperature ustrezno izračunane.

1.2 Potek meritev

Termopari so bili v peč vstavljeni skozi obstoječe odprtine. Za postavitev zaznaval pri sintrancih je bil uporabljen endoskop, ker se zapiranje peči izvaja z dvigom pladnjev v komoro. Na sliki 1 je shematsko prikazana namestitev zaznaval v peči. Temperaturni zaznavali na steni (st1 in st3) sta bili nameščeni na izolacijo. Feriti so bili razvrščeni na treh pladnjih.V vsaki plasti je bilo nameščeno po eno zaznavalo 10 mm od sintranca (fsp, fsr, fzg). Eno zaznavalo je bilo položeno na grelnik (gre), eno pa je bilo nameščeno pod grelnikom (amb). Termopar "st3" je bil tip K, vsi drugi pa tip S.

were used to test the calculation. The differences between the conventional true and the calculated values were within the range of correction, therefore, we considered the calculated values suitable.

1.2 Measuring procedure

The thermocouples were inserted into the furnace through existing holes. An endoscope was used to position the sensors near the ferrites because the furnace is closed by lifting the ferrite trays into the chamber. The locations of the sensors in the furnace are shown schematically in Fig.1. The thermocouples on the wall (st1 and st3) were placed onto the insulation. The ferrites were arranged on three trays. In each level the sensor was placed 10 mm from the ferrite (fsp, fsr, fzg). One sensor was put on the heater (gre) and one was placed in the area under the heater (amb). The thermocouple "st3" was type K, the others were type S.

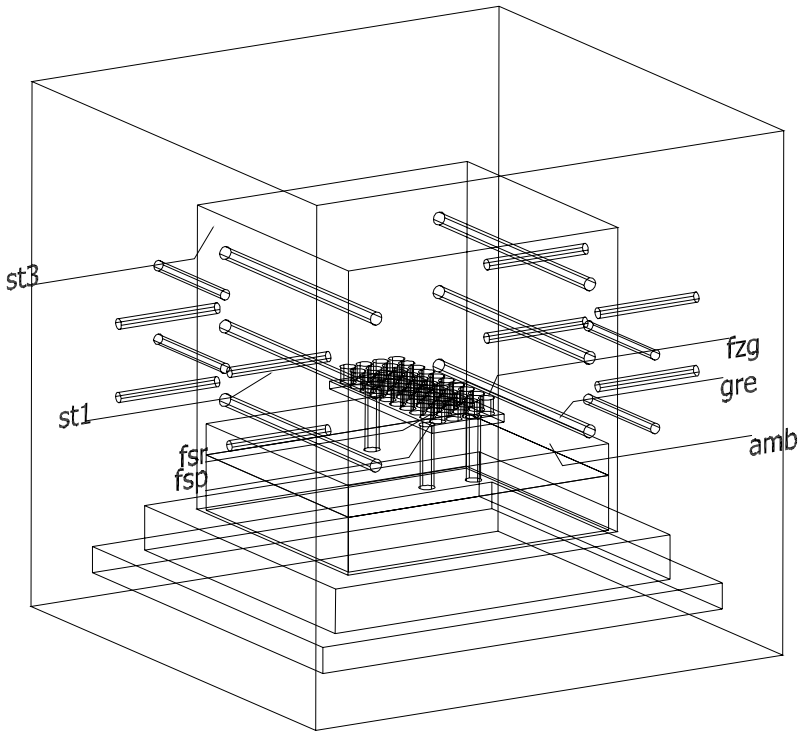

Sl. 1. *Shema eksperimentalne komorne peči za sintranje feritov in merilna mesta v komorni peči*
Fig. 1. *Schematic of the experimental furnace for sintering of ferrites and measuring locations in the furnace*

2 NUMERIČNO SIMULIRANJE

2.1 Prenosna enačba energije

Temperaturno polje v komorni peči za sintranje feritov je opisano z enačbo ohranitve energije [4]:

2 NUMERICAL SIMULATION

2.1 Energy transport equation

Temperature field in the furnace for ferrites sintering is governed by the equation for energy conservation [4]:

$$\rho c_p \frac{\partial T}{\partial t} = \nabla \cdot (\lambda \nabla T) + S \qquad (1),$$

pri čemer so: c_p specifična toplota pri nespremenljivem tlaku, ρ gostota, λ toplotna prevodnost in S viri toplote. Za temperaturno odvisnost toplotne

where c_p denotes the specific heat at constant pressure, ρ is the density, λ is the heat conductivity and S are the heat sources. The dependence of the temperature on

prevodnosti je uporabljen Sutherlandov zakon [5]:

$$\lambda = \frac{2.502 \cdot 10^{-3} T^{1.5}}{T + 194.4} \quad (2).$$

Natančnost približka je 2% na temperaturnem območju med 160 K in 1000 K.

Ker imamo v našem primeru več različnih materialov (zrak, feriti, keramika), morajo na stiku veljati združljivostni pogoji:

$$T^1 = T^2 \quad (3),$$

$$\lambda_1 \frac{\partial T^1}{\partial n} = -\lambda_2 \frac{\partial T^2}{\partial n} \quad (4),$$

torej enakost temperatur in nasprotna enakost gostote toplotnih tokov.

heat conduction is described by Sutherland's law [5]:

The accuracy of the approximation is 2%, in the range between 160 K in 1000 K.

Because there are different materials air, ferrites, ceramics – the compatibility conditions have to be satisfied:

i.e. equality of the temperatures and the heat fluxes.

2.2 Difuzijski model sevanja

Sevalna temperatura T_r je določena z integralom intenzivnosti sevanja i po prostorskem kotu ([6] do [8]):

$$\frac{1}{4\pi} \int_{4\pi} i \, d\Omega = \frac{\sigma T_r^4}{\pi} \quad (5).$$

Po analogiji za gostoto sevalnega toplotnega toka pri difuzijski meji je gostota sevalnega energijskega toka definirana kot:

$$\vec{q}_r = -\frac{4\sigma}{3K_e} \nabla T_r^4 \quad (6).$$

Difuzijska meja obstaja, če je dejanska absorpcija K_{ζ} velika, in je po Gibbu definirana kot:

$$K_e = K_a + K_p'(\bar{e}_p + \bar{p}_p(1 - f)) \quad (7).$$

V našem primeru je $K'_p=0$, ker v zraku ni trdnih delcev. Ko enačbo (6) vstavimo v prenosno enačbo sevanja in integriramo po vsem območju valovnih dolžin, dobimo:

$$-\nabla \cdot \left(\frac{1}{3K_e} \nabla T_r^4 \right) = K_a (T_f^4 - T_r^4) \quad (8),$$

kjer je T_f temperatura zraka. Celoten energijski tok iz zraka na sevalno fazo je:

$$\dot{Q}_f = 4\sigma K_a (T_f^4 - T_r^4) \quad (9).$$

Ta člen je treba v prenosni enačbi toplotne energije (1) odšteti.

2.2 Diffusion model for radiation

The radiation temperature T_r is defined with the integral of the radiant intensity i over all directions ([6] to [8]):

By analogy with the radiant heat flux in the diffusion limit, the radiant energy flux is defined as:

A diffusion limit exists if the effective absorption K_{ζ} is large, and was defined by Gibb to be:

In our case $K'_p=0$, because there are no particles in the air. When equation (6) is substituted into the radiation transport equation and integrated over all wavelengths we obtain:

where T_f is the air temperature. The net energy transfer from the air to the radiant phase is:

This term is subtracted from the thermal energy equation (1).

Robni pogoj

Ob predpostavki, da na steni sevanje prihaja in jo zapušča neodvisno od smeri, za robni pogoj na steni velja:

$$\vec{n} \cdot \vec{q}_r = -\frac{4\sigma}{3K_e} \frac{\partial T_r^4}{\partial n} = \frac{2\sigma\epsilon_w}{2 - \epsilon_w} \left(T_w^4 - T_r^4 \right) \quad (10),$$

Boundary conditions

From the assumption that the radiant intensity arriving at and leaving from the wall are directionally independent, the boundary conditions at the walls are:

kjer je ***n*** enotska normala, T_w je temperatura stene in $\sum_w$ sevalnost stene.

Začetni pogoj

Po naravi je porazdelitev T_r po območju veliko bolj enakomerna kakor T_f, zato lahko izberemo nespremenljivo začetno vrednost. Določimo jo z integracijo enačbe (9) po vsem območju Ω:

$$4\sigma \int_{\Omega} K_a (T_f^4 - T_r^4)\, dV = \int_{\partial\Omega} \frac{2\sigma\epsilon_w}{2-\epsilon_w} \left(T_w^4 - T_r^4\right) dA \qquad (11).$$

Če zanemarimo prispevek robnega integrala, je začetna vrednost:

$$\overline{T}_r^4 = \frac{1}{V} \int_{\Omega} T_f^4\, dV \qquad (12).$$

2.3 Robni pogoji

Če želimo rešiti sitem ločenih enačb, moramo predpisati smiselne robne pogoje. V našem primeru predpišemo temperaturo na notranji steni peči in na grelnikih. Vrednosti so dobljene z meritvami.

2.4 Mrežasti model

2.4.1 Komorna peč

Ker je geometrijska oblika peči zelo zapletena, saj so v notranjosti grelniki, kjer predpišemo robni pogoj, moramo računsko območje razdeliti na tri dele. Za vsak del posebej naredimo mrežo, ki jih na koncu združimo v eno celotno - strukturirano mrežo, ki ima 32422 vozlišč.

Določitev mreže pri delu 2 je zelo zahtevna, ker so v računskem območju telesa, ki prevajajo toploto: nosilci, podstavki, pladnji in feriti. Vsa ta notranja telesa je treba upoštevati in tudi ločiti, pri tem pa paziti, da mreža ni preveč spačena, saj se lahko pri reševanju enačb pojavijo problemi s konvergenco.

2.4.2 Pladenj s feriti

Mrežasti model pladnja s feriti je sestavljen iz treh delov: pladenj, feritna podlaga in feriti. Za vsak del posebej naredimo mrežo, ki poteka v naslednjih fazah:

1. geometrijski opis problema (koordinate točk, krivulje),
2. določitev vozlišč na robovih računskega območja,
3. določitev vozlišč v notranjosti računskega območja,
4. sprememba 2D mreže v 3D mrežo.

Ko imamo za vsak del narejeno strukturirano računsko mrežo, jih združimo v eno celotno - strukturirano mrežo, ki ima 101077 vozlišč.

Čeprav je geometrijska oblika peči simetrična, tega pri izračunu ne moremo uporabiti ker je: 1. mrežasti model zasnovan tako, da lahko z najmanjšimi spremembami obravnavamo različne oblike feritov in različne nalagalne sheme; 2. robni

where ***n*** is the unit vector outward normal to the wall, T_w is the wall temperature and $\sum_w$ is the wall emissivity.

Initial condition

By its nature, T_r is more uniform throughout the domain than T_f, therefore a constant value can be set for the initial value. It is determined by integrating equation (9) over the entire domain Ω:

Without taking into account the contribution from the boundary integral, the initial value is

2.3 Boundary conditions

To solve the system of discrete equations, consistent boundary conditions have to be prescribed. In our case the temperature at the inside wall of the furnace is known. Values are obtained by measurements.

2.4 Discrete model

2.4.1 Furnace

Because the geometry of the furnace is very complex, i.e. there are heaters where the boundary conditions are set, we have to split our domain into three segments. A mesh is generated for each segment. At the end all meshes are joined into one block-structured mesh which has 32422 nodes.

Mesh generation for segment 2 is very difficult due to the conjugate heat transfer (CHT) objects in the domain: bearers, supports, plates and ferrites. All these CHT objects have to be discretized as well. The mesh must not be too deformed because convergence problems could appear.

2.4.2 Ferrite plate

The discrete model of the ferrite plate is composed of three segments: plate, ceramic ferrite base and ferrites. A mesh is generated for each segment according to the following steps:

1. Geometric description (point coordinates, curves)
2. Generation of nodes at the edges of the domain boundary
3. Generation of nodes on the inside of the domain
4. Transformation of 2D mesh into 3D mesh

The meshes of all three segments are joined into one block-structured mesh with 101077 nodes.

Although the geometry of the furnace is symmetrical, this cannot be taken into account in the simulation because: 1. the discrete model is designed in such way that various types of ferrites and different load schemes can be studied with minimal changes; 2.) the

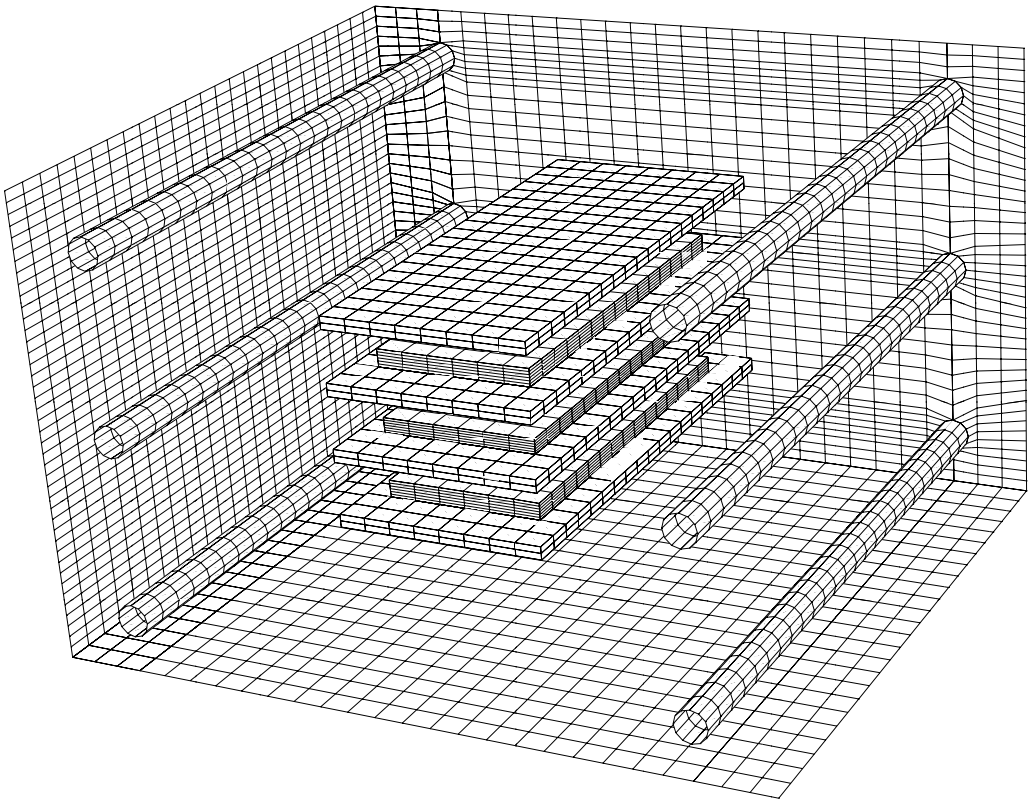

Sl. 2. *Računska mreža komorne peči*
Fig. 2. *Computational mesh for furnace.*

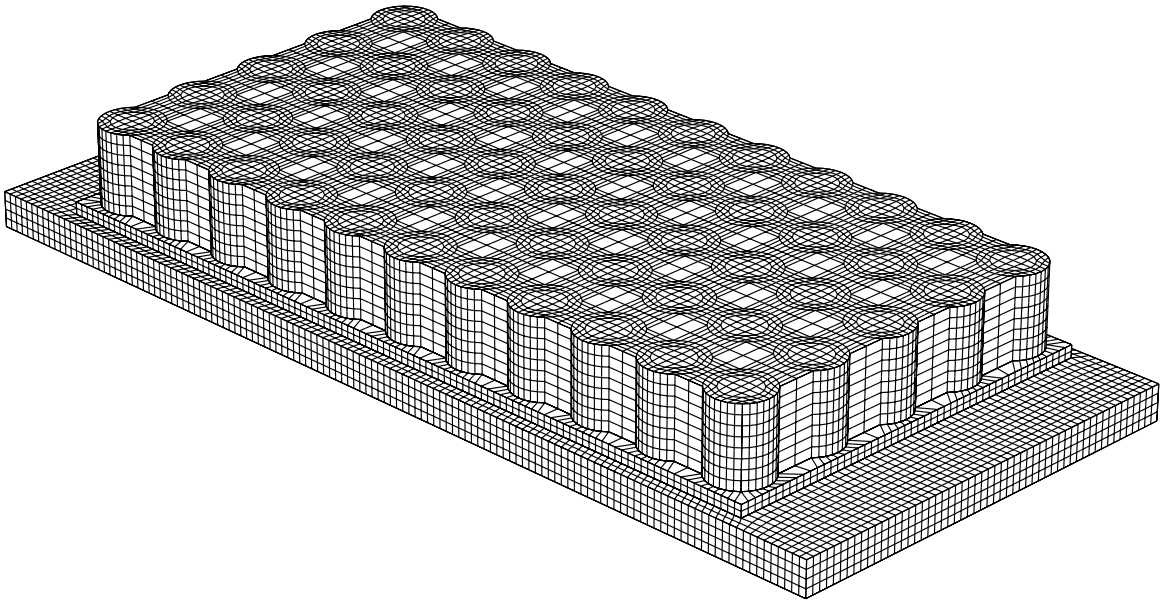

Sl. 3. *Računska mreža pladnja s feriti*
Fig. 3. *Computational mesh for ferrite plate.*

pogoj za temperaturo ni nujno simetričen (meritve).

Za simuliranje prenosa toplote je bil uporabljen poslovni programski paket TASCflow, ki za reševanje prenosnih enačb uporablja metodo nadzornih prostornin.

boundary conditions for the temperature are not necessarily symmetrical (measurements).

The simulation of the heat-transport equation is performed with a commercial package called TASCflow, where the transport equations are solved using the control volume method.

2.5 Analiza rezultatov

2.5.1 Temperatura v peči

Na sliki 4 je prikazana razlika med izračunano in izmerjeno temperaturo v peči v opazovani točki (fsp). Točka je tik ob feritih na spodnjem pladnju. Ujemanje numerične rešitve in izmerjenih vrednosti je dobro. Največja relativna napaka se pojavi v izgonski fazi in ne presega 20%. Nekaj večje je odstopanje tudi v fazi segrevanja, kjer je največja napaka 12%. To je tudi razumljivo, saj je hitrost spremembe temperature zelo velika. V fazi sintranja so razlike majhne, relativna napaka je <0,1%. Tudi to je smiselno, saj so razmere ustaljene (dT/dt=0). V fazi ohlajanja se razlika zopet povečuje na 12%).

2.5.2 Temperatura v feritih

Sliki 5 in 6 prikazujeta temperaturno polje vodoravni ravnini skozi središče feritov v prvi plasti, tj. feriti na podlagi, med fazo segrevanja (dT/dt>0) in fazo ohlajanja (dT/dt<0). S slik se jasno vidi, da so največji temperaturni gradienti v feritih na robu pladnja. To je tudi razumljivo, saj zunanji deli feritov prejmejo največ sevalne energije zaradi neposredne izpostavljenosti grelnikom. Temperaturno polje v notranjih feritih je bolj homogeno.

2.5 Analysis of the results

2.5.1 Temperature in the furnace

Figure 4 shows the difference between the computed and measured temperatures in the furnace at the monitoring point (fsp). The location of the monitoring point is close to the ferrites on the bottom plate. Agreement between the numerical results and the measured values is good. The largest relative error appears at the expulsion phase, and does not exceed 20%. A somewhat worse deviation also appears at the heating phase, where the maximum error is 12%. This is understandable, because the rate of change in temperature is very high. The differences in the sintering phase are minimal, the relative error is <0.1%. This also make sense because the conditions are steady (dT/dt=0). In the cooling phase the error again increases up to 12%.

2.5.2 Temperature in the ferrites

Figures 5 and 6 show the temperature field on the horizontal plane through the centre of the ferrites in the first layer, e.g. the ferrites near the ceramic ferrite base, during the heating phase (dT/dt>0) and during the cooling phase (dT/dt<0). It can be clearly seen that the largest temperature gradients appear in the ferrites at the plate edge. This is understandable because the outer parts of the ferrites receive the majority of the radiation heat due to direct exposure to the heaters. The temperature field in the other ferrites is more homogeneous.

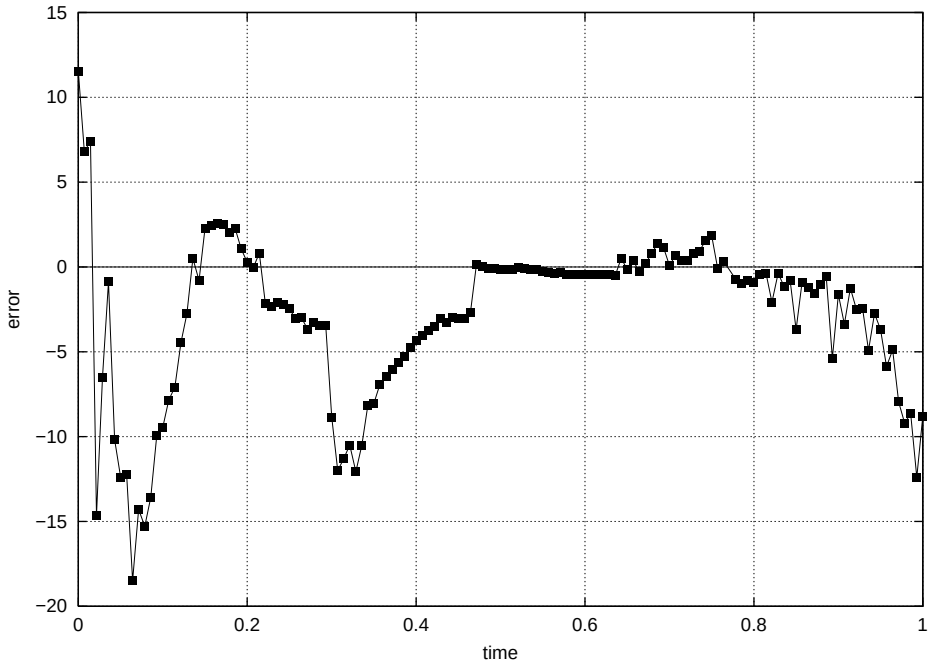

Sl. 4. *Razlika med izmerjeno in izračunano temperaturo*
Fig. 4. *Difference between computed and measured temperatures*

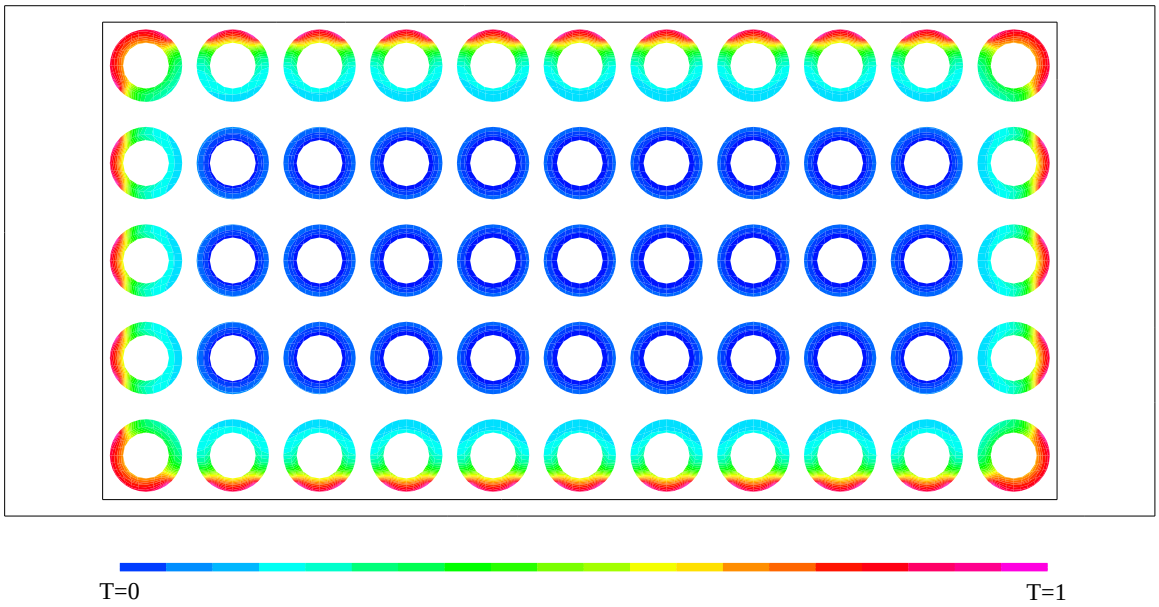

Sl. 5. *Temperaturno polje v feritih v fazi segrevanja*
Fig. 5. *Temperature field in the ferrites during the heating phase*

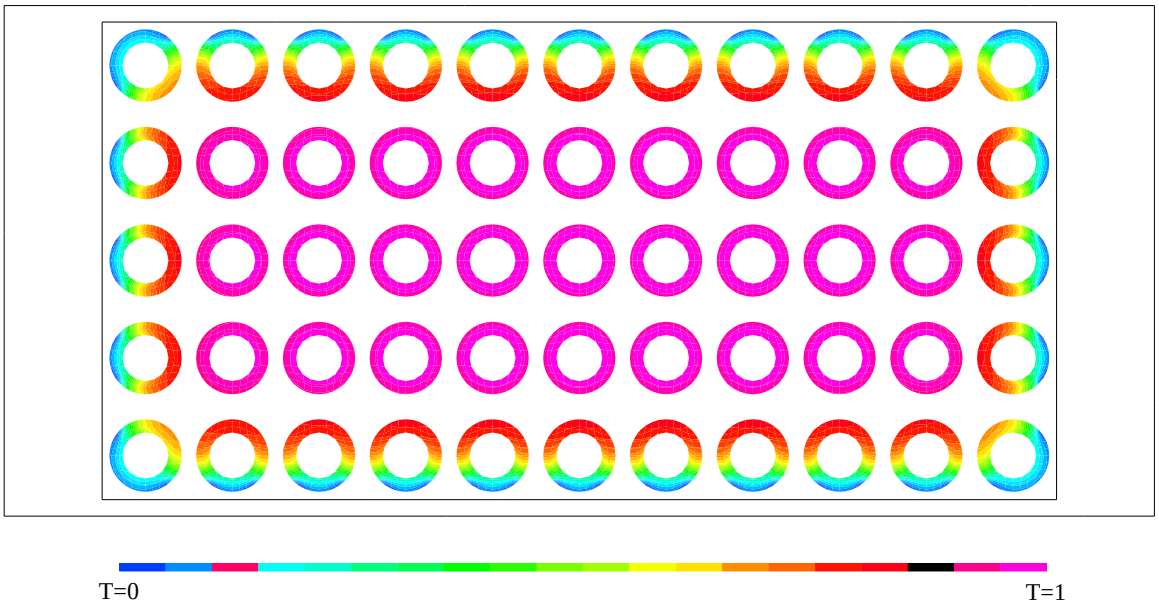

Sl. 6. *Temperaturno polje v feritih v fazi ohlajanja*
Fig. 6. *Temperature field in the ferrites during the cooling phase*

3 SKLEPI

V prispevku je prikazan postopek numeričnega simuliranja temperaturnega polja v laboratorijski komorni peči za sintranje feritov in temperaturnega polja v feritih. Narejena sta bila dva mrežasta modela: peč z notranjimi telesi (feriti, pladnji, nosilci, podstavki) in pladenj s feriti za dve numerični simuliranji.

Za preverbo numeričnega modela je bilo treba izvesti meritve temperatur. Za merjenje temperatur znotraj peči so bili uporabljeni umerjeni termopari tipa S in tipa K. Temperature zunaj peči so bile izmerjene z digitalnimi termometri.

3 CONCLUSIONS

This article shows a numerical simulation of the development of the temperature field in a laboratory furnace for sintering ferrites. Two discrete models were made, the furnace with CHT objects (ferrites, plates, bearers, supports) and a single ferrite plate, for two numerical simulations.

Testing of the numerical model required temperature measurements. The temperatures inside the furnace were measured with calibrated type S and type K thermocouples. The temperatures outside the furnace were measured with digital thermometers.

Ker postopek sintranja poteka pri visokih temperaturah, je glavni mehanizem prenosa toplote iz grelnikov na ferite sevanje. Za reševanje sistema diferencialnih enačb v različni obliki je bila uporabljena metoda nadzornih prostornin. Časovno odvisni robni pogoji, ki so potrebni za rešitev tega sistema, so bili dobljeni z meritvami.

Zaradi zahtevnosti problema je bilo narejenih nekaj poenostavitev. Ker so feriti zelo majhni v primerjavi s preostalimi telesi, jih ni mogoče razbiti na dele. V prvi fazi so bili obravnavani kot enoten del. Ker se med seboj ne dotikajo, med postopkom sintranja pa se še skrčijo, je bilo treba zračne reže upoštevati pri izračunu koeficienta prevodnosti feritnega dela.V drugi fazi je bilo izvedeno numerično simuliranje časovno spremenljivega temperaturnega polja v feritih med postopkom sintranja. Obravnavan je bil keramičen pladenj, 220 svitkov feritov, naloženih po štiri v stolpec in feritne ploščice za podlago feritom. Porazdelitev temperature v feritih je pričakovana. V fazah izgona in segrevanja je temperatura višja v feritih, ki so na robu pladnja, na sredini pa nižja. Po fazi sintranja, tj. je v fazi ohlajanja, pa je slika obrnjena. Na sredini je temperatura višja kakor na robu. Zaradi geometrijske simetrije in simetrije robnih pogojev je tudi temperaturno polje simetrično.

Iz primerjave meritev in rezultatov numeričnega simuliranja lahko sklenemo, da je numerični model ustrezen in da z njim dovolj natančno opišemo dogajanje v komorni peči.

Zahvala

Avtorji se zahvaljujejo Računalniškemu centru na Institutu Jožef Stefan za uporabo programskega paketa TASCflow za numerično simuliranje. Prav tako se zahvaljujejo g. Lepoldu Knezu in dr. Andreju Žnidaršiču iz Iskra Feriti, d.o.o. za pregled članka in pripombe.

Due to the high temperatures of the sintering process the main heat-transfer mechanism from the heaters to the ferrites is radiation. The system of differential equations in a discrete form is solved by the control volume method (CVM). The time-dependent boundary conditions, which are needed to solve the system, are obtained by measurement.

A few simplifications are used because of the complexity of the problem. Because the ferrites are very small when compared to the other objects they could not be discretized. In the first step they are treated as a single block. Because they are not touching each other, and because they shrink during the sintering process, the air gap must be taken into account when computing the heat conduction coefficient of the ferrite block. In the second step a numerical analysis of the time-dependent temperature field in the ferrites during the sintering process was performed. It deals with a ceramic plate with 220 toroidal ferrites stacked in columns of four on a ceramic base. The temperature distribution is as expected. In the expulsion and heating phase the temperature is higher in the ferrites at the edge of the plate and lower at the plate's centre. After the sintering phase, i.e. during the cooling phase, the picture is reversed. The temperature is higher at the centre and lower at the edge. Due to the geometry, and the symmetry of the boundary conditions, the temperature field is also symmetrical.

From a comparison of the measurements and the numerical simulation results we can conclude that the numerical model is appropriate and that the process in the furnace is well described.

Acknowledgements

The authors wish to thank the Computer Centre at the Jožef Stefan Institute for allowing us to use the TASCflow software for the numerical simulation. We also thank Mr. Lepold Knez and Dr. Andrej Žnidaršič from Iskra Feriti Ltd. for their review of the article and their valuable comments.

4 LITERATURA
4 REFERENCES

[1] Rek, Z., I. Žun (1998) Numerična simulacija temperaturnega polja v komorni peči. Poročilo FERITI 02 - 97/98. *Poročilo o raziskovalni nalogi*. Fakulteta za strojništvo, Ljubljana.
[2] Rek, Z., I. Žun (2000) Numerična simulacija temperaturnega polja v feritih Poročilo FERITI 03 - 00. *Poročilo o raziskovalni nalogi*. Fakulteta za strojništvo, Ljubljana.
[3] Perpar, M., I. Žun, D. Petrič (1998) Meritve temperatur in deleža kisika v komorni peči. Poročilo FERITI 01 - 97. *Poročilo o raziskovalni nalogi*. Fakulteta za strojništvo, Ljubljana.
[4] Isachenko, V.P., V.A. Osipova, A.S. Sukomel (1977) Heat transfer. *Mir Publishers*, Moskva.
[5] TASCflow (1996) Version 2.5 Documentation: User documentation. *Advanced Scientific Computing Ltd*., Waterlo, Ontario, Canada.
[6] TASCflow (1996) Version 2.5 Documentation: Theory documentation – diffusion model for radiation. *Advanced Scientific Computing Ltd.,* Waterlo, Ontario, Canada.
[7] Siegel, R. and J.R. Howell (1972) Thermal radiation heat transfer . *Mc Graw-Hill Book Company*, New York.
[8] Edwards, D.K. (1981) Radiation heat transfer notes. *Hemisphere Publishing Corporation*, New York.

Naslov avtorjev: dr. Zlatko Rek
dr. Matjaž Perpar
prof. dr. Iztok Žun
Laboratorij za dinamiko fluidov in termodinamiko
Fakulteta za strojništvo
Univerza v Ljubljani
Aškerčeva 6
1000 Ljubljana
zlatko.rek@fs.uni-lj.si
matjaz.perpar@fs.uni-lj.si
iztok.zun@fs.uni-lj.si

Author's Address: Dr. Zlatko Rek,
Dr. Matjaž Perpar
Prof. Dr. Iztok Žun
Laboratory for Fluid Dynamics and Thermodynamics
Faculty of Mechanical Eng.
University of Ljubljana
Aškerčeva 6
SI-1000 Ljubljana, Slovenia
zlatko.rek@fs.uni-lj.si
matjaz.perpar@fs.uni-lj.si
iztok.zun@fs.uni-lj.si

Prejeto: 9.4.2002
Received:

Sprejeto: 22.11.2002
Accepted:

© Strojniški vestnik 48(2002)9,482-490
ISSN 0039-2480
UDK 62-714:621.565:536.2
Izvirni znanstveni članek (1.01)

© Journal of Mechanical Engineering 48(2002)9,482-490
ISSN 0039-2480
UDC 62-714:621.565:536.2
Original scientific paper (1.01)

Analiza vezanega prenosa toplote v hladilniku elektronskega čipa

An Analysis of Conjugate Heat Transfer in the Heat Sink of an Electronic Chip

Andrej Horvat - Ivan Catton

Prispevek opisuje razvoj algoritma za izračun vezanega prenosa toplote z namenom izbire najugodnejše geometrijske oblike za hladilnik elektronskega čipa. Struktura hladilnika je bila modelirana kot homogena porozna snov z uporabo teorije prostorninskega povprečenja (TPP - VAT). Geometrijska oblika simulacijskega območja in robni pogoji so bili povzeti po eksperimentalni napravi v laboratoriju za prenos toplote "Morrin-Martinelli-Gier" na Univerzi Kalifornije v Los Angelesu. Primeri numeričnih simulacij so bili izvedeni za izotermno testno sekcijo kakor tudi za toplotno prevodno testno sekcijo iz aluminija. Primerjava koeficienta upora celotne proge $\overline{C}_d$ kot funkcije Reynoldsovega števila Re_h razkriva dobro ujemanje z objavljenimi rezultati, medtem ko primerjava porazdelitev Nusseltovega števila $\overline{Nu}$ kaže večje razlike. Končna toplotna prevodnost trdnine zmanjša koeficient prestopa toplote in Nusseltovo število $\overline{Nu}$. Vpliv toplotne prevodnosti na rezultate se zvečuje s povečevanjem Reynoldsovega števila.

(Ključne besede: prenosniki toplote, hladilniki čipov, prenos toplote, razvoj algoritmov)

This paper describes the construction of an algorithm for conjugate heat-transfer calculations in order to find the most suitable form for the heat sink of an electronic chip. Applying volume averaging theory (VAT) to a system of transport equations, a heat-sink structure was modeled as a homogeneous porous medium. The geometry of the simulation domain and the boundary conditions followed the experimental set-up used in the Morrin-Martinelli-Gier Memorial Heat Transfer Laboratory at the University of California, Los Angeles. The example numerical simulations were performed for the test section with an isothermal structure as well as for the heat-conducting aluminum pin-fins. A comparison of the whole-section drag coefficient $\overline{C}_d$ as a function of Reynolds number Re_h reveals good agreement with existing data, whereas the comparison of the Nusselt number $\overline{Nu}$ distributions shows larger discrepancies. The finite conductivity of the solid decreases the heat-transfer coefficient and Nusselt number $\overline{Nu}$. The influence of conductivity becomes larger with increasing Reynolds number.

(Keywords: heat exchangers, heat sinks, heat transfer, algorithms)

0 UVOD

Prenosniki toplote so ena od osnovnih komponent ne samo v termoenergetski in procesni industriji ampak tudi v proizvodnji elektronske opreme. Navkljub pomembni vlogi, je v konstrukcijski postopek prenosnikov toplote še vedno vpleteno mnogo izkustvenih spoznanj. V preteklosti sta se namreč razvoj in uporaba prenosnikov toplote razvijala ločeno na številnih, največkrat nepovezanih področjih, zlasti v avtomobilski in letalski industriji, v kriogeni in hladilniški tehniki. Pri tem so se tehnologije, dobro znane v enem področju, le počasi širile na druga področja [1]. Zaradi tega lahko skupen način izbire in optimizacije konstrukcije prenosnikov toplote pomembno zmanjša stroške v industriji.

0 INTRODUCTION

Heat exchangers are one of the basic installations, not only in power and process industries, but also in the production of electronic equipment. Despite their crucial role, there is still a great deal of empiricism involved in the design procedure of heat exchangers. The development and application of heat exchangers and their surfaces has taken place in a piecemeal fashion in a number of rather unrelated areas, principally those of the automotive, aerospace, cryogenic and refrigeration sectors. A lot of detailed technology, familiar in one sector, progressed only slowly over the boundary into another sector [1]. Therefore, a unifying approach to select and to optimize a heat-exchanger design can bring significant cost reduction to industry.

Prispevek je del širših prizadevanj za razvoj znanstvenega prostopa k problemu optimizacije geometrijske oblike prenosnikov toplote. Opisuje gradnjo algoritma za hiter izračun vezanega prenosa toplote z namenom izbire najugodnejše geometrijske oblike za hladilnik elektronskega čipa.

Struktura hladilnika je bila modelirana kot homogen porozen medij z uporabo teorije prostorninskega povprečenja (TPP) ([2] do [4]) sistema prenosnih enačb. Medsebojni vpliv tekočine in strukture je bil opisan s koeficienti lokalnega upora C_d in prestopa toplote h, ki so bili prevzeti iz razpoložljive literature ([7] do [9]) in vstavljeni v računalniški program.

Izračunani koeficient upora celotne proge $\overline{C}_d$, toplotna učinkovitost $\bar{Q}/\bar{W}$ in Nusseltovo število $\overline{Nu}$ so bili primerjani z razpoložljivimi eksperimentalnimi podatki [5]. Primerjava kaže dobro ujemanje s preskusi kljub poenostavitvam predstavljenega modela.

1 MODELNI PRISTOP

Zračni tok skozi hladilnik čipa lahko opišemo z osnovnimi enačbami prenosa snovi, gibalne količine in energije [6]. Zaradi zahtev po kratkem računskem času modela, je treba prenosnim enačbam izračunati povprečje po periodični nadzorni prostornini (za podrobnosti glej [4]). To prostorninsko računanje povprečja vodi do problema sklenitve sistema enačb, pri katerem je treba prenos gibalne količine in toplote med tekočino in trdnino opisati z empiričnimi razmerji, npr. s koeficientoma lokalnega upora C_d in prestopa toplote h.

Da bi še nadalje poenostavili simuliran sistem, smo predpostavili tok tekočine le v vzdolžni smeri z nespremenljivim znižanjem tlaka (sl. 1). Zaradi tega se profil hitrosti spreminja le prečno na smer toka. To pomeni, da je tlačna sila čez celotno simulacijsko območje v ravnovesju s strižnimi silami. Tako je mogoče enačbo prenosa gibalne količine zapisati v diferencialni obliki kot:

$$-\alpha_f \mu_f \left(\frac{\partial^2 u_f}{\partial y^2} + \frac{\partial^2 u_f}{\partial z^2} \right) + \frac{1}{2} C_d \rho_f u_f^2 S = \frac{\Delta p}{L} \qquad (1),$$

kjer so: α_f delež tekočine, C_d koeficient lokalnega upora, S specifična površina porozne snovi, Δp padec tlaka čez simulacijsko območje in L dolžina simulacijskega območja.

Temperaturno polje v tekočini se oblikuje pod vplivom ravnovesja med toplotno konvekcijo v smeri toka, toplotno difuzijo in toploto, ki se prenese s trdnine na tekočino. Iz tega izhaja diferencialna oblika energijske enačbe za tekočino:

$$\alpha_f \rho_f c_f u_f \frac{\partial T_f}{\partial x} = \alpha_f \lambda_f \left(\frac{\partial^2 T_f}{\partial x^2} + \frac{\partial^2 T_f}{\partial y^2} + \frac{\partial^2 T_f}{\partial z^2} \right) - h \left(T_f - T_s \right) S \qquad (2),$$

kjer sta: T_f temperatura tekočine in T_s temperatura trdnine. Prenos toplote med trdnino in tekočino je

This paper is part of a broader effort to develop a scientific procedure for optimization of heat-exchanger geometries. It describes the construction of an algorithm for fast calculations of conjugate heat transfer in order to find the most suitable form for an electronic chip heat sink.

Applying volume averaging theory (VAT) ([2] to [4]) to a system of transport equations, a heat-sink structure was modeled as a homogeneous porous media. The interaction between the fluid and the heat-sink structure was described with local drag and heat-transfer coefficients, which were taken from the available literature ([7] to [9]) and inserted into a computer code.

The calculated whole-section drag coefficient $\overline{C}_d$, thermal effectiveness $\bar{Q}/\bar{W}$ and Nusselt number $\overline{Nu}$ were compared with available experimental data [5]. The comparison shows a good agreement with the experimental data despite model simplifications.

1 MODEL APPROACH

The airflow through a chip-cooler structure can be described with basic mass, momentum and heat-transport equations [6]. Due to the requirement for the model to have short computing times, the transport equations have to be averaged over a periodic control volume (see [4] for details). This volumetric averaging leads to a closure problem, where an interface exchange of momentum and heat between a fluid and a solid has to be described with additional empirical relations, e.g. a local drag coefficient C_d and a local heat-transfer coefficient h.

To further simplify the simulated system, fluid flow was taken as unidirectional with a constant pressure drop in the streamwise direction (Fig. 1). As a consequence, velocity only changes transverse to the flow direction. This means that the pressure force across the entire simulation domain is balanced with shear forces. Thus, the momentum equation can be written in differential form as:

$$-\alpha_f \mu_f \left(\frac{\partial^2 u_f}{\partial y^2} + \frac{\partial^2 u_f}{\partial z^2} \right) + \frac{1}{2} C_d \rho_f u_f^2 S = \frac{\Delta p}{L} \qquad (1),$$

where α_f is the fluid fraction, C_d the local drag coefficient, S the specific surface of porous media, Δp the pressure drop across the simulation domain and L the simulation domain's length.

The temperature field in the fluid is formed as a balance between thermal convection in the streamwise direction, thermal diffusion, and the heat that is transferred from the solid to the fluid. Thus, the differential form of the energy equation for the fluid is:

$$\alpha_f \rho_f c_f u_f \frac{\partial T_f}{\partial x} = \alpha_f \lambda_f \left(\frac{\partial^2 T_f}{\partial x^2} + \frac{\partial^2 T_f}{\partial y^2} + \frac{\partial^2 T_f}{\partial z^2} \right) - h \left(T_f - T_s \right) S \qquad (2),$$

where T_f and T_s are the fluid and solid temperatures, respectively. The heat transfer between the solid and the

modeliran kot linearna odvisnost temperatur obeh faz, kjer je *h* koeficient lokalnega prestopa toplote.

V vsaki nadzorni prostornini je struktura hladilnika le šibko povezana v vodoravni smeri (sl. 1). Zaradi tega je le toplotna difuzija v navpični smeri v ravnovesju s toploto, ki odteka skozi stično površino kapljevine in trdnine, medtem ko lahko toplotno difuzijo v vodoravni smeri zanemarimo. To poenostavi energijsko enačbo trdnine:

$$0 = \alpha_s \lambda_s \frac{\partial^2 T_s}{\partial z^2} + h \left(T_f - T_s\right) S \qquad (3),$$

kjer je α_s delež trdnine.

Enačbe (1) do (3), ki so zapisane s povprečenimi veličinami, so enačbe ravnovesnega prenosa gibalne količine in toplote skozi homogeno porozno snov. Zanesljive podatke za dva dodatna parametra, to sta koeficienta lokalnega upora C_d in prestopa toplote *h*, smo poiskali v [7] do [9].

2 SIMULACIJSKO OBMOČJE

Geometrijska oblika simulacijskega območja kakor tudi robni pogoji enačb (1) do (3) sledijo geometrijski obliki eksperimentalne testne sekcije, ki je bila uporabljena v laboratoriju za prenos toplote "Morrin-Martinelli-Gier" na Univerzi Kalifornije v Los Angelesu za pridobitev eksperimentalnih podatkov, opisanih v [5].

fluid is modeled as a linear relation between both phase temperatures, where *h* is a local heat-transfer coefficient.

The chip-cooler structure in each control volume is only loosely connected in the horizontal directions (see Fig. 1). As a consequence, only the thermal diffusion in a vertical direction is in balance with the heat leaving the structure through the fluid-solid interface, whereas the thermal diffusion in horizontal directions can be neglected. This simplifies the energy equation for the solid to:

where α_s is the solid fraction.

Equations (1) to (3), written with the phase averaged variables, are equations for the steady-state transport of momentum and heat through homogeneous porous media. The reliable empirical data for two additional parameters, a local drag coefficient C_d and heat-transfer coefficient *h*, were found in [7] to [9].

2 SIMULATION DOMAIN

The geometry of the simulation domain as well as the boundary conditions for Eqs. (1-3) follow the geometry of the experimental test section used in the Morrin-Martinelli-Gier Memorial Heat Transfer Laboratory at the University of California, Los Angeles, where the experimental data described in [5] were taken.

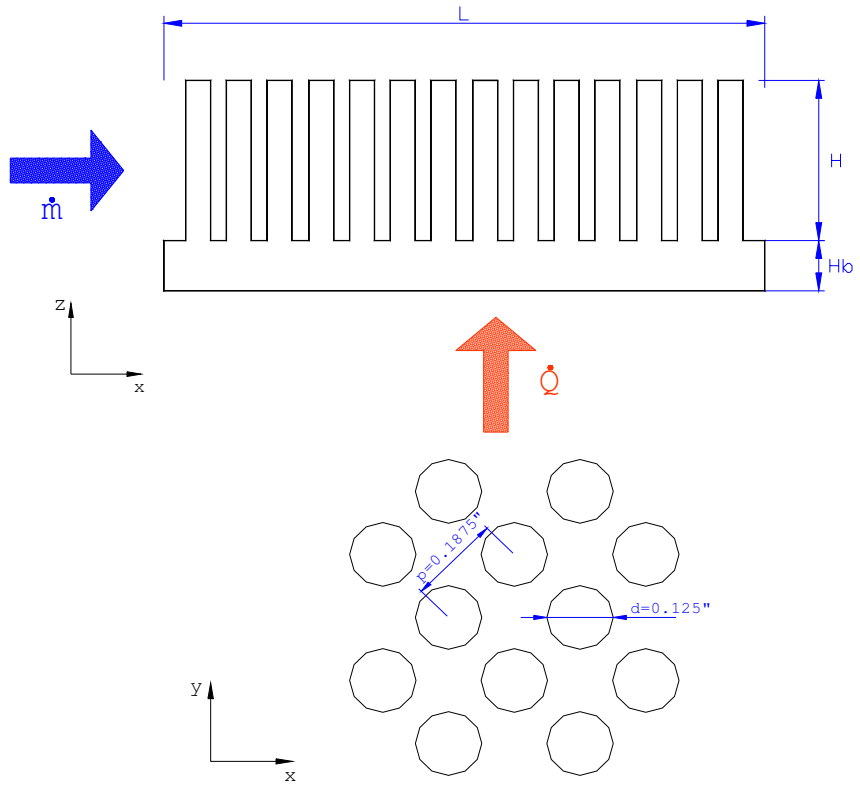

Sl. 1. *Eksperimentalna testna proga*
Fig. 1. *Experimental test section*

Splošna razporeditev palčnih reber hladilnika je podana na sliki 1. Premer palčnih reber je znašal d = 0,003175 m (0,125"). Razmerje medpalčnega razmika in premera v smeri toka je bilo p_x/d = 1,06 in v smeri prečno na tok p_y/d = 2,12. Simulacijsko območje je zajemalo 34 vrst palčnih reber v smeri toka in 17 vrst prečno na smer toka. Dolžina hladilnika L kakor tudi širina W sta znašali 0,1145 m , medtem ko je višina H znašala 0,0381 m.

Robni pogoji trdne stene brez zdrsa so bili uporabljeni za enačbo prenosa gibalne količine (1) na vseh štirih stenah, ki so vzporedne s smerjo toka:

The general arrangement of the heat-sink pin-fins is given in Fig. 1. The diameter of the pin-fins was d = 0.003175 m (0.125"). The pitch-to-diameter ratio in the streamwise direction was set to p_x/d = 1.06, and in the transverse direction to p_y/d = 2.12. The simulation domain consisted of 34 rows of pin-fins in the streamwise direction and 17 rows of pin-fins in the transverse direction. The length L as well as the width W of the heat sink were 0.1145 m, whereas the height H was 0.0381 m.

The no-slip boundary conditions for the momentum equation (1) were implemented for all four walls, which are parallel to the flow direction:

$$u_f(0,z)=0,\ u_f(W,z)=0,\ u_f(y,0)=0,\ u_f(y,H)=0 \quad (4).$$

Kot gonilna sila toka je bil podan tlačni padec vzdolž celotnega simulacijskega območja. Absolutne vrednosti so zbrane v preglednici 1.

Pri enačbi prenosa energije v tekočini (2) smo predpostavili izotermni vtok tekočine kot tudi izotermno spodnjo steno:

As a flow driving force, the whole-section pressure drop Δp was prescribed. The absolute values are summarized in Table 1.

For the fluid energy equation (2), the simulation domain inflow and the bottom wall were taken as isothermal:

$$T_f(0,y,z)=T_{in},\ T_f(x,y,0)=T_g \quad (5),$$

medtem ko so bile druge stene adiabatne:

whereas the other walls were considered as adiabatic:

$$\frac{\partial T_f}{\partial x}(L,y,z)=0,\ \frac{\partial T_f}{\partial y}(x,0,z)=0,\ \frac{\partial T_f}{\partial y}(x,W,z)=0,\ \frac{\partial T_f}{\partial z}(x,y,H)=0 \quad (6).$$

Pri enačbi prenosa energije v trdnini (3) je bila spodnja stena privzeta kot izotermna, medtem ko je bila zgornja stena adiabatna:

For the solid energy equation (3), the bottom wall was prescribed as isothermal, whereas the top wall was assumed to be adiabatic:

$$T_s(x,y,0)=T_g,\ \frac{\partial T_s}{\partial z}(x,y,H)=0 \quad (7).$$

Predpostavka o izotermnosti spodnje stene (5) in (7) se pomembno razlikuje od eksperimentalne postavitve [5], pri kateri so palčna rebra spojena s toplotno prevodno bazno ploščo. Kljub vsemu bodo rezultati pokazali, da sedanji model daje zadovoljiv približek izmerjenih vrednosti.

Absolutne temperature robnih pogojev za različne simulirne primere so zbrane v preglednici 1.

The assumption about the isothermal bottom wall (5) and (7) significantly differs from the experimental set-up [5], where the pin-fins were joined with a conductive base plate. Nevertheless, as the results will show, the presented model still gives a satisfactory approximation to the measured values.

The absolute temperatures in different simulation cases are summarized in Table 1.

3 NUMERIČNE METODE

Prenosne enačbe (1) do (3) in robni pogoji (4) do (7) so bili preoblikovani v brezdimenzijsko obliko in diskretizirani, upoštevajoč načela metode končnih

3 NUMERICAL METHODS

The transport equations (1) do (3) and boundary conditions (4) to (7) were transformed into the dimensionless form and then discretized following

Preglednica 1. *Robni pogoji - izbrane vrednosti*
Table 1. *Boundary conditions - pre-set values*

Št. No.	**Δp Pa**	**T_{in} °C**	**T_g °C**	**Št. No.**	**Δp Pa**	**T_{in} °C**	**T_g °C**
1	5,0	23,00	54,90	**5**	74,7	23,02	30,30
2	10,0	23,00	43,43	**6**	175,6	23,02	27,90
3	20,0	23,00	37,20	**7**	266,5	23,04	27,30
4	40,0	23,00	33,00	**8**	368,6	22,85	26,64

prostornin ([6] in [10]). Pri vseh izvedenih numeričnih simulacijah smo uporabili 34x17x70 končnih prostornin v smereh x, y in z.

Zaradi robnih pogojev (4) do (7), sta bili hitrost u_f in temperatura trdnine T_s zapisani kot dvodimenzionalno skalarno polje, medtem ko je bila temperatura tekočine T_f zapisana kot tridimenzionalno skalarno polje. Zaradi diskretizacijskega postopka je nastal, v primeru dvodimenzionalnih skalarnih polj, pet-diagonalni matrični sistem in, v primeru tridimenzionalnega skalarnega polja, sedem-diagonalni matrični sistem.

Za učinkovito obračanje matričnega sistema enačb je bila za ta poseben primer privzeta metoda spremenjenih vezanih gradientov (MSVG - PCGM), ki je podrobneje opisana v [11].

4 REZULTATI IN RAZPRAVA

Rezultati izračunov za primer aluminijastega (Al) hladilnika so predstavljeni na slikah 2 in 3. Tlačni padec Δp = 368,6 Pa povzroči zračni tok z Reynoldsovim številom Re_h = 1904, pri čemer je Reynoldsovo število definirano na podlagi hidravličnega premera d_h hipotetičnega kanala porozne snovi:

Slika 2 prikazuje temperaturno polje v Al strukturi v Celzijevi skali, medtem ko slika 3 razkriva temperaturno polje v zračnem toku.

Kakor prikazuje slika 2, ima Al struktura najvišjo temperaturo blizu izotermne spodnje stene in najnižjo temperaturo ob levem zgornjem robu, kjer je struktura izpostavljena vtoku zraka z nizko temperaturo. Slika 3 kaže, kako se zrak postopoma segreva od vtoka na levi do iztoka na desni strani. Spodnji del temperaturnega polja prav tako razkriva intenzivno segrevanje s spodnje izotermne meje, kar ima za posledico vodoravno toplotno razslojenost prehajajočega zraka.

the principles of the finite-volume methods ([6] and [10]). In all the performed numerical simulations, 34x17x70 finite volumes were used in x, y and z directions, respectively.

Due to the boundary conditions (4) to (7), the velocity u_f as well as the solid temperature T_s were described as two-dimensional scalar fields, whereas the fluid temperature T_f was described as a three-dimensional scalar field. This resulted in a non-symmetric five-diagonal matrix system for the two-dimensional scalar fields and a seven-diagonal matrix system for the three-dimensional scalar field.

In order to invert the matrix systems efficiently, the preconditioned conjugate gradient method (PCGM), as described in [11], was adopted for this specific problem.

4 RESULTS AND DISCUSSION

The results of an example calculation for an aluminum (Al) heat sink are presented in Figs. 2 and 3. The imposed pressure drop Δp = 368.6 Pa causes airflow of the Reynolds number Re_h = 1904, where the definition of the Reynolds number is based on a hydraulic diameter d_h of a hypothetical porous media channel:

$$\mathrm{Re}_h = \frac{\overline{u}_f}{\nu_f} d_h = \frac{\overline{u}_f}{\nu_f}\left(4\frac{\alpha_f}{S}\right) \qquad (8).$$

Fig. 2 shows the temperature field in the Al structure in degrees Celsius, whereas Fig. 3 reveals the temperature field in the airflow.

In Fig. 2, the Al structure has its highest temperature close to the isothermal bottom, and the lowest close to the left upper edge, where the structure is exposed to a low-temperature inflow. Fig. 3 shows how the air is gradually heated from the inlet on the left side to the outlet on the right side. The lower part of the temperature field also shows intensive heating from the isothermal bottom boundary, which results in horizontal thermal stratification of the passing air.

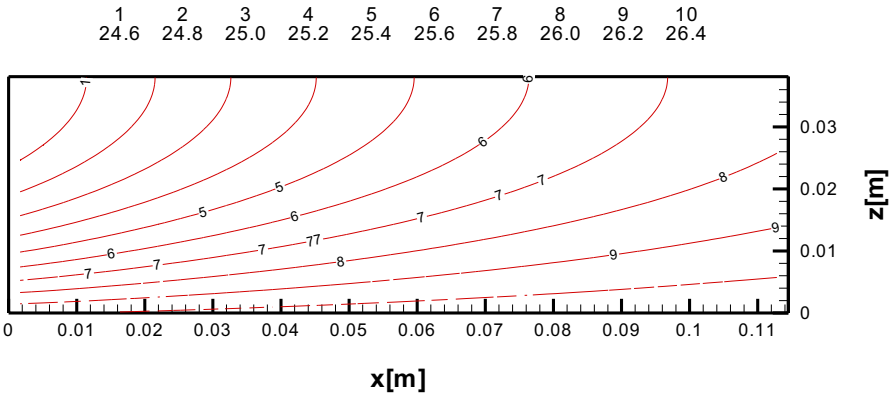

Sl. 2. *Temperaturno polje v trdnini pri* Re_h = 1904, T_{in} = 22,85 °C, T_g = 26,64 °C
Fig. 2. *Temperature fields in the solid at* Re_h = 1904, T_{in} = 22.85 °C, T_g = 26.64 °C

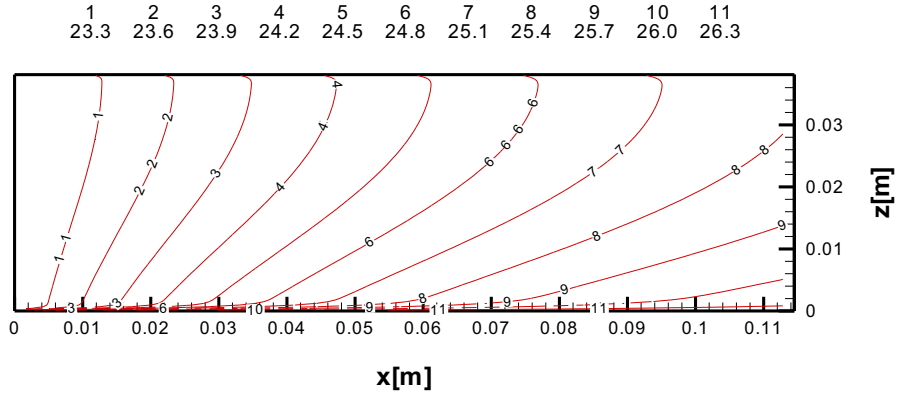

Sl. 3. *Temperaturno polje v zraku pri* $Re_h = 1904$, $T_{in} = 22{,}85\ ^oC$, $T_g = 26{,}64\ ^oC$
Fig. 3. *Temperature fields in the air at* $Re_h = 1904$, $T_{in} = 22.85\ ^oC$, $T_g = 26.64\ ^oC$

Poleg vzorčnega izračuna sta bili opravljeni še dve seriji izračunov pri osmih različnih tlačnih padcih. Pri izračunih uporabljeni robni pogoji so zbrani v preglednici 1. V obeh serijah smo za tok hladiva vzeli snovske lastnosti zraka. Pri prvi seriji izračunov smo za hladilnik vzeli snovske lastnosti aluminija, medtem ko je bila v drugi seriji predpostavljena izotermičnost strukture.

Kakor je običajno pri tovrstnih simuliranjih, sta bila izračunana koeficient upora $\bar{C}_d$ (9) in Nusseltovo število $\overline{Nu}$ (10) za celotno sekcijo, dobljene vrednosti pa primerjane z eksperimentalnimi rezultati [5].

Besides the example calculation, two other series of calculations with eight different pressure drops were performed. The boundary conditions for these calculations are summarized in Table 1. In both series the air material properties were taken for coolant flow. For the first set of calculations the Al material properties were taken for the heat sink, whereas in the second set the heat sink was considered as isothermal.

As is usually the case in such calculations, the whole-section drag coefficient $\bar{C}_d$ (9) and Nusselt number $\overline{Nu}$ (10) were calculated and compared with the experimental results [5].

$$\bar{C}_d = \frac{2\ \Delta p}{\rho_f \bar{u}_f^2 L\ \ S} \tag{9},$$

$$\overline{Nu} = \frac{Q\ \ d_h}{\Delta T A_g\ \ \lambda_f} \tag{10},$$

kjer sta: $A_g = L \cdot W$ površina gretega dna in $\Delta T = T_g - T_{in}$ temperaturna razlika med greto spodnjo steno in vtokom zraka. Pri definiciji Nusseltovega števila $\overline{Nu}$ je konvektivni toplotni tok definiran kot:

where $A_g = L \cdot W$ is the area of the heated bottom and $\Delta T = T_g - T_{in}$ is the temperature difference between the heated bottom and the inflow air. In the Nusselt number $\overline{Nu}$ (10) definition, the convective heat-flow rate is defined as:

$$\bar{Q} = \alpha_f \rho_f c_f \bar{u}_f \ \ \left(\bar{T}_{out} - \bar{T}_{in}\right)\ \ A_\perp \tag{11}.$$

kjer je $A_\perp = H \cdot W$.

Primerjava na sliki 4 kaže koeficient upora celotne proge $\bar{C}_d$ kot funkcijo Reynoldsovega števila Re_h. Slika kaže dobro ujemanje z že objavljenimi rezultati. Kljub temu pa se pri večji vrednosti Reynoldsovega števila Re_h zaradi naraščajoče turbulence, ki ni bila zajeta v model, pokaže razlika v velikosti nekaj odstotkov.

Primerjava porazdelitev Nusseltovega števila celotne proge $\overline{Nu}$ na sliki 5 prikazuje večje odstopanje. Zaradi razlike v toplotnih robnih pogojih kažejo izračuni za 20 odstotkov večji toplotni tok od eksperimentalnih vrednosti [5]. Nadalje je razvidno, da končna toplotna prevodnost aluminijaste strukture (na slikah 5 in 6 označeno z Al) znižuje koeficient prestopa toplote in Nusseltovo število $\overline{Nu}$ v primerjavi s strukturo z neskončno toplotno

where $A_\perp = H \cdot W$.

The comparison in Fig. 4 shows the whole-section drag coefficient $\bar{C}_d$ as a function of Reynolds number Re_h. It reveals good agreement with already published data. Nevertheless, at a higher Reynolds number a difference of a few percent appears due to increasing turbulence, which was not taken into account in the model.

The comparison of the Nusselt number $\overline{Nu}$ distributions in Fig. 5 shows larger discrepancies. Due to the difference in the thermal boundary conditions, the calculated data reveal up to 20 percent higher heat-transfer rate than the measured values [5]. Furthermore, it is evident that the finite thermal conductivity of the Al structure (in Figs. 5 and 6 marked with Al) decreases the heat-transfer coefficient and the Nusselt number $\overline{Nu}$ in comparison

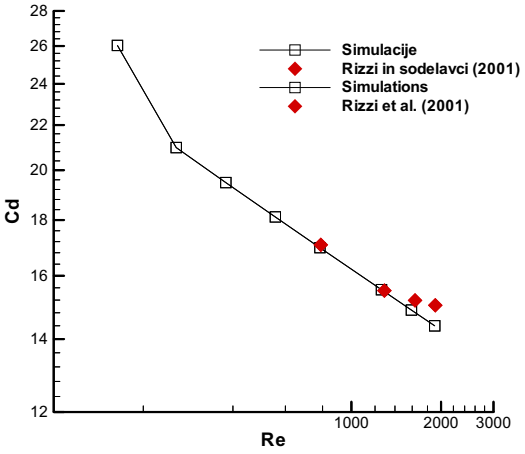

Sl. 4. *Koeficient upora celotne sekcije kot funkcija Reynoldsovega števila*
Fig. 4. *Whole-section drag coefficient as a function of Reynolds number*

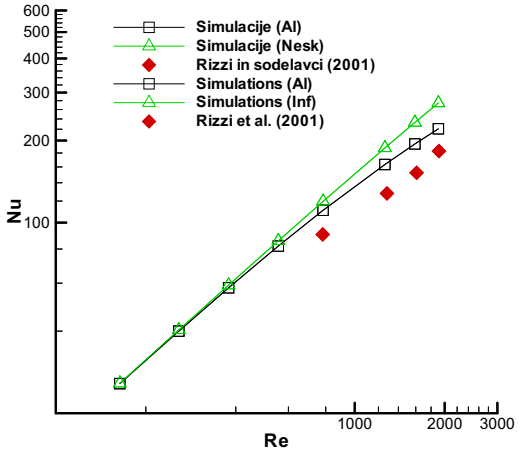

Sl. 5. *Nusseltovo število celotne sekcije kot funkcija Reynoldsovega števila*
Fig. 5. *Whole-section Nusselt number as a function of Reynolds number*

prevodnostjo (na slikah 5 in 6 označeno z Nesk). Ta vpliv končne toplotne prevodnosti trdnine se z večanjem vrednosti Reynoldsovega števila še povečuje.

Konstrukcija prenosnikov toplote mora upoštevati tako vrednosti toplotnega toka kakor tudi mehanskega dela, ki je potrebno za premagovanje trenja tekočine in za premikanje le-te skozi samo strukturo. V tem pogledu je glavni cilj konstrukcije povečati toplotni tok $\bar{Q}$ (11) pri najmanjši moči črpanja:

with the infinite thermal conductivity case (in Figs. 5 and 6 marked with Inf). This influence of finite thermal conductivity of the solid becomes larger with increasing Reynolds number.

The design of a heat sink involves consideration of the heat-transfer rate and the mechanical pumping power expended to overcome fluid friction and move the fluid through a structure. Thus, the main design goal is to maximize the heat-transfer rate $\bar{Q}$ (11) for the minimum pumping power:

$$\bar{W} = \alpha_f \quad \Delta p \quad A_\perp \quad \bar{u}_f \tag{12}.$$

Slika 6 prikazuje toplotno učinkovitost prenosa toplote, ki je definirana kot razmerje med toplotnim tokom $\bar{Q}$ in mehansko močjo $\bar{W}$. Razvidno je, da so eksperimentalni in numerični rezultati blizu skupaj. Pri padajoči toplotni učinkovitosti $\bar{Q}/\bar{W}$ se vpliv toplotne prevodnosti poveča in povzroči 35 odstotkov razlike pri vrednosti Reynoldsovega števila $Re_h = 1904$.

Fig. 6 shows the thermal effectiveness of the heat-transfer process, which is defined as the ratio between the heat-transfer rate $\bar{Q}$ and the mechanical power $\bar{W}$. It is evident that the experimental and numerical results are close. With decreasing thermal effectiveness $\bar{Q}/\bar{W}$, the influence of the structure's thermal conductivity increases and causes a 35 percent difference at the Reynolds number $Re_h = 1904$.

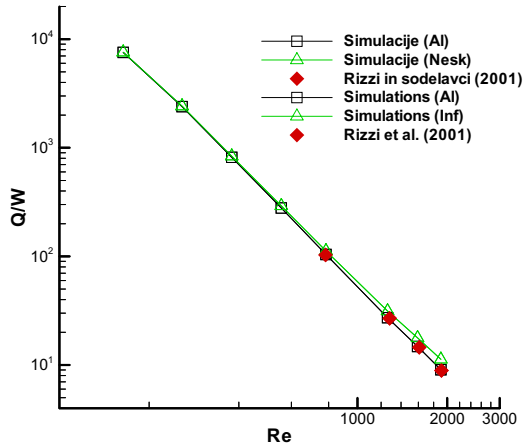

Sl. 6. *Toplotna učinkovitost hladilnika v odvisnosti od Reynoldsovega števila*
Fig. 6. *Heat-sink effectiveness as a function of Reynolds number*

Kakor je prikazano, se toplotna učinkovitost $\bar{Q}/\bar{W}$ hladilnika zmanjšuje z večanjem vrednosti Reynoldsovega števila Re_h (8). Kljub temu, da manjše vrednosti Reynoldsovega števila Re_h prinašajo večjo toplotno učinkovitost, pa morajo biti rezultirajoči majhni toplotni tokovi nadomeščeni z večjo površino in zaradi tega z večjimi dimenzijami samega hladilnika. V nekaterih primerih to ni mogoče zaradi gospodarnosti in omejitev velikosti.

5 SKLEPI

Prispevek opisuje delo, ki je bilo vloženo v razvoj računsko hitrega numeričnega algoritma za izračun prenosnikov toplote. Namen naloge je bil posvečen numerični raziskavi odvoda toplote iz elektronskega čipa. Pri tem je bila notranja struktura hladilnika, v obliki paličastih reber s premaknjeno postavitvijo, obravnavana kot homogena porozna snov. Vrednosti koeficientov lokalnega upora C_d in prestopa toplote h, ki so bile potrebne za zaprtje prenosnih enačb, smo prevzeli iz [7] do [9]. Razvite parcialne diferencialne enačbe so bile diskretizirane z upoštevanjem ohranitvenih lastnosti metode nadzornih prostornin. Sistem pol-linearnih enačb je bil nato rešen z metodo spremenjenih vezanih gradientov. Za preveritev postopka izračuna smo uporabili eksperimentalne podatke laboratorija za prenos toplote "Morrin-Martinelli-Gier".

Izvedeni sta bili dve seriji izračunov za hladilnik čipa, ki je bil hlajen z zračnim tokom. Izračunane vrednosti koeficienta upora celotne proge $\bar{C}_d$ kažejo dobro ujemanje z že objavljenimi podatki, medtem ko izračunane vrednosti Nusseltovega števila $\overline{Nu}$ celotne proge razkrivajo odstopanje zaradi razlik v toplotnih robnih pogojih. Prav tako smo raziskali vpliv končne toplotne prevodnosti trdne strukture. Izkazalo se je, da končna toplotna prevodnost aluminija zmanjša toplotno učinkovitost $\bar{Q}/\bar{W}$ za 35 odstotkov pri Re_h = 1904. Prav tako je pričakovati večji vpliv toplotne prevodnosti pri večjih vrednostih Reynoldsovega števila.

Prikazani rezultati potrjujejo ustreznost izbranega načina za preračun hladilnika, kjer je treba upoštevati toplotno prevodnost trdne strukture. Vzorčni izračuni prav tako potrjujejo, da razvit numerični program daje rezultate z zadostno natančnostjo za razširitev njegove uporabe na druge bolj zahtevne geometrijske oblike.

Zahvala

Prvi avtor se želi zahvaliti za finančno podporo skladu Kerze-Cheyovich in Ministrstvu za šolstvo, znanost in šport Republike Slovenije.

The thermal effectiveness $\bar{Q}/\bar{W}$ of the examined heat sink is reduced with increasing Reynolds number Re_h. Although the lower Reynolds numbers Re_h bring higher effectiveness, the resulting low-heat-transfer rates have to be compensated with a larger heat-transfer surface and consequently with a larger heat sink. In some cases this is not possible due to economics and size limitations.

5 CONCLUSIONS

The present paper describes an effort to develop a fast-running numerical algorithm for heat-exchanger calculations. The purpose of the task was to numerically investigate heat removal from an electronic chip. The heat sink's internal structure, in the form of a staggered arrangement of pin-fins, was treated as a homogenous porous media. The local values of drag coefficient C_d and heat-transfer coefficient h, which were needed to close the transport equations, were taken from [7] to [9]. The resulting partial differential equations were discretized using conservation properties of the finite-volume method. The system of semi-linear equations was solved with the preconditioned conjugate gradient method. To test the calculation procedure, experimental data obtained in the Morrin-Martinelli-Gier Memorial Heat Transfer Laboratory were used for the comparison.

Two series of calculations were performed for the heat sink cooled with airflow. The calculated values of the whole-section drag coefficient $\bar{C}_d$ show a good agreement with already published data, whereas the calculated whole-section values of the Nusselt number $\overline{Nu}$ reveal some discrepancies due to differences in the thermal boundary conditions. Also, the influence of the finite thermal conductivity of the solid structure was examined. It was shown that the finite thermal conductivity of aluminum decreases the thermal effectiveness $\bar{Q}/\bar{W}$ by 35 percent at Re_h = 1904. Furthermore, it is expected that at a higher Reynolds number this thermal conductivity effect would increase.

The presented results demonstrate that this approach is appropriate for heat-sink calculations where the thermal conductivity of a solid structure has to be taken into account. The example calculations also verify that the developed numerical code yields sufficiently accurate results to be also applicable for other more demanding geometries.

Acknowledgements

The first author's financial support by the Kerze-Cheyovich scholarship and the Ministry of Education, Science and Sport of the Republic of Slovenia is gratefully acknowledged.

6 LITERATURA
6 REFERENCES

[1] Hesselgreaves, J.E. (2001) Compact heat exchangers selection, *Design and Operation, Pergamon Press*.
[2] Whitaker, S. (1967) Diffusion and dispersion in porous media, *AIChE Journal*, Vol. 13, No. 3, 420-427.
[3] Travkin, V.S., I. Catton (1995) A two temperature model for fluid flow and heat transfer in a porous layer, *J. Fluid Engineering*, Vol. 117, 181-188.
[4] Travkin, V.S., I. Catton (1999) Transport phenomena in heterogeneous media based on volume averaging theory, *Advans. Heat Trasfer*, Vol. 34, 1-143.
[5] Rizzi, M., Canino, M., Hu, K., Jones, S., Travkin, V., Catton, I. (2001) Experimental investigation of pin fin heat sink effectiveness, *Procs. of the 35th National Heat Transfer Conference*, Anaheim, California.
[6] Horvat, A., I. Catton (2001) Development of an integral computer code for simulation of heat exchangers, *Procs. of the Conf. "Nuclear Energy in Central Europe 2001",* Portorož, Slovenia, Sept. 10-13, No. 213.
[7] Launder, B.E., T.H. Massey (1978) The numerical prediction of viscous flow and heat transfer in tube bank. *Trans, ASME J. Heat Transfer*, Vol. 100, 565-571.
[8] Kays, W.M., A.L. London (1998) Compact heat exchangers, *3rd Ed. Krieger Publishing Company,* Malabar, Florida, 146-147.
[9] Žukauskas, A.A., R. Ulinskas (1985) Efficiency parameters for heat transfer in tube banks, *J. Heat Transfer Engineering*, Vol.5, No.1, 19-25.
[10] Versteeg, H.K., W. Malalasekera (1995) An introduction to computational fluid dynamics, The Finite Volume Method, *Longman Scientific & Technical: England*, 103-1335.
[11] Ferziger, J.H., M. Perić (1996) Computational method for fluid mechanics, Chapter 5: Solution of linear equation systems, *Springer Verlag: Berlin*, 85-127.

Naslova avtorjev:

dr. Andrej Horvat
Odsek za reaktorsko tehniko
Institut "Jožef Stefan"
Jamova 39
1111 Ljubljana

prof.dr. Ivan Catton
Morrin-Martinelli-Gier Memorial Heat Transfer Laboratory
Department of Mechanical and Aerospace Engineering
School of Engineering and Applied Science
University of California, Los Angeles
420 Westwood Plaza, Eng. IV, 90095
Los Angeles, California, USA

Author's Addresses:

Dr. Andrej Horvat
Reactor Engineering Division
Institute "Jožef Stefan"
Jamova 39
SI-1111 Ljubljana, Slovenia

Prof.Dr. Ivan Catton
Morrin-Martinelli-Gier Memorial Heat Transfer Laboratory
Department of Mechanical and Aerospace Engineering
School of Engineering and Applied Science
University of California, Los Angeles
420 Westwood Plaza, Eng. IV, 90095
Los Angeles, California, USA

Prejeto: 6.5.2002
Received:

Sprejeto: 22.11.2002
Accepted:

© Strojniški vestnik 48(2002)9,491-500
ISSN 0039-2480
UDK 621.311.21:621.224.1
Strokovni članek (1.04)

© Journal of Mechanical Engineering 48(2002)9,491-500
ISSN 0039-2480
UDC 621.311.21:621.224.1
Speciality paper (1.04)

Nekateri vidiki terenskih preskusov peltonovih turbin v HE "Perućica"

Some Aspects of the Research Carried out on the Power Generation Units at the Perućica Hydroelectric Power Plant

Milo Mrkić - Zoran Culafić

V delu so predstavljeni osnovni delovni parametri HE "Perućica", prikazana je analiza delovnega procesa v Peltonovi turbini in eksperimentalno-analitična metoda za določitev pretočne karakteristike šob vgrajenih v HE "Perućica" pri obratovalnih pogojih.

(Ključne besede: turbine Peltonove, parametri energetski, karakteristike procesov, metode eksperimentalne)

This paper describes the basic power parameters of the "Perućica" HEPP. Also included is an analysis of the work process in the Pelton turbine and an experimental-analytical method for determining the nozzle-flow characteristics under real working conditions.

(Keywords: Pelton turbines, power parameters, process characteristics, experimental methods)

0 UVOD

Hidroelektrarna "Perućica" ima moč 307 MW. Zgrajena je bila v treh fazah, prva faza se je začela leta 1960. Hidroelektrarna je derivacijskega tipa in ima skupaj sedem agregatov vodoravne izvedbe s Peltonovimi turbinami.

Prvi avtor prispevka je delo začel kot hidroinženir v tej elektrarni leta 1964, zaposlen z reševanjem obratovalnih problemov. V dolgem času delovanja elektrarne so bila opravljena raziskovanja mnogih pojavov v dejanskih razmerah, da bi zagotovili pogonske stabilnosti. Pri neposrednem učenju pogonskega osebja so bila v raziskovanja vključene domače strokovne institucije. Avtor je pri vseh raziskovanjih sodeloval neposredno ali kot svetovalec.

Glede na bogato znanje in izkušnje, pridobljene v času delovanja hidroelektrarne, je avtor v svojem delu podal vidike, pridobljene pri eksperimentalnih raziskovanjih v dejanskih razmerah in iz tega izhajajoče metode analitičnega določanja pretočnih karakteristik Peltonovih turbin, vgrajenih v obravnavani hidroelektrarni.

0 INTRODUCTION

The Perućica hydroelectric power plant (HEPP) has an installation power of 307 *MW*. It was built in three phases, and the first phase began operating in 1960. It was built as a derivative type, and it has seven power-generation units of the horizontal type with Pelton turbines.

One of the authors of this paper started work as a hydro engineer at this HEPP in 1964, when he was working on some problems concerning exploitation. During the long exploitation period of this HEPP a lot of research was conducted on many occurrences in stationary and non-stationary regimes under real conditions. In order to acquire operational staff, other qualified domestic and scientific institutions were engaged. In all this research the author participated directly or as a consultant.

Having gained much experience during the exploitation period of this HEPP, from the very beginning to the present day, the author presents some aspects of the completed experimental research under real conditions, and the method of analytically determining the flowing exploitation characteristic of the Pelton turbines mounted in this HEPP.

1 OSNOVNI ENERGETSKI PARAMETRI TURBIN V PRIMERU HE PERUĆICA

Za vsak hidroenergetski sistem so karakteristični osnovni delovni parametri bruto in čisti padec ter instalirani pretok. V že zgrajenih hidroelektrarnah obratujejo turbine pod določenimi energetskimi parametri, od katerih so nekateri lahko stalni, večina pa se jih spreminja glede na funkcijo delovnega režima. Med osnovne parametre vodnih turbin spadajo: moč (P), pretok (Q), specifična energija (Y), izkoristek (η) in število vrtljajev turbine (n).

Specifični energiji vodnega toka (Y_g, Y_d) na gladini vode zgornje akumulacije V̇ GNV (indeks g) in na gladini vode spodnje akumulacije V̇ DNV (indeks d) sta za splošni primer hidroenergetskega sistema izraženi z enačbama:

1 BASIC POWER PARAMETERS OF THE PELTON TURBINES ON THE PERUĆICA HEPP

The basic characteristic working parameters of any hydroelectric power plant are the gross and the net fall and the installed flow. On the hydroelectric power plants that are already built the turbines operate with certain power parameters, some of which can be permanent, whereas most of them change depending on the function of the working mode. The basic parameters of water turbines include the following: power (P), flow (Q), specific energy (Y), degree of efficiency (η) and the number of revolutions (n).

The specific energies of the water flow (Y_g, Y_d) on the surface of the upstream reservoir V̇ GNV (index g) and on the surface of the downstream reservoir V̇ DNV (index d) on the Perućica hydroelectric power plant with Pelton turbine are:

$$Y_g = \frac{p_g}{\rho} + g \cdot z_g + \frac{c_g^2}{2} \quad (1),$$

$$Y_d = \frac{p_d}{\rho} + g \cdot z_d + \frac{c_d^2}{2} \quad (2).$$

Razlika energij Y_g in Y_d pomeni bruto specifično energijo hidroelektrarne (Y_{br}).

The difference between the specific energies Y_g and Y_d represents the gross specific fall in the flow of the electrical power plant (Y_{br}).

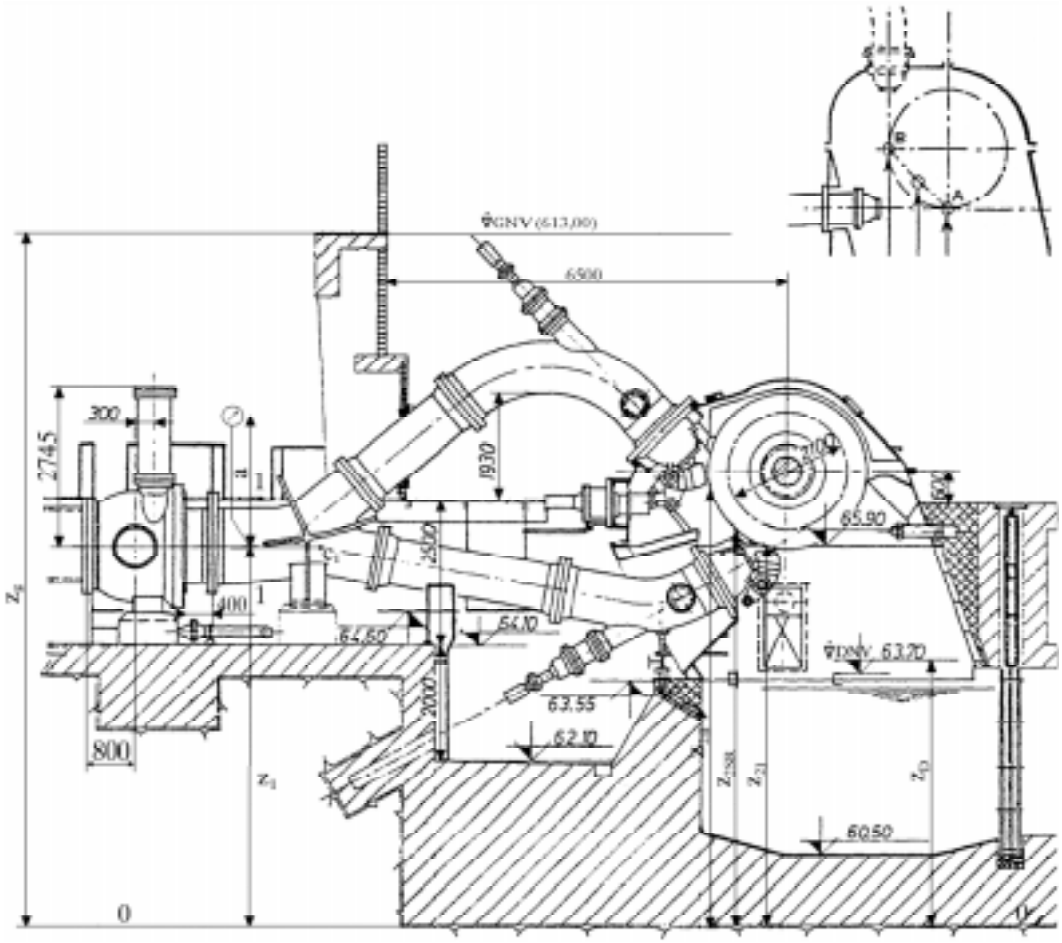

Sl. 1. *Razporeditev hidroagregata s Peltonovo turbino, vgrajenega v HE "Perućica"*
Fig. 1. *General arrangement of power generation unit with Pelton turbine in the Perućica HEPP*

V (1) in (2) so: p_g in p_d tlaka na nivojih *(g - g)* in *(d - d)*, c_g in c_d srednji hitrosti v prerezih, z_g in z_d koti zgornjega in spodnjega nivoja vode hidroelektrarne, g je zemeljski pospešek.

Za Peltonove (akcijske) turbine z eno šobo (agregati I do V v HE "Perućica") je razpoložljiva specifična energija:

$$Y = g \cdot H = \frac{p_m}{\rho} + \frac{c_1^2}{2} + g \cdot (z_1 + a - z_2) \quad (3),$$

kjer so: z_1 - kota vstopnega prereza turbine, a - oddaljenost kote težišča vstopnega prereza do kote vgradnje manometra, z_2 - kota točke, kjer os šobe tangira osnovni krog turbinskega kolesa, p_m - manometrični tlak, H - neto padec.

Hitrost c_2 na izstopnem prerezu turbine (izhodni rob Peltonove turbine) je zanemarljiva ($c_2 << c_1$).

V primeru, ko ima turbina dve šobi z enakim pretokom (agregati VI in VII v HE "Perućica"), se kota $z_{2\,sr}$ določa kot srednja vrednost kot točk A in B (sl. 1). Vse hitrosti, podane v prejšnjih enačbah, so srednje hitrosti, ki se določajo s pretokom Q in pretočnim prerezom A, tj. po enačbi $c_i = Q_i / A_i$.

Moč vodnega toka se določa z enačbo:

The designations in (1) and (2) are as follows: p_g and p_d - absolute pressure at levels (*g- g*) and (*d - d*), c_g and c_d - mean velocities in the cross-sections, z_g and z_d - elevations of upstream and downstream water surface, g - acceleration due to gravity.

For the Pelton (action) turbines with one nozzle (power generation units I–V) the available specific energy:

where: z_1 - the elevation of the turbine inlet cross section, a - the distance between the elevation of the centre of gravity of the inlet cross section and the elevation of the installation of the pressure gauge, z_2 - the elevation of the point where the nozzle axis touches the basic circle of the turbine wheel, p_m - the overpressure indicated by the pressure gauge, H - the net turbine fall.

The velocity c_2 at the turbine outlet cross section (outlet edge of the Pelton turbine) is low ($c_2 << c_1$).

In the event that the turbine has two nozzles with the same flow rate (units VI–VII) the elevation $z_{2\,mean}$ is determined as the mean value of the elevation of points A and B (Figure 1.). All velocities given in the preceding equation are the mean velocities determined by means of the flow (Q) and the flow cross section A, i.e. according to the equation $c_i = Q_i / A_i$.

The power of the water flow is determined with the following equation :

$$P_s = \rho \cdot g \cdot Q \cdot H \quad (4),$$

na gredi turbine pa z enačbo:

and the mechanical power of the turbine:

$$P_s = \rho \cdot g \cdot Q \cdot H \cdot \eta \quad (4'),$$

pri čemer je ρ gostota vode

where ρ is water density.

2 KARAKTERISTIKE DELOVNEGA POSTOPKA V PELTONOVI TURBINI

Slika 2 prikazuje karakteristike moči in izkoristka dvojne Peltonove turbine $2 \cdot P_2 \cdot 2{,}1 / 255$ (pri čemer so: 2 - število delovnih koles hidroagregata; P_2 - Peltonova turbina z dvema delovnima kolesoma; 2,1 – premer delovnega kolesa v m; 255 – premer vstopa v mm),

Karakteristike so dobljene pri preskusu garantiranih parametrov III faze HE "Perućica" pri padcu $H = 526$ m in pretoku $Q = 12{,}75$ m^3/s.

Gonilnik Peltonove turbine izkorišča samo kinetično energijo vodnega toka. Zaradi tega mora spremeniti pretočni aparat turbine (šob) ustrezno rezervo energije vodnega toka v kinetično energijo.

Razpoložljivi padec (višina) na izstopu iz šobe je:

2 CHARACTERISTICS OF THE WORK PROCESS IN A PELTON TURBINE

Figure 2 shows the characteristics of the power and the degree of efficiency of the double Pelton turbine $2 \cdot P_2 \cdot 2.1 / 255$ (where: 2 is the number of working wheels of the power generation unit, P_2 is the Pelton turbine with two nozzles, 2.1 is the diameter of working wheel [m], and 255 is the nozzle diameter [mm]).

The characteristics are obtained experimentally when testing the guaranteed parameters of the stage III of the Perućica HEPP at the fall $H = 526$ m and the flow $Q = 12.75$ m^3/s.

The runner of the Pelton turbine only uses the kinetic energy of the water flow. Therefore, the flow device of the turbine (nozzle) must convert the relevant reserve of the water flow energy into kinetic energy.

The kinetic energy at the nozzle outlet is:

$$\frac{c^2}{2 \cdot g} = H \cdot \eta_m \quad (5),$$

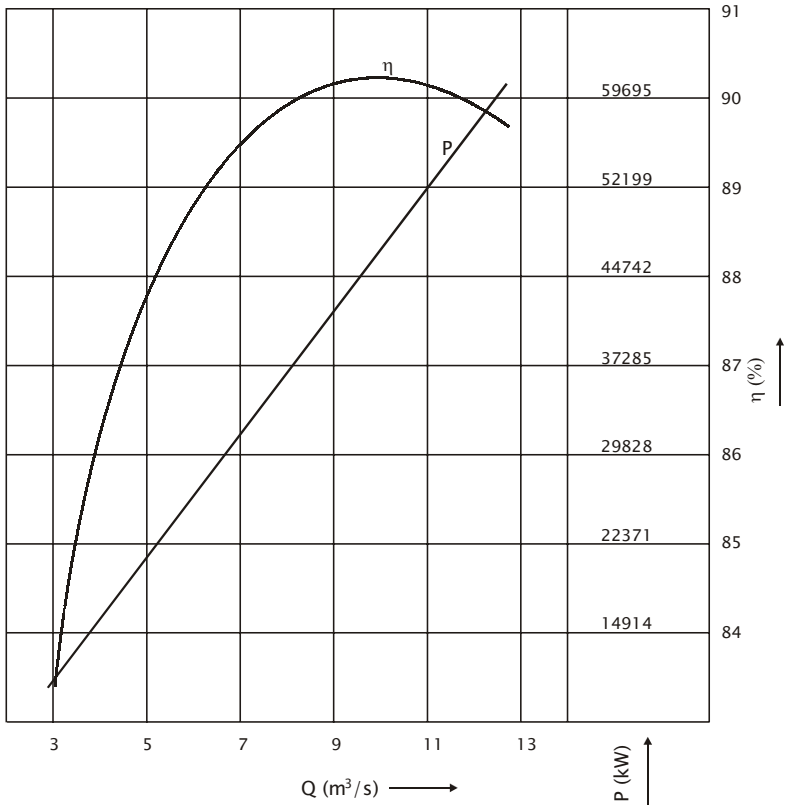

Sl. 2 *Diagram izkoristka in moči Peltonove turbine 2 · P_2 · 2,1/255 (padec H=526 m , pretok Q=12,75 m³/s)*
Fig. 2 *Diagram of degree of efficiency and power of the Pelton turbine 2 · P_2 · 2.1/255 in case of fall H = 526 m and Q = 12.75 m³/s*

pri čemer so: *H* - razpoložljiva višina pred šobo; *c* - pretočna hitrost; η_m - izkoristek šobe.

Torricellijeva enačba za hitrost iztekanja tekočine skozi odprtino pri nespremenljivi višini je:

where: *H* - the available height at the nozzle, *c* - the flow velocity, η_m - the degree of efficiency of the nozzle.

The well-known Torricellian formula for the velocity of a liquid flow from an opening at constant water level is:

$$c = \sqrt{2g \cdot H \cdot \eta_m} = \varphi\sqrt{2g \cdot H} \qquad (6),$$

pri čemer je: $\varphi = \sqrt{\eta_m}$ - koeficient hitrosti iztekanja.

Šoba Peltonove turbine ima krožno izhodno odprtino in osnosimetrični natok, kar zagotavlja

where: $\varphi = \sqrt{\eta_m}$ - the coefficient of the discharge velocity.

The nozzle of the Pelton turbine has a circular outlet opening and axially symmetrical in flow

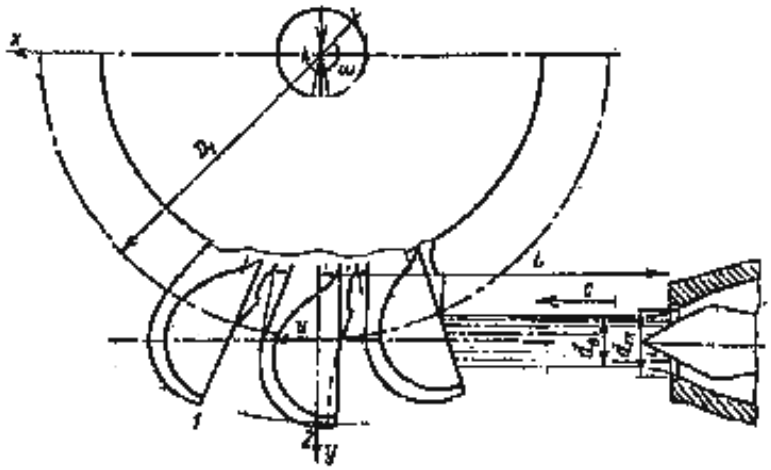

Sl. 3. *Lega delovnega kolesa in šobe Peltonove turbine*
Fig. 3 *Position of mounting of the runner and nozzle of the Pelton turbine*

stabilne, praktično valjne tokove na izhodu (slika 3).

Specifičnost delovnega postopka v Peltonovi turbini je v tem, da sprememba hitrosti vrtljajev gonilnika ne vpliva na pretočno moč turbine, tj. med momentom na osi turbine in parametri vodnega toka ni povratnega vpliva. Pretočna karakteristika šobe ni odvisna od obratovalnega režima, profila in izmer gonilnika. Odprtja šobe so v karakterističnem diagramu Q_{11} - n_{11} (Q_{11} je enotski pretok, n_{11} je enotska vrtilna frekvenca) predstavljena s premicami, ki so vzporedne z absciso (n_{11}). Zaradi tega pri Peltonovih turbinah odprtino pretočnega aparata, gib igle šobe (s) ne definiramo glede na premer delovnega kolesa. Relativni gib igle s' se izraža glede na premer izhodne odprtine šobe d_m po enačbi (sl. 3):

ensuring stable, practically cylindrical flow at the outlet (Figure 3).

It is a specific feature of the working process in the Pelton turbine that the change of rotating speed of the runner does not affect the flow rate of the turbine, i.e. there is no return influence between the turbine shaft torque and the water flow parameters. The flow characteristic of the nozzle does not depend on the mode of working, the runner contours and the dimensions. The nozzle openings in the characteristic diagram Q_{11} – n_{11} (Q_{11} is the unit pressure, n_{11} is the unit rotating speed) are given with straight lines parallel to the abscissa (n_{11}). Therefore, for these turbines it is not rational to express the flow device opening, nozzle needle motion (s), with regard to the working wheel diameter. The relative needle motion (s') is expressed with regard to the diameter of the nozzle outlet opening (d_m) (Figure 3), i.e.:

$$s' = s/d_m \tag{7}.$$

Pri Peltonovih turbinah izrazimo karakteristično površino A_{xm} in pretok šobe Q_{xm} z enačbami ($c_x = \sqrt{2 \cdot g \cdot H}$):

It is appropriate in the case of the Pelton turbine to express the characteristic surface and nozzle flow (A_{xm}; Q_{xm}) by means of equations ($c_x = \sqrt{2 \cdot g \cdot H}$):

$$A_{xm} = d_m^2 \cdot \pi/4 \quad \text{in / and} \quad Q_{xm} = c_x \cdot A_{xm} \tag{8},$$

pri čemer indeks "x" označuje poljuben delovni režim, D_1 – osnovni premer gonilnika.

Z uporabo karakterističnih veličin (8) definiramo brezdimenzijski pretočni koeficient šobe Peltonove turbine k_g:

where the index "x" designates the characteristic mode of working, D_1 is the basic diameter of the working wheel.

By means of these characteristic values (8) the unit flow of the nozzle of the Pelton turbine (k_g) is defined :

$$k_g = \frac{Q_m}{Q_{xm}} = \frac{4 Q_m}{\sqrt{2}\,\pi\, d_m^2 \sqrt{g\,H}} = 0{,}901 \frac{Q_m}{d_m^2 \sqrt{g\,H}} \tag{9}.$$

Glede na enačbo (6) lahko pretok šobe izrazimo takole:

On the basis of equation (6) it is possible to express the nozzle flow as follows:

$$Q_m = \frac{d_o^2\,\pi}{4} \varphi \sqrt{2 g H} \tag{10},$$

pri čemer je d_0 premer vodnega curka, d_m pa premer šobe (sl. 3).

where d_o is the diameter of the water jet, d_m is the diameter of the nozzle (Figure 3.).

Nadalje lahko enotni pretok šobe izrazimo tudi z enačbo:

Further, the unit nozzle flow can be expressed by the equation:

$$k_g = \varphi \left(d_o / d_m \right)^2 \tag{11}.$$

3 GEOMETRIJSKI PARAMETRI ŠOB, VGRAJENIH V HE "PERUĆICA"

V HE "Perućica" je vgrajenih 7 agregatov z dvojno Peltonovo turbino vodoravne izvedbe. Na petih agregatih so turbinska kolesa izvedena z eno šobo tipa $2 \cdot P_1 \cdot 2{,}4 / 300$, na dveh agregatih pa kolesa z dvema šobama tipa $2 \cdot P_2 \cdot 2{,}1 / 255$.

Na sliki 4 je prikazan profil izstopnega dela šobe na agregatih HE "Perućica". Osnovni geometrijski parametri šobe so: d_m - premer izhodne odprtine (d_m = 300 mm), $A_m = d_m^2 \cdot \pi / 4$ - površina

3 GEOMETRIC PARAMETERS OF NOZZLES INSTALLED ON THE PERUĆICA HEPP

On the Perućica HEPP seven power-generation units with double Pelton turbines in the horizontal position are installed. On five units the turbine wheels are equipped with one nozzle of type $2 \cdot P_1 \cdot 2.4/300$, and on two units the wheels are equipped with two nozzles of type $2 \cdot P_2 \cdot 2.1/255$.

Figure 4 shows the contour of the outlet part of the nozzle on the Perućica HEPP. The basic geometrical parameters of the nozzle are: d_m is the diameter of outlet opening (d_m = 300 mm), $A_m = d_m^2 \cdot \pi / 4$ is the surface of

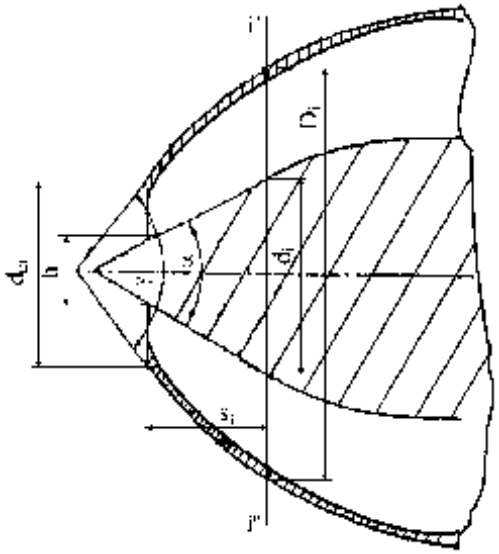

Sl. 4 *Profil izstopnega dela šobe, vgrajene v HE "Perućica" v poljubni legi "i-i"*
Fig.4. *Contour of outlet part of the nozzle installed on the Perućica HEPP in arbitrary position "i-i"*

izhodnega pretočnega prereza (A_m = 70650 mm^2), s - gib igle šobe, s_{maks} - največji gib šobe (s_{maks} = 195 *mm*), α - kot igle šobe (α=57,2^o), h - višina odprtine šobe, h_{imax} - največja višina odprtine šobe, (h_{imax} = 90 mm), D_i - premer okrova na "i - i", d_i - premer igle v prerezu (i - i), γ - izstopni kot šobe.

4 DOLOČITEV PRETOČNE KARAKTERISTIKE ŠOBE NA IZVEDBI

Pretok šobe se lahko glede na enačbi (10) in (11) izrazi kot:

$$Q_m = k_g \, A_m \sqrt{2g\,H} \qquad (12).$$

Razpoložljiva višina šobe (H) je definirana z enačbo:

$$H = H_b - \Delta H_1 - \Delta H_2 \qquad (13),$$

pri čemer sta: H_b - bruto višina HE "Perućica" ($H_b \cong$ 550 m), ΔH_1 - hidravlične izgube v dovodnem sistemu od vtočne zgradbe do izhoda iz razvejanja (sl. 1).

Izgube v dovodnem sistemu HE "Perućica" (ΔH_1) so izmerjene po delih na vstopni rešetki, v predoru, na razvejanju v izravnalniku in v dovodnih cevovodih (slika 5).

Rezultati meritev izgub po posameznih cevovodih (leta 1998) so:
- cevovod 1 (agregati 1, 2; dolžina L = 1851 m; premer D = 2,2 m - 1,8 m): $\Delta H_{c1} \cong 0{,}0563 \cdot Q^2_{c1}$,
- cevovod 2 (agregati 3, 4, 5; dolžina L = 1883 m; premer D = 2,2 m - 2,1 m): $\Delta H_{c2} \cong 0{,}0407 \cdot Q^2_{c2}$,
- cevovod 3 (agregati 6, 7; dolžina L = 1931 m; premer D = 2,5 m - 2,2 m): $\Delta H_{c3} \cong 0{,}02297 \cdot Q^2_{c3}$.

4 DETERMINATION OF NOZZLE FLOW CHARACTERISTICS UNDER REAL CONDITIONS

With respect to equations (10) and (11) the nozzle flow can be expressed as:

The available height of the nozzle (H_m) is defined by the equation:

where: H_b is the gross water level of the Perućica HEPP ($H_b \cong$ 550 m), ΔH_1 is the hydraulic loss in the supplying system from the intake structure to the bifurcation outlet (Figure 1).

The losses in the supply system of the Perućica HEPP (ΔH_1) are measured according to the sections in entering the trash rack, in the tunnel, in the surge tank and in the supply pipelines. (Figure 5).

The measured results of the losses according to the branches of the pipeline (in 1998) are:
- pipeline 1 (units 1, 2; length L = 1851 m; diameter D = 2.2 m - 1.8 m): $\Delta H_{c1} \cong 0.0563 \cdot Q^2_{c1}$,
- pipeline 2 (units 3, 4, 5; length L = 1883 m; diameter D = 2.2 m - 2.1 m): $\Delta H_{c2} \cong 0.0407 \cdot Q^2_{c2}$,
- pipeline 3 (units 6, 7; length L = 1931 m; diameter D = 2.5 m - 2.2 m): $\Delta H_{c3} \cong .0.02297 \cdot Q^2_{c3}$.

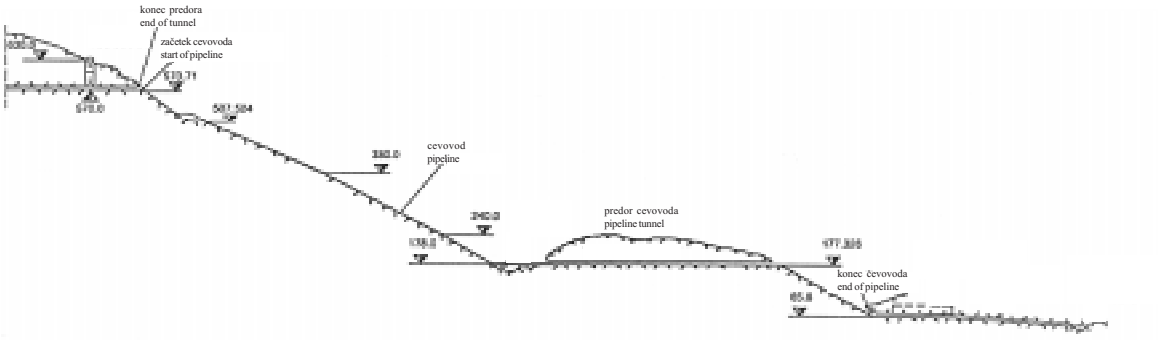

Sl. 5 *Pretočni sistem HE "Perućica"*
Fig. 5 *Flow system of Peručica HEPP*

Srednja vrednost koeficienta izgub je:
a) rešetka: $k_r = 0{,}749.10^{-3}$
b) predor: $k_t = 1{,}261.10^{-3}$
c) izravnalnik: $k_{1=} 6{,}50.10^{-3}$
$k_2 = 4{,}66.10^{-3}$
$k_3 = 5{,}31.10^{-3}$

Pretok šobe oziroma koeficient pretoka sta odvisna od giba igle šobe *s*:

The average value of the loss coefficient is :
a) in trashrack: $k_r = 0.749.10^{-3}$
b) in tunnel: $k_t = 1.261.10^{-3}$
c) in surge tank: $k_{1=} 6.50.10^{-3}$
$k_2 = 4.66.10^{-3}$
$k_3 = 5.31.10^{-3}$

The nozzle flow and/or the flow coefficient depend on the nozzle needle motion (*s*), therefore:

$$k_{g(s)} = \frac{Q_{m(s)}}{A_m \sqrt{2g \cdot H}} \qquad (14).$$

V primeru hidroelektrarne "Perućica" lahko predpostavimo nespremenljivo vrednost višine H pri vseh delovnih režimih elektrarne (glede na veliko bruto višino ($H_b \approx 550$ m) in s tem tudi relativno zanemarljiv vpliv izgub višine v dovodnem sistemu pri spremembah pretokov v delovnem področju turbine).

Z merjenjem pretoka $Q_{m(s)}$ za znane vrednosti A_m in H_m lahko s preskusi določimo odvisnost koeficienta pretoka $k_{q(s)}$ od relativnega giba igle šobe *s'* (enačba 7).

V obsegu raziskav nestalnih režimov obratovanja v sistemu HE "Perućica", je bila določena karakteristika šobe $k_q = f(s/d_m)$ agregatov I-V. Karakteristika je grafično prikazana na sliki 6. Delovno področje agregatov VI - VII je:

In the case of the Perućica HEPP the constant value of height H for all working modes of the power plant (with respect to the great gross water level ($H_b \approx 550$ m) and, consequently, a relatively unimportant influence of height losses in the adduction system in the case of changes to the flow in the turbine working area is assumed.

Thus, by measuring the flow $Q_{m(s)}$ for the known values A_m and H_m the dependence of the flow coefficient $k_{q(s)}$ on the flow $Q_{(s)}$ and/or on the relative nozzle needle motion (equation 7) is experimentally determined.

Within the scope of research on the unstable working modes of the Perućica HEPP the nozzle characteristic $k_q = f(s/d_m)$ of units I–V graphically shown in Figure 6 was determined. The working range for the Peručica III power generation units is :

$H_{max} = 526$ m; $H_{min} = 520$ m; $n = 428{,}5$ min^{-1};
$Q_{11} = 63{,}0$ l/s; $n_{11} = 39{,}2$ min^{-1}; $P = 59$ MW;
($D_1 = 2100$ mm, $d_0 = 225$ mm, $\varphi = 0{,}614$)

Parametri agregatov I - V so:

The parameters of the units I–V are :

$n = 375$ min^{-1}, $P = 39$ MW, $Q = 8{,}5$ m^3/s, $D_1 = 2400$ mm, $d_0 = 300$ mm

Ker se pretok Q_m na izhodu iz šobe s spremembo giba igle *s* spreminja zaradi spremembe površine dejanskega pretočnega prereza, skozi katerega prehaja voda in spremembe polja hitrosti vode v šobi, lahko enačbo za pretok napišemo v obliki:

As the flow Q_m at the nozzle outlet changes with the needle motions due to the change of surface of the effective flow cross section through which the water passes and the change of the water speed in the nozzle, the equation for the flow can be written in the following form:

$$Q(s/d_m) = c(s/d_m)\, A(s/d_m) \qquad (15).$$

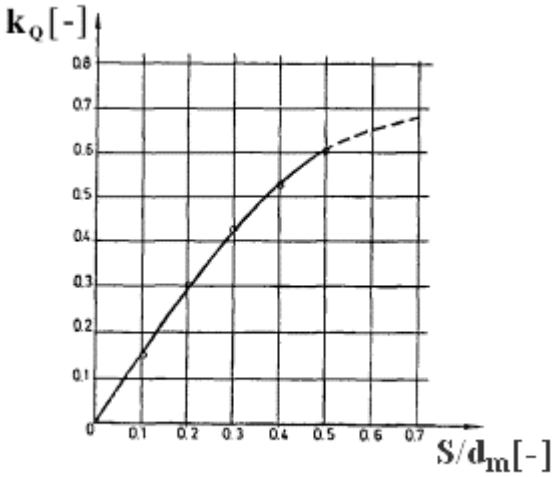

Sl. 6. *Karakteristika šobe $k_Q = f(s/d_m)$ agregatov I-IV*
Fig. 6. *Nozzle characteristic $k_Q = f(s/d_m)$ of units I-IV*

Glede na (12) velja:

Taking into account (12), the following applies:

$$k_Q A_m \sqrt{2gH} = c A(s/d_m) \quad (16).$$

5 SKLEP

Prvo vprašanje, na katerega mora odgovoriti projektant Peltonove turbine, je izbira njenih osnovnih parametrov; konstrukcijske skice same turbine, hitrosti vrtenja, število šob, premer delovnega kolesa, premer šobe itn. Pri tem se razume, da so meje sprememb vodnega padca in mejna moč po navadi podane s projektno nalogo.

Rešitev te naloge ni enolična. Praktično je treba analizirati več možnih variant. Za končno rešitev se odločimo po vsestranski tehnično-gospodarni analizi.

Svetovne izkušnje potrjujejo, da so v 60. letih v gradili Peltonove turbine z vodoravno gredjo z eno ali največ dvema šobama na en gonilnik. Po tem obdobju pa so prišli iz vodoravne v navpično izvedbo. Namen projektantov je bil, da se poveča število šob na gonilnik. Tako so sodobne velike Peltonove turbine najpogosteje izvedene z navpično gredjo in šestimi šobami na en gonilnik.

Peltonove turbine v HE "Perućica" imajo vodoravno gred z dvema gonilnikoma na enoto (I do V) oziroma dvema šobama na enoto (VI in VII) za en gonilnik.

Rezultat raziskav nestalnih režimov obratovanja je pretočna karakteristika šobe $2 \cdot P_1 \cdot 2.4 / 300$ Peltonove turbine $2 \cdot P_1 \cdot 2.4 / 300$ (enote I do V) (slika 6).

5 CONCLUSION

The first question that should be answered by the design engineer of the Pelton turbine is the selection of its basic parameters: the design sketch of the turbine alone, the number of revolutions, the nozzle number, the diameter of the runner, the diameter of the nozzle, etc. It goes without saying that the limits of the changing fall and the limited power are usually set in the design assignment.

The solution of this assignment is not uniform. It is necessary to analyze practically several possible variants. The final solution to the problem is adopted after the comprehensive tech-eco analysis.

General practice around the world showed that in the 1960s Pelton horizontally mounted turbines with one or a maximum of two nozzles for one runner were built. After that period they moved from horizontal to vertical mounting. That is, in the first place, the result of the designer's desire to increase the nozzle number for the runner. The modern Pelton turbines are usually built with a vertical shaft and with six nozzles in one working circle.

Pelton turbines' HEPPs have a horizontal shaft with two runners and with one (I–V) or two nozzles for one runner (VI and VII).

A result of the research into unstable operating modes is the nozzle flow characteristic $k_g = f(s/d_m)$ of the Pelton turbine $2 \cdot P_1 \cdot 2.4 / 300$ (units I–V) (Fig. 6) .

6 OZNAKE
6 SYMBOLS

oddaljenost kote težišča vstopnega prereza do kote vgradnje manometra	a	distance between the elevation of the centre of gravity of the inlet cross section and the elevation of the pressure gauge fastening
površina izhodnega pretočnega prereza	A_m	surface of outlet flow cross section
pretočna hitrost	c	flow velocity
srednja hitrost v prerezu (g - g)	c_g	average velocity in cross section (g – g)
srednja hitrost v prerezu (d - d)	c_d	average velocity in cross section (d – d)
osnovni premer gonilnika	D_1	basic diameters of runner
premer okrova na "i - i"	D_i	diameters of housing on "i - i"
premer igle v prerezu (i - i)	d_i	diameter of needle in cross section (i – i)
premer vodnega curka	d_o	diameter of water jet
premer izhodne odprtine šobe	d_m	diameter of nozzle outlet opening
čisti padec	H	net fall
bruto padec hidroelektrarne	H_{br}	gross fall of HEPP
višina odprtine šobe	h	height of nozzle opening
največja višina odprtine šobe	h_{imax}	maximum height of nozzle opening
koeficient izgub	k	loss coefficient
brezdimenzijski pretočni koeficient šobe Peltonove turbine	k_q	non–dimensional flow coefficient of Pelton turbine nozzle
število vrtljajev turbine	n	number of turbine revolutions
moč	P	power
tlak na ravni (g - g)	p_g	pressure at level (g – g)
tlak na ravni (d - d)	p_d	pressure at level (d – d)
manometrični tlak	p_m	gauge pressure
pretok	Q	flow
pretok šobe	Q_m	nozzle flow
gib igle šobe	s	nozzle needle movement
relativni gib igle	s'	relative needle movement
največji gib šobe	s_{max}	maximum nozzle movement
specifična energija	Y	specific energy
specifična energija vodnega toka na gladini vode zgornje akumulacije	Y_g	specific energy of water flow on water surface of upstream reservoir
specifična energija vodnega toka na gladini vode spodnje akumulacije	Y_d	specific energy of water flow on water surface of downstream reservoir
bruto specifična energija hidroelektrarne	Y_{br}	gross specific energy of HEPP
kota vstopnega prereza turbine	z_1	elevation of turbine inlet cross section
kota točke, kjer os šobe dotika osnovni krog turbinskega kolesa	z_2	elevation of point where the nozzle are s touches the basic circle of the turbine wheel
kot igle šobe	α	nozzle needle angle
koeficient hitrosti iztekanja	φ	coefficient of discharge velocity
gostota vode	ρ	water density
izstopni kot šobe	γ	nozzle outlet angle
izkoristek	η	efficiency
izkoristek šobe	η_m	nozzle efficiency
hidravlične izgube v dovodnem sistemu	ΔH_1	hydraulic losses in supplying system

7 LITERATURA
7 REFERENCE

[1] Ispitivanje energetskih karakteristika i prelaznih pojava na agregatima HE "Perućica" – Institut "Jaroslav Černi" (Beograd 1984, 1987, 1998).

Naslov avtorjev: prof.dr. Milo Mrkić
prof.dr. Zoran Culafić
Univerzitet Crne Gore
Mašinski fakultet Podgorica
Cetinjski put bb
81000 Podgorica, ZRJ
milom@cg.ac.yu

Authors' Address: Prof. Dr. Milo Mrkić
Prof.Dr. Zoran Culafić
University of Montenegro
Faculty of Mech. Eng. Podgorica
Cetinjski put bb
81000 Podgorica, ZRJ
milom@cg.ac.yu

Prejeto:
Received: 21.2.2001

Sprejeto:
Accepted: 22.11.2002

© Strojniški vestnik 48(2002)9,501-515
ISSN 0039-2480
UDK 621.791.92:621.795:621.9.02
Strokovni članek (1.04)

© Journal of Mechanical Engineering 48(2002)9,501-515
ISSN 0039-2480
UDC 621.791.92:621.795:621.9.02
Speciality paper (1.04)

Struženje navarov z orodji podjetja Walter

The Turning of Overlays Using Tools Produced by the Company Walter

Milan Brožek

Tehnologija navarjanja se v praksi uporablja za oblikovanje površinskih plasti s specifičnimi lastnostmi v primeru na novo narejenih sestavnih delov oziroma pri popravilih obrabljenih funkcijskih ploskev sestavnih delov. Pri veliki večini sestavnih delov je glede na želeno obliko, izmero in površino navarjenega predmeta te treba tudi obdelati. Takšna obdelava ima v primerjavi z obdelovanjem vlečenih ali valjanih polizdelkov nekatere posebnosti. Zaradi optimizacije rezalnih razmer se po navadi izhaja iz rezultatov dolgoročnih preskusov obstojnosti orodja. Pri njih se eksperimentalno ugotavlja časovna odvisnost obrabljenosti orodja pri različnih stopnjah rezalne hitrosti za vsako kombinacijo materialov navarjenega predmeta in orodja. Iz te odvisnosti se za mejno velikost obrabljenosti orodja določi odvisnost obstojnosti orodja za rezalno hitrost. Tako ugotovljene odvisnosti T - v_c so izhodiščne vrednosti za lastno optimizacijo rezalnih razmer. Ta pa se najpogosteje izvaja po kriteriju najmanjših proizvodnih stroškov. Optimalen izračun obsega vse osnovne gospodarske kazalnike obrata. Sestavni del izvedenih preskusov je merjenje trdote navara HRC (po Rockwellu) in hrapavosti R_a in R_t obdelane površine. V prispevku so podrobno objavljeni rezultati obstojnostnih preskusov orodja, narejenih pri obdelavi navara žice C 508 ob uporabi orodja podjetja Walter. V preskuse je bilo uvrščenih šest tipov materiala orodja v obliki izmenljivih ploščic, od katerih se lahko trije priporočijo kot primerni za obdelavo takšnega tipa navarjenega predmeta. Najboljši rezultati so bili doseženi z uporabo orodja WNMG 080412 WTA 13 (HC K 10). Pri preskusih je bilo ugotovljeno, da se hrapavost obdelane površine v poteku obdelave postopoma počasi povečuje, pri čemer na koncu obratovalne dobe orodja prihaja do očitnega poslabšanja.

(Ključne besede: struženje navarov, hrapavost površin, pogoji rezanja, ploščice ostrilne)

Surfacing technology is used to produce layers with special properties for new parts or worn out functional surfaces. For many parts it is necessary to machine them to fulfill the requirements for shape, size and roughness. But the machining of overlays is, in comparison with the machining of drawn or rolled semi-products, specialized. Usually, the optimization of the cutting conditions comes from long-term tool-life test results. For these tests we have experimentally determined time dependences of tool wear at different cutting speeds for every combination of overlay and cutting materials. These dependences are the basis for the determination of the relationship between tool-life and cutting speed for the limit of tool wear. The relationships between cutting speed and tool-life determined in this way are the initial values for one's own optimization of the cutting conditions. It is usual for the optimum to be determined for the minimum machining costs criterion. In the calculation all the economic indexes of the workshop are included. Measuring of the overlay hardness, HRC, and the overlay surface roughness, R_a and R_t, after machining was also part of the tests. In this article we publish the results of long-term tool-life tests, made during the turning of an overlay made by welding wire C 508 using a tool from the firm Walter. In the tests we used six types of tool material in the form of inserts. Three of them can be recommend for the turning of this overlay. The best results were achieved using the WNMG 080412 WTA 13 (HC K 10) insert. During the tests we found that the roughness of the turned surface slowly increases and that extensive deterioration occurs at the end of the tool-life.

(Keywords: overlays turning, surface roughness, cutting conditions, inserts)

0 UVOD

Navarjanje je z vidika razdelitve tehnologije gradnje strojev uvrščeno v varjenje. Izhaja iz njegovih teoretičnih osnov, pri čemer so nekateri znaki skladni,

0 INTRODUCTION

In terms of engineering technology, surfacing is classed together with welding. This is based on theoretical considerations: some aspects are the same,

drugi spet bolj ali manj drugačni. S postopnim razvojem se je iz navarjanja razvila samostojna stroka, ki se še posebej v zadnjih letih hitro razvija.

Tehnologija navarjanja se v praksi uporablja tako v proizvodnji novih sestavnih delov, za oblikovanje površinskih plasti s specifičnimi lastnostmi, kakor pri popravilih obrabljenih funkcijskih ploskev sestavnih delov. V obeh primerih lahko uporaba primernega navara prinese očitne snovne in energijske prihranke, zmanjšanje težavnosti dela in v veliko primerih tudi podaljšanje dobe trajanja navarjenega sestavnega dela.

Razvoj obeh zgoraj navedenih področij se lahko utemeljuje s številnimi prispevki, ki so bili objavljeni v strokovni literaturi, znanstvenih revijah, na konferencah ipd. Tehnologija navarjanja se uporablja v različnih panogah gospodarstva, npr. v metalurgiji, jedrski energetiki, medicini, prometu, rokovanju z materialom, petrokemiji, pa tudi pri popravilih stiskalnic za opeko, starih kulturnih spomenikov in v drugih panogah. Očitno razširitev je navarjanje doseglo v kmetijstvu, kjer se uporablja v obeh zgoraj navednih smereh, in to tako pri proizvodnji novih sestavnih delov (npr. navari, odporni proti obrabi na funkcijskih ploskvah plužnih rezil) kakor pri popravilih sestavnih delov, ki so obrabljeni zaradi delovanja (npr. navari vreten, zatičev ipd.) ([1], [5], [6] in [9]).

Velik pomen pripisujejo tehnologiji navarjanja tudi proizvajalci dodajanih materialov. Praktično vsa podjetja ponujajo v svoji zalogi navadno tudi posebne navarjene materiale ([1] in [10]).

V nekaterih primerih je mogoče sestavni del z navarjeno površino uporabiti brez dodatnih posegov, drugje je treba navar izravnati, nekje pa je zopet nujno potrebno navarjeno površino iverasto obdelati. Razlogi za mehansko obdelavo navara so predvsem zahteve po obliki in izmerah sestavnih delov, morebitno hrapavost površine izdelka.

Navari pa imajo v primerjavi z vlečenimi ali valjanimi polizdelki nekatere različne lastnosti, ki izhajajo iz značaja tehnologije navarjanja, predvsem:

- površina navara je neravna – zaradi tega nastopa prekinjevano rezanje, kar povča obremenitev rezalnega robu,
- kemična sestava navarjenega materiala se pod vplivom segrevanja in mešanja navarjenega ter osnovnega materiala pri navarjanju razlikuje od kemične sestave navarjene plasti,
- lastnosti navara so občutljive na razmere pri hlajenju po navarjanju – to povzroča spremembe mehanskih lastnosti in njihovo večjo razpršitev.

Do sedaj še niso bili objavljeni povzeti normativi o obdelavi navarov in pri iskanju rezalnih pogojev moramo izhajati iz posamezno objavljenih informacij ali pa iz rezultatov lastnih preskusov. V nekaterih objavljenih prispevkih pa žal niso navedeni potrebni podatki. Avtorji so se na primer omejili samo na ugotovitev, da "je bil navar obdelan", vendar niso

some are more or less different. Today, the surfacing has become a separate field of engineering that has developed very rapidly in recent years.

Surfacing technology is used in practice for both the production of new parts with laxers that have specific properties, and for the renovation of worn out surfaces. In both cases the use of a suitable overlay may result in savings in terms of material, power and work, and in many cases in an increase of the overlay's service life.

The development of both the above-mentioned fields is evidenced by the number of contributions in special literature, scientific journals, and at conferences, etc. Surfacing technology is used in many different fields, e.g. metallurgy, nuclear-power supply, medicine, traffic, materials handling, petrochemistry, renovation of brick moulding presses, old cultural monuments and other fields. Surfacing is also often employed in agriculture, where surfacing is used for the production of new part, e.g. wear-resistant overlays on the functional surfaces of plough shares, and for the renovation of worn out in-service parts, e.g. overlays on shafts, pins, etc. ([1], [5], [6] and [9]).

Manufacturers of filler materials are also involved in surfacing technology. In practice, all such firms offer coventional and special filler materials in their range ([1] and [10]).

In some cases it is possible to use the part with an overlay without any additional finish, but sometimes it is necessary to machine the welded-on surface. The reasons for the additional machining of the overlay are based on the requirements for the shape and size of the part, and on the surface roughness.

The overlays have, in comparison with drawn or rolled semi-products, some different properties, which follow from the principle of surfacing technology. These are as follows:

- major uneveness of the overlay surface – the cutting changes in the zone of the interrupted cut, which taxes the tool heavily,
- the chemical composition of the overlay is different from the chemical composition of the wire for welding owing to loss by burning and by mixing of the basic and the wire materials,
- the overlay properties are sensitive to the cooling conditions after surfacing – it affects changes to the mechanical properties and so introduces significant scatter in their range of values.

So far there have been no complete standards published, and so when deciding on cutting conditions it is necessary to start with partial published information or with the results of one's own tests. But in some published information the necessary data is not included. The authors only state that "the overlay was machined", and do not

navedli morebitnih pogojev za to obdelavo. Zato je uporaba teh rezultatov v praksi problematična [1].

Na naši katedri se s problematiko obdelave različnih tipov navarov z različnimi rezalnimi materiali ukvarajmo že vrsto let. V tem obdobju smo preskusili orodja iz karbidnih trdnin, kubičnega borovega nitrida in rezalne keramike ([1] do [4]). Namen izvedenih preskusov je, da na osnovi dolgotrajnih preskusov obstojnosti orodja pridobimo temelje za določitev optimalnih rezalnih parametrov za struženje navarjenih plasti. V naslednjem prispevku so povzeti rezultati preskusov, narejenih z orodji podjetja Walter.

1 TEORIJA

1.1 Preskusi obstojnosti

Eden od temeljev, potrebnih za izvedbo optimizacije rezalnih razmer je poznavanje odvisnosti med obstojnostjo in rezalnimi parametri: $T = f(v_c)$ oziroma $T = f(v_c, f, a_p)$. Ta spada med najpomembnejše odvisnosti teorije rezanja. Iz teh matematičnih razmerij izhajamo tako pri izbiri optimalnih rezalnih parametrov z vidika varčnosti postopka obdelave kakor tudi pri ugotavljanju rezalnih sposobnosti materiala orodja in obdelovalnosti obdelovanega materiala ipd. [8].

Odvisnost obstojnosti od rezalne hitrosti ugotavljamo eksperimentalno, s t.i. obrabnimi preskusi. V bistvu razlikujemo dva osnovna tipa teh preskusov – dolgotrajne in kratkotrajne.

Postopek pri dolgotrajnih preskusih je naslednji [7]:

– določimo časovni potek obrabe (sl. 1), npr. $VC = f(t)$, za različne rezalne hitrosti v_{c1}, v_{c2}, v_{c3}, ... (drugi parametri so nespremenljivi),
– določimo dopustno obrabo, npr. VC_{adm} in iz značilnih krivulj obrabe odberemo vrednosti obstojnosti za posamezne rezalne hitrosti in

publish the machining conditions. Making use of such results is problematic [1].

In our department we have engaged in the problems of machining various overlay types using various cutting materials for a number of years. During this time we have tested tools with cemented carbides, cubic boron nitride and ceramics ([1] to [4]). The aim of the long-term tool-life tests was to determine the basis for finding the optimum cutting conditions for the turning of overlays. In this paper we present the results of tests made using Walter tools.

1 THEORY

1.1 Tool-life tests

Knowledge of the relationship between tool-life and cutting conditions $T = f(v_c)$, resp. $T = f(v_c, f, a_p)$ is one of the basic elements needed for optimizing the cutting conditions. This relationship is one of the most important relationships in cutting theory. These equations are the basis both for the selection of the optimum cutting conditions, from the point of view of cutting economy, and for the determination of the cutting property of the tool material and the machinability of the machined material, etc. [8].

The relationship tool-life to cutting speed is determined experimentally by so-called durability tests. In principle, we distinguish two basic classes of these tests: long-term and short-term tests.

The procedure for the long-term tests is as follows [7]:

– we determine the time course wear (Fig. 1), e.g. $VC = f(t)$ for different cutting speeds v_{c1}, v_{c2}, v_{c3}, ... (the other parameters are constant),
– we determine the terminal flank wear, e.g. VC_{adm}, and from the characteristic wear curves we read the tool-life values relevent to single cutting

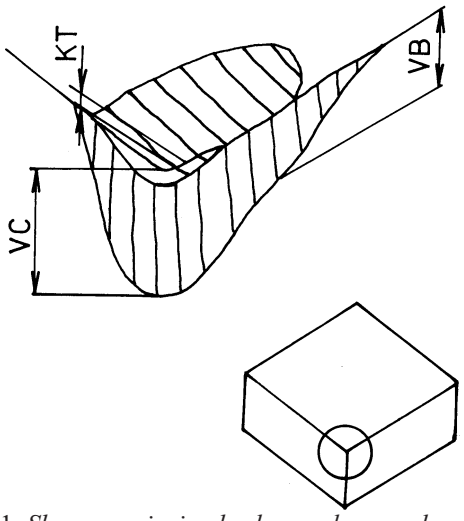

Sl. 1. *Shema merjenja obrabe rezalnega robu orodja*
Fig. 1. *Measuring diagram of tool edge wear*

meritve,
– vrednosti obstojnosti, ki ustrezajo posameznim rezalnim hitrostim, prenesemo v logaritemske koordinate T - v_c (primer na sl. 7).

Zaradi večje natančnosti ugotovljenih odvisnosti je treba ves postopek izpeljati večkrat, da bo vsaj delno izločen vpliv nepričakovanih naključnih pojavov, ki povzročijo razpršitev vrednosti obstojnosti. Rezultati, pridobljeni z dolgotrajnimi preskusi, so razmeroma natančni, vendar zelo dragi zaradi porabe časa in materiala.

1.2 Optimizacija rezalnih parametrov

Optimizacija rezalnih parametrov predstavlja enega od najpomembnejših členov vse optimizacije proizvodnega procesa (optimizacija tehnoloških postopkov, orodij, strojev, strege ipd.). Optimalni rezalni parametri so tesno povezani z gospodarskimi, količinskimi oziroma kakovostnimi vidiki proizvodnje in vplivajo tako na ceno posameznih sestavnih delov kakor tudi na ves izdelek.

Optimizacijo rezalnih parametrov razumemo kot določitev optimalnih rezalnih razmer s poudarkom na tehničnih in organizacijskih omejitvah in kriterijih optimalnega poteka oziroma rezultata rezalnega postopka.

Obdelovalni postopek lahko presojamo z različnimi merili optimalnosti glede na zahtevo njegovega poteka oziroma rezultata.

Za izračun se lahko uporabijo tile kriteriji:
– kriterij najmanjših proizvodnih stroškov,
– kriterij najmanjše produktivnosti,
– kriterij največjega dobička.

Kot najpomemebnejši od vseh kriterijev se šteje kriterij najmanjših proizvodnih stroškov [8].

Grafično je kriterij najmanjših proizvodnih stroškov ponazorjen na sliki 2. Člen K_1/n, ki pada z rezalno hitrostjo, izraža stroške za delovanje stroja, člen $K_2/n \cdot T$, ki se povečuje z rezalno hitrostjo, izraža stroške za uporabo orodja. Člen K izraža stroške, ki so neodvisni od rezalne hitrosti (npr. vpenjanje in izpenjanje obdelovanca, merjenje ipd.), katerih velikost pa ne vpliva na izračun [1].

S slike 2 je očitno, da ima kakršenkoli odmik od optimalne rezalne hitrosti k manjšim ali večjim vrednostim za posledico povečanje stroškov za obdelavo želene dolžine navara. Iz oblike krivulje skupnih stroškov lahko presodimo velikost rasti stroškov ob neupoštevanju optimalne rezalne hitrosti. Najpogostejši nujni razlog odmika je uporaba obdelovalnega stroja s stopenjsko spremembo vrtljajev, na katerem ni mogoče natančno nastaviti vrtljajev, ki bi ustrezali izračunani optimalni rezalni hitrosti. Zato, če je to le mogoče, uporabljamo obdelovalne stroje z večjim številom stopenj vrtljajev ali moderne obdelovalne stroje z brezstopenjskim spreminjanjem vrtljajev.

speeds and measurements,
– we plot the tool-life values of single cutting speeds using logarithmic coordinates T - v_c (cf Fig. 7).

For an increase in accuracy it is necessary to repeat the whole process in order to eliminate at least some of the influence of unforeseeable random events that induce scattering when determining tool-life values. The results acquired by long-term tests are relatively accurate, but in terms of time and material they are very expensive.

1.2 Optimization of the cutting conditions

Optimization of the cutting conditions is one of the most important elements in the manufacturing process (optimization of the technological process, of the tools, of the machines, of the handling etc.). Optimum cutting conditions are closely connected with the economic, quantitative and qualitative aspects, and in this way they affect the price of individual parts, and so the price of the whole product.

Optimization of the cutting conditions is understood as the determination of the optimum cutting conditions with regard to technical limitation, organizational limitation and the criterion of optimum course of the cutting process result.

It is possible to consider the cutting process according to different criteria, the requirement on this course is the result.

For the calculation it is possible to use the following criteria:
– the criterion of minimum production costs,
– the criterion of maximum productivity,
– the criterion of maximum profit.

The criterion of minimum production costs is considered as the most important [8].

The criterion of minimum production costs is graphically represented in Fig. 2. Line K_1/n, decreases when the cutting speed increases, this represents machine-tool service costs; line $K_2/n \cdot T$, increases when the cutting speed increases, this represents tool service costs. Line K represents costs that do not depend on the cutting speed (e.g. workpiece clamping, size measuring etc.), which have no influence on the calculation [1].

From Fig. 2 it follows that any kind of deviation from the optimum cutting speed to lower or higher values results in an increase in the machining costs of a given overlay length. From the form of the total costs line it is possible to judge how the costs grow when the optimum cutting speed is not achieved. The most common reason for deviation is the use of a machine-tool with a speed that changes in steps, when it is not possible to set the exact spindle revolutions according to the calculated optimum cutting speed. If possible, therefore, we use machine-tools with more revolution steps or modern machine-tools with stepless speed variation.

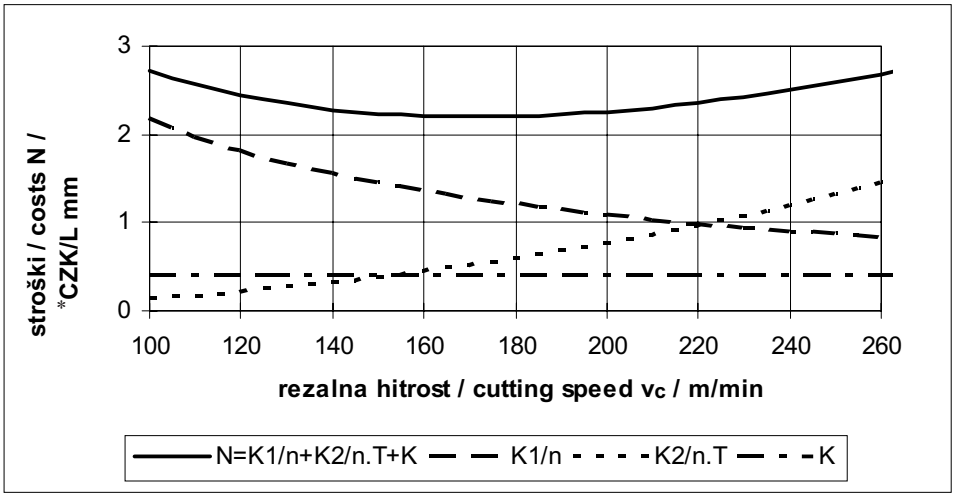

*CZK - češka krona (denarna enota) / czech crown (monetary unit)

Sl. 2. *Grafična ponazoritev kriterija najmanjših stroškov proizvodnje*
Fig. 2. *Graphical representation of the minimum machining costs criterion*

Matematično je mogoče kriterij proizvodnih stroškov pri enoizmenskem delu in operaciji na namenskem stroju, ob uporabi orodij z izmenljivimi ploščicami, izraziti z enačbo:

$$N = \min\left(\frac{K_1}{n} + \frac{K_2}{n.T} + K\right) \quad (1),$$

kjer sta $n = f(v_c)$, $T = f(v_c)$.

Posamezne stroškovne postavke se izračunajo iz naslednjih enačb:

$$K1 = \frac{L}{f}.N_{sCm}$$

$$K2 = \frac{L}{f}.(t_{102}.N_{102Cm} + N_{nT})$$

$$N_{sCm} = k_c.\frac{T_{fo}}{60}(1 + \frac{R_d}{100}) + \frac{N_{hs}}{60}$$

$$N_{hs} = O_s.k_{us} + C_E$$

$$O_s = \frac{C_s}{Z_s.C_f}$$

$$N_{nT} = \frac{C_d.z_d}{z_b.s_b} + (1 + k_{ut}).\frac{C_{tn}}{z_o}$$

kjer je pomen simbolov podan v preglednici 1.

Grafični rezultat izračuna je prikazan na sliki 2. Računalniški program omogoča, ob kakršnikoli spremembi katere od zgoraj navedenih veličin, zelo hiter izračun spremenjenih optimalnih rezalnih parametrov.

The minimum machining costs criterion during single-shift operation, single-machine operation and using tools with inserts can be expressed mathematically with equation:

where $n = f(v_c)$, $T = f(v_c)$.

The single costs are calculated from following equations:

where the symbols are identified in Tabel 1.

The graphical result of this calculation is in Figure 2. The PC program enables the rapid calculation of changed optimum cutting conditions for any change of the above-mentioned inputs.

2 EKSPERIMENTALNI DEL

2.1 Osnovni in navarjeni material

Preskusni vzorci za navarjanje so bili narejeni iz jekla 14 220 (po ČSN 41 4220). Kemična sestava jekla po normi je: C = 0,14 – 0,19, Si = 0,17 – 0,37, Mn = 1,10 – 1,40, Cr = 0,8 – 1,4, P_{maks} = 0,035, S_{maks} = 0,035; kemična sestava po analizi pa je bila:

2 EXPERIMENTAL SECTION

2.1 Basic and welded-on materials

The test samples for surfacing were made from the steel 14 220. The nominal percentage composition of the steel (according to ČSN 41 4220) is: C = 0.14 – 0.19, Si = 0.17 – 0.37, Mn = 1.10 – 1.40, Cr = 0.8 – 1.4, P_{max} = 0.035, S_{max} = 0.035; the composition according to the analysis

Preglednica 1. *Pomen simbolov v enačbi (1) (simboli so uporabljeni po [8])*
Table 1. *Symbols used in equation (1) (the symbols are used according to [8])*

L	dolžina obdelave / section length, mm	n	vrtljaji / revolutions, min^{-1}
D	premer dela po navarjenju / section diameter after surfacing, mm	v_c	rezalna hitrost / cutting speed, $m.min^{-1}$
f	podajanje / feed, $mm.rev^{-1}$	T	obstojnost orodja / tool life, min
k_c	dodatek za delo v izmenah / addition to shift time, -	T_{fo}	urna postavka delavca / workman's wages tariff, $CZK.h^{-1}$
R_d	stroški režije obrata / shop overhead, %	k_{us}	koeficient vzdrževanja in popravila strojev / machine maitenance and repair coefficient, -
C_E	stroški energije / electrical energy costs, $CZK.h^{-1}$	C_s	nabavna cena stroja / machine price, CZK
Z_s	obratovalna doba stroja / machine service life, leto / year	C_f	razpoložljive ure / time fund, $ura.leto^{-1}$ / $h.year^{-1}$
t_{102}	čas za zamenjavo ploščic / insert changing time, min	N_{102Cm}	ali / here = N_{sCm} (ali je strugar ali hkrati tudi skrbi za stroj / turner is also tool setter)
C_d	cena ploščic / insert price, CZK	z_d	število ploščic v držalu / insert number on toolholder, -
z_b	število rezalni robov ploščice / number of cutting edges on the insert, -	s_b	izkoristek ploščice / insert utilization factor, -
k_{ut}	koeficient vzdrževanja orodja / tool maintenence coefficient, -	C_{tn}	stroški držala / toolholder price, CZK
z_o	domnevno število obrabljenih robov / supposed number of cutting edges worn out, -		

C = 0,156, Si = 0,32, Mn = 1,18, Cr = 0,97, Ni = 0,04. Mo = 0,034, V = 0,009, P = 0,014 and S = 0,008. Jeklo 14 220 približno ustreza npr. jeklu TYPE 5 po normi ISO 683/11, jeklu 16MnCr5 (po normi EN 10084), jeklu 16MnCr5 (DIN 17 210), jeklu 18ChG (GOST 4543), jeklu 16MC5 (NF A 35-551) ali jeklu Gr. 5120 (ASTM A506). To jeklo je bilo izbrano glede na njegovo uporabo pri gradnji kmetijskih strojev. Za preskuse so bile uporabljene palice z navari s premerom 55 mm in z dolžino 400 mm. Oblika in dimenzije preskusnih palic so razvidne s slike 3.

Navar je bil izdelan z uporabo pulznega MIG/MAG varjenja v zaščitni atmosferi ogljikovega dioksida (CO_2) z žico C 508. Deklarirana kemična sestava žice je: C = 0,3, Si = 1,1, Mn = 1,0, Cr = 1,0 [10]; kemična sestava po analizi: C = 0,302, Si = 1,13, Mn = 1,01, Cr = 1,03, Ni = 0,03, Mo = 0,007, V = 0,005, P = 0,018 and S = 0,008 (material C 508 približno ustreza npr. materialu OK AUTROD 13.89 podjetja ESAB ali materialu FOX DUR 250 IG podjetja Böhler [10]), s premerom 1,2 mm. Uporabljen je bil avtomat za navarjanje NVE 301 z virom varilnega toka Kv 200 in pozicionirno napravo PSH 02.

is: C = 0.156, Si = 0.32, Mn = 1.18, Cr = 0.97, Ni = 0.04. Mo = 0.034, V = 0.009, P = 0.014 and S = 0.008. The steel approximates, for example, to the steel TYPE 5, according to the standard ISO 683/11, to the steel 16MnCr5, according to the standard EN 10084, to the steel 16MnCr5 (DIN 17 210), to the steel 18ChG (GOST 4543), to the steel 16MC5 (NF A 35-551) or to the steel Gr. 5120 (ASTM A506). This steel was chosen because it is used widely in agricultural machinery. For the tests we used rods with overlays of 55-mm diameter and 400-mm length. The shapes and dimensions of the tested rods with overlays are evident in Fig. 3.

The overlay was deposited pulsed MAG surfacing under a carbon dioxide (CO_2) shield using C 508 wire. The nominal percentage composition of the wire is: C = 0.3, Si = 1.1, Mn = 1.0, Cr = 1.0 [10], the composition according to the analysis is: C = 0.302, Si = 1.13, Mn = 1.01, Cr = 1.03, Ni = 0.03, Mo = 0.007, V = 0.005, P = 0.018 and S = 0.008 (the material C 508 approximates, for example, to the material OK AUTROD 13.89 of the firm ESAB or to the material FOX DUR 250 IG of the firm Böhler [10]), 1.2-mm diameter. The NVE 301 automatic welder, the Kv 200 power supply and the positioner PSH 02 were used.

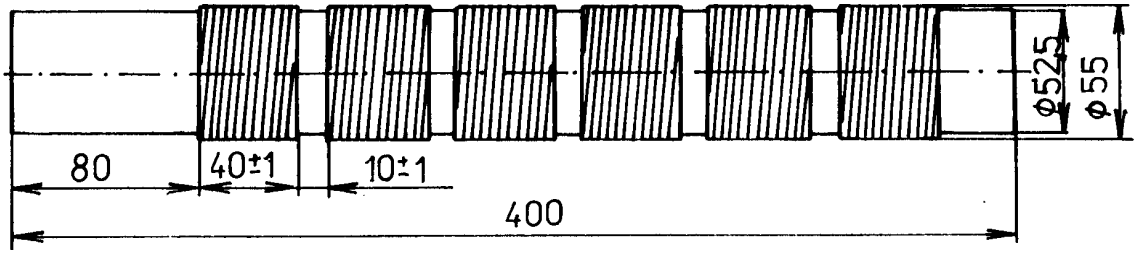

Sl. 3. *Oblika in izmere preskusnih palic z navari*
Fig. 3. *Shapes and dimensions of tested rods with overlays*

Žico C 508 proizvajalec priporoča za pulzno navarjanje (predvsem valjanih) površin sestavnih delov z manjšimi premeri (min. 20 mm). Navarjanje je potekalo pod pogoji, ki so običajni v praksi (pregl. 2). Povprečna trdota navarjene plasti je bila 44 HRC.

2.2 Material orodja

V celoti smo preskusili šest rezalnih materialov podjetja Walter. Vsi testirani orodni materiali so bili dobavljeni v obliki IP, vrste „trigon“. Njihova natančnejša opredelitev je očitna iz preglednice 3. Pri preskusih so bile IP pritrjene v držalo podjetja Walter, tipa PWLNR 2525 M 08.

Za vsa ta orodja so bili izvedeni orientacijski preskusi obstojnosti. Zadovoljivi rezultati so bili doseženi pri rezalnih materialih WAK 10 in WTA 13, s katerimi so bili izvedeni preskusi dolgotrajne obstojnosti. Njihov namen je bilo določiti odvisnost obstojnosti T v min - od rezalne hitrosti v_c v m.min^{-1}. Na temelju rezultatov, doseženih pri drugih, v preskuse uvrščenih rezalnih materialih, lahko poudarimo, da za obdelavo navara žice C 508 niso primerni.

3 REZULTATI

Preskusi obstojnosti IP so bili pri obdelavi navarov izpeljani na stružnici C 11 A (najv. premer obdelovanca = 425 mm, najv. dolžina obdelovanca 1050 mm). Stružnica ima vrtljaje razdeljene po stopnjah v vrsti, s koeficientom 1,4. Realne vrednosti obstojnosti IP so

The manufacturer recommends the wire C 508 for pulsed surfacing of worn out (especially cylidrical) parts with a small diameter (but a minimum of 20 mm). The surfacing was made under the usual conditions (Tab. 2). The mean overlay hardness was 44 HRC.

2.2 Tool material

Altogether we tested six tool materials from the firm Walter. All the tested tool materials were delivered in the form of “trigon” inserts. More details can be found in Tab. 3. The inserts were clamped in the PWLNR 2525 M 08 holder from Walter.

For all these tools we tested the short-term orientation tests of tool-life. For the tool materials WAK 10 and WTA 13 we obtained favourable results. Using these tool materials we made the long-term tests. The aim was to determine the relationship between tool-life T [min] and cutting speed v_c [m.min^{-1}]. On the basis of the test results of other tested tool materials it is possible to state that for the machining of a C 508 overlay these materials are not useful.

3 RESULT SECTION

When machining the overlay the tool-life tests were made on C 11 A lathe (maximum workpiece diameter 425 mm, maximum turning length 1050 mm), enabling the gradual setting of the number of revolutions with a multiplier of 1.4. The real tool-life

Preglednica 2. *Parametri navarjanja*
Table 2. *Surfacing parameters*

Tok navarjanja / surfacing current	regulacijska stopnja / current setting	stopnja 6 step 6
napetost polkroga / voltage	V	12,5
frekvenca vibracij / vibration frequency	Hz	70
podajanje žice / wire feed	m.min^{-1}	2,3
vrtljaji vretena pričvrščevalne priprave / positioner spindle revolutions	min^{-1}	5,3
pomik vozička / carriage feed	mm.rev^{-1}	2,07
količina CO_2 / CO_2 feed rate	l.min^{-1}	11
premer varjenca pred navarjanjem / sample diameter before surfacing	mm	52,0
premer varjenca po navarjanju / sample diameter after surfacing	mm	55,0
debelina navara / layer thickness	mm	1,5

Preglednica 3. *Pregled preskušenih rezalnih materialov [10]*
Table 3. *Summary of tested cutting materials [10]*

Tip NOP / insert type	označitev materiala orodja / tool material	oblika orodja / chip former shape
WNMG 080404	WAP 10 / HC P 10	NM4
WNMG 080404	WAP 20 / HC P 20	NM 4
WNMA 080404	WAK 10 / HC K 10	x
WNMG 080404	WMG 20 / HC K 20 - 30	NM4
WNMA 080412	WAK 10 / HC K 10	x
WNMG 080412	WTA 13 / HC K 10	NM 5

bile za preskusne rezalne materiale ugotovljene pri vrtljajih $n = 710$ min^{-1}, $n = 1\,000$ min^{-1} oziroma $n = 1\,400$ min^{-1}. Iz rezultatov preskusov izhaja, da bi se pri obdelavi z najbližjimi višjimi oziroma nižjimi nastavljivimi vrtljaji na stružnici dosegle nerealno majhne oziroma nerealno velike vrednosti obstojnosti IP. Zaradi tega je bilo vedno izvedeno nekaj meritev pri vrtljajih $n = 710$ min^{-1}, $n = 1000$ min^{-1} oziroma $n = 1400$ min^{-1}. Tem vrtljajem ustreza (pri premeru obdelovanca 55 mm) rezalna hitrost $v_c = 122{,}7$ m.min^{-1}, $v_c = 172{,}8$ m.min^{-1} oziroma $v_c = 241{,}9$ m.min^{-1}. Vsi preskusi so bili izvedeni pri podajanju $f = 0{,}2$ mm.vrt^{-1} in globini reza $a_p = 1$ mm.

3.1 Merjenje obrabe pri rezanju

Pri preskusih je bila izmerjena obraba cepilne ploskve orodja (parameter *VC* v mm, ki je bila z vidika obrabljenosti pri rezanju prevladujoča) in hrapavost dokončane površine (parametri R_a v μm a R_t v μm) v odvisnosti od trajanja obdelave. Obraba pri rezanju je bila izmerjena z orodjarskim mikroskopom. Pri preskusih je bila izbrana mejna vrednost $VC_{adm} = 0{,}8$ mm. Pri prekoračitvi te vrednosti je prišlo do zelo naglega povečanja obrabe in takšna obdelava ni bila varčna.

Časovna odvisnot obrabe cepilne ploskve IP iz materiala WNMA 080412 WAK pri rezalni hitrosti $v_c = 172{,}8$ m.min^{-1} je prikazana na sliki 4.

3.2 Meritev hrapavosti obdelane površine

Hrapavost obdelane površine je bila izmerjena z napravo SURFTEST 301 podjetja MITUTOYO. Rezultati merjanja hrapavosti obdelane površine za tri preskušane orodne materiale so navedeni v nadaljevanju.

Rezultati meritev časovne odvisnosti hrapavosti R_a in R_t po obdelavi navara žice C 508 z

values for the tested tool materials were reached at revolutions of $n = 710$ min^{-1}, $n = 1\,000$ min^{-1}, and $n = 1\,400$ min^{-1}. From the test results it follows that the machining at the next higher and the next lower revolutions would result in unreasonably low and high tool-life values. Therefore, we made measurements at revolutions $n = 710$ min^{-1}, $n = 1000$ min^{-1} and $n = 1400$ min^{-1}. The corresponding cutting speeds were then (at a workpiece diameter of 55 mm) $v_c = 122.7$ m.min^{-1}, $v_c = 172.8$ m.min^{-1} and $v_c = 241.9$ m.min^{-1}. All tests were made at a feed $f = 0.2$ mm.rev^{-1} and a depth of cut $a_p = 1$ mm.

3.1 Chip wear measurement

We measured the flank wear (parameter *VC* [mm]), which was, from the point of view of chip wear, dominant, and the machined surface roughness (parameters R_a [μm] and R_t [μm]) related to the machining time. The chip wear was measured using a toolmaker's microscope. The limit value was $VC_{adm} = 0.8$ mm. Exceeding this limit resulted in a large increase in the wear, and the cutting was uneconomical.

The flank wear of the insert WNMA 080412 WAK 10 related to the time can be seen in Fig. 4, for a cutting speed $v_c = 172.8$ m.min^{-1}.

3.2 Machined surface roughness measurements

The surface roughness of the machined surface was measured using the SURFTEST 301 apparatus from MITUTOYO. The results of the roughness measurements for the three tested tool materials are shown below.

The surface roughness measurement results R_a and R_t after machining the overlay from C 508 wire

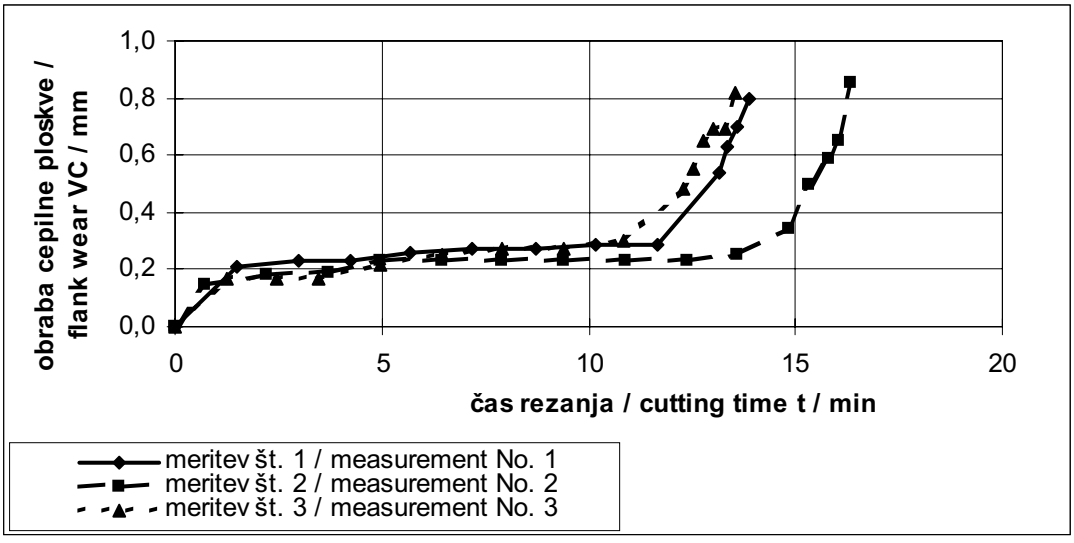

Sl. 4. *Časovni potek obrabe pri 1., 2. in 3. meritvi (WNMA 080412 WAK 10)*
Fig. 4. *Wear versus time during measurement No. 1, 2 and 3 (WNMA 080412 WAK 10)*

rezalnim materialom WNMA 080404 WAK 10 so prikazani na sliki 5 (R_a, v_c = 172,8 m.min^{-1}) in sliki 6 (R_t, v_c = 172,8 m.min^{-1}).

3.3 Ovrednotenje preskusov

Iz krivulje časovne odvisnosti obrabe cepilne plsokve so bili za vrednost dopustne obrabe VC_{adm} = 0,8 mm določene vrednosti obstojnosti orodja. Te so navedene v naslednjih preglednicah: za orodje WNMA 080404 WAK 10 v pregl. 4, za WNMA 080412 WAK 10 v pregl. 5 in za WNMG 080412 WTA 13 v pregl. 6.

Z vstavitvijo izmerjenih vrednosti (Preglednice 4, 5 in 6), v logaritemski v_c-T diagram (sl. 7), smo na osnovi premic lahko ugotovili odvisnosti obstojnosti orodja T od rezalne hitrosti v_c za tri preskušene kombinacije material navara – materiala orodja (pregl. 7).

with the tool material WNMA 080404 WAK 10 related to the time are illustrated in Fig. 5 (R_a, v_c = 172.8 m.min^{-1}) and Fig. 6 (R_t, v_c = 172.8 m.min^{-1}).

3.3 Tests evaluation

From the flank wear course related to the time we read values of the tool-life for the flank wear of VC_{adm} = 0.8 mm. These values are shown in the following tables: for the tool WNMA 080404 WAK 10 in Tab. 4, for WNMA 080412 WAK 10 in Tab. 5 and for WNMG 080412 WTA 13 in Tab. 6.

These values (Tab. 4, 5 and 6) were plotted in a logarithmic diagram for time T and cutting speed v_c. After the straight line interlining (Fig. 7) we established the equation for the relationship between tool-life T and cutting speed v_c for the three tested combinations of overlay material and tool material. (Tab. 7).

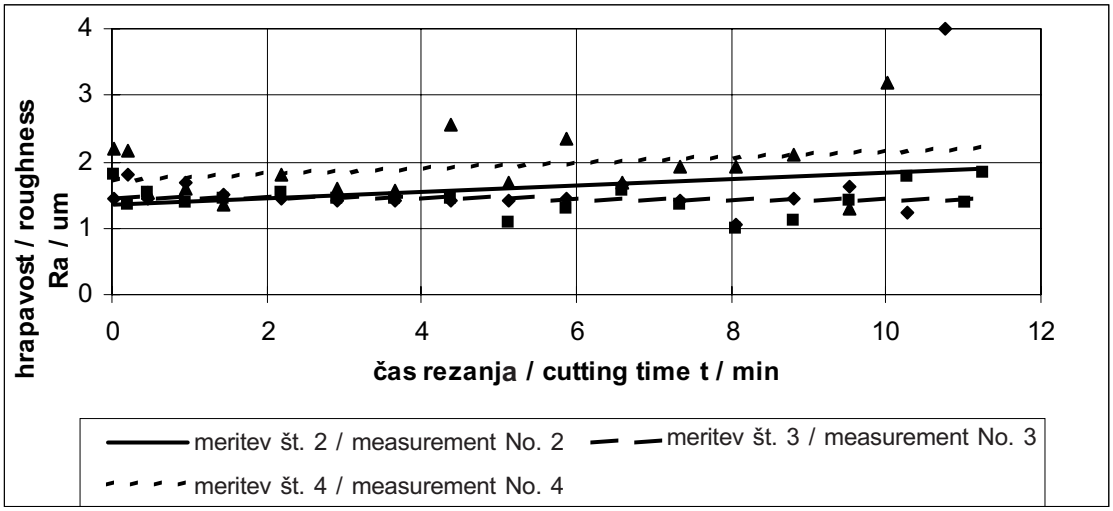

Sl. 5. *Časovni potek hrapavosti R_a pri 2., 3. in 4. merivi (WNMA 080404 WAK 10)*
Fig. 5. *Roughness R_a versus time during measurements No. 2, 3 and 4 (WNMA 080404 WAK 10)*

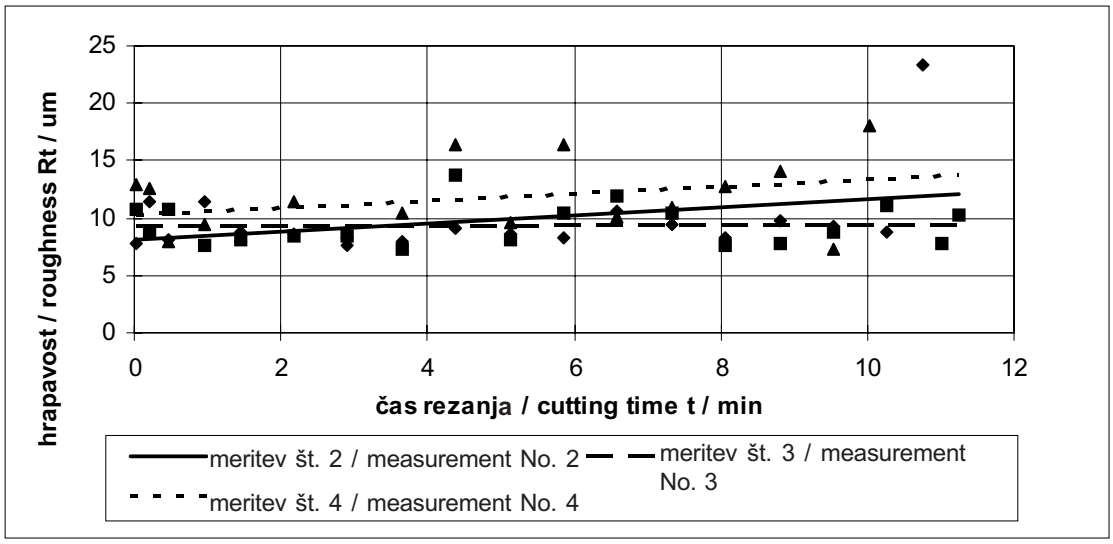

Sl. 6. *Časovni potek hrapavosti R_t pri 2., 3. in 4. meritvi*
Fig. 6. *Roughness R_t versus time during measurements No. 2, 3 and 4*

3.4 Optimizacija rezalnih razmer

Optimizacija rezalnih razmer na osnovi kriterija najmanjših proizvodnih stroškov je bila izvedena z upoštevanjem odvisnosti navedenih v teoretičnem delu prispevka. Za izračun smo uporabili osebni računalnik. Pri izračunu smo uporabili dejanske dekonomske kazalnike stružilnega obrata in cene, veljavne v Češki republiki (stanje v februarju 2002). Računalniški program je omogočil zelo hiter izračun optimalnih rezalnih pogojev ob spremembi kateregakoli od vstopnih parametrov.

Pri izračunu, ki ga je avtor izvedel z lastnim programom [1], so bile dosežene naslednje vrednosti: L = 40 mm, D = 55 mm, f = 0,2 mm.rev^{-1}, n = 710; 1 000 in 1 400 min^{-1}, v_c = 122,7; 172,8 in 241,9 m.min^{-1}, T = (2), (3) in (4) v pregl. 7, k_c = 1,1, T_{fo} = 60 CZK.h^{-1}, R_d = 400 %, k_{us} = 1,3, C_E = 0 (pri optimizaciji ni bila upoštevana), C_s = 450 000 CZK (vključno 22 % davka na dodano vrednost, DDV), $Ž_s$ = 6 let, $Č_f$ = 2 008 h.leto^{-1}, t_{102} = 0,5 min, z_d = 1, z_b = 6, s_b=1, C_d = 377,0 CZK (WAK 10), 380.6 CZK (WTA 13) (vključno 22 % DDV), K_{ut} = 0,25, C_{tn} = 3 035,40 CZK, z_o = 1 000.

3.4 Optimization of the cutting conditions

Optimization of cutting conditions for the minimum production costs criterion was calculated using the relations mentioned in the theoretical part of this article. The calculation was made using a PC. We used the real economic indexes of a turning shop and the prices valid in the Czech Republic (February 2002). The PC program enables a rapid calculation of the optimum cutting conditions for any change of the input parameters.

In the calculation, using the author's own program [1], the following values were used: L = 40 mm, D = 55 mm, f = 0.2 mm.rev^{-1}, n = 710; 1 000 and 1 400 min^{-1}, v_c = 122.7; 172.8 and 241.9 m.min^{-1}, T = (2), (3) and (4) in table 7, k_c = 1.1, T_{fo} = 60 CZK.h^{-1}, R_d = 400 %, k_{us} = 1.3, C_E = 0 (it was not taken into consideration), C_s = 450 000 CZK (including 22 % value added tax, VAT), $Ž_s$ = 6 years, $Č_f$ = 2 008 h.year^{-1}, t_{102} = 0.5 min, z_d = 1, z_b = 6, s_b=1, C_d = 377.0 CZK (WAK 10), 380.6 CZK (WTA 13) (including 22 % VAT), K_{ut} = 0.25, C_{tn} = 3 035.40 CZK, z_o = 1 000.

Preglednica 4. *Rezultati preskusov (C 508, WNMA 080404 WAK 10)*
Table 4. *Test results (C 508, WNMA 080404 WAK 10)*

Meritev / measurement	rezalna hitrost / cutting speed v_c / m.min^{-1}	obstojnost orodja / tool-life T / min
1	122,7	68,1
2	172,8	11,26
3	172,8	9,87
4	1728	10,68

Preglednica 5. *Rezultati preskusov (C 508, WNMA 080412 WAK 10)*
Table 5. *Test results (C 508, WNMA 080412 WAK 10)*

Meritev / measurement	rezalna hitrost / cutting speed v_c / m.min^{-1}	obstojnost orodja / tool-life T / min
1	172,8	13,86
2	172,8	16,26
3	172,8	13,50
4	241,9	2,33
5	241,9	2,65
6	241,9	2,17
7	241,9	2,95

Preglednica 6. *Rezultati preskusov (C 508, WNMG 080412 WTA 13)*
Table 6. *Test results (C 508, WNMG 080412 WTA 13)*

Meritev / measurement	rezalna hitrost / cutting speed v_c / m.min^{-1}	obstojnost orodja / tool-life T / min
1	172,8	21,67
2	172,8	23,72
3	172,8	29,97
4	241,9	5,75
5	241,9	6,95
6	241,9	8,37
7	241,9	11,50

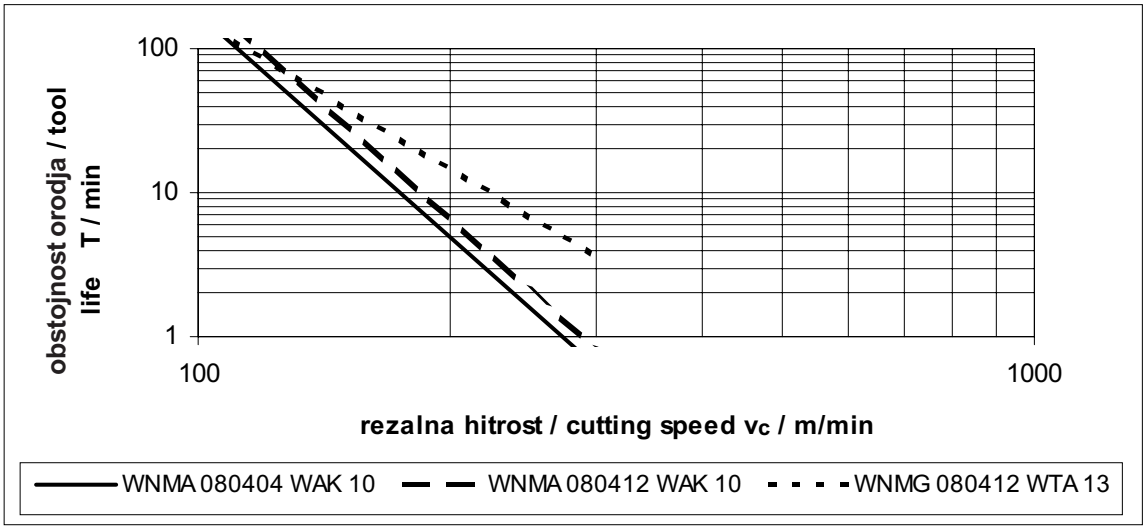

Sl. 7. *Odvisnost obstojnosti T od rezalne hitrosti v_c (C 508, WALTER)*
Fig. 7. *T - v_c relationship (C 508, WALTER)*

Preglednica 7. *Odvisnost obstojnosti T od rezalne hitrosti v_c*
Table 7. *T - v_c relationship*

Izmenljiva ploščica / insert	$T - v_C$	
WNMA 080404 WAK 10	$T = 3{,}5798.10^{12} .v^{-5.1525}$	(2)
WNMA 080412 WAK 10	$T = 6{,}7542.10^{12} .v^{-5.2149}$	(3)
WNMG 080412 WTA 13	$T = 1{,}1169.10^{9} .v^{-3.4199}$	(4)

Grafični rezultat izračuna optimuma je za IP WNMA 080404 WAK 10 naveden na sliki 8, za IP WNMA 080412 WAK 10 na sliki 9 in za IP WNMG 080412 WTA 13 na sliki 10; skupaj za vse tri preskušene IP pa na sliki 11.

The result of the calculation is graphically represented in Fig. 8 for the insert WNMA 080404 WAK 10, in Fig. 9 for the insert WNMA 080412 WAK 10 and in Fig. 10 for the insert WNMG 080412 WTA 13, and a summary of all three tested inserts is in Fig. 11.

4 RAZPRAVA

Skupni rezultati optimizacije rezalnih razmer, izračunani na osnovi podatkov gospodarskih kazalnikov stružilnega obrata v pogojih Češke

4 DISCUSSION

The summary of the results of the cutting-conditions optimization calculated on the basis of the economic indexes of the turning shop for the

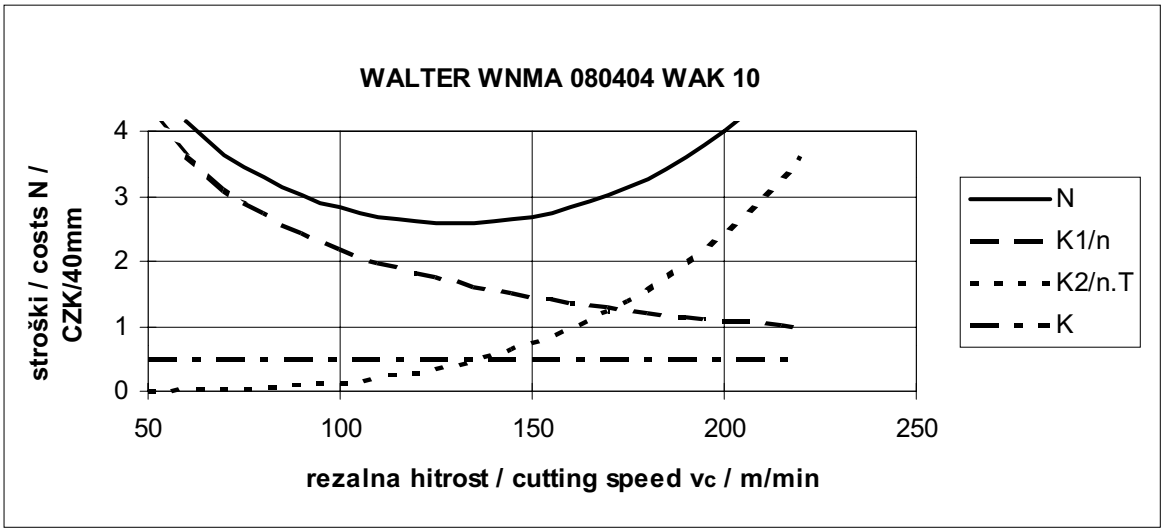

Sl. 8. *Grafična ponazoritev kriterija najmanjših stroškov obdelave*
Fig. 8. *Graphical expression of minimum machining costs criterion*

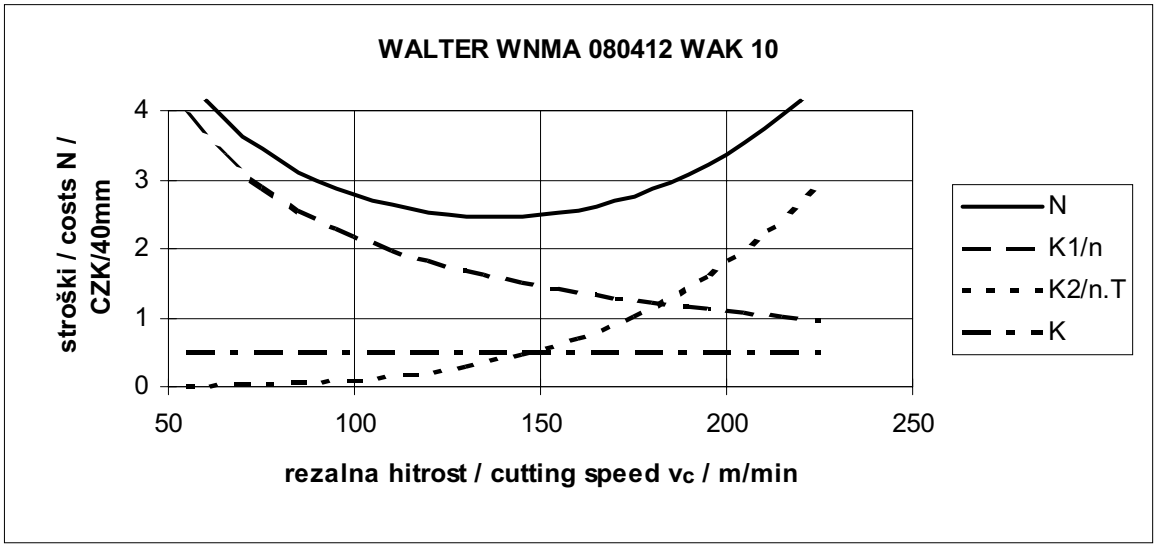

Sl. 9. *Grafična ponazoritev kriterija najmanjših stroškov obdelave*
Fig. 9. *Graphical expression of minimum machining costs criterion*

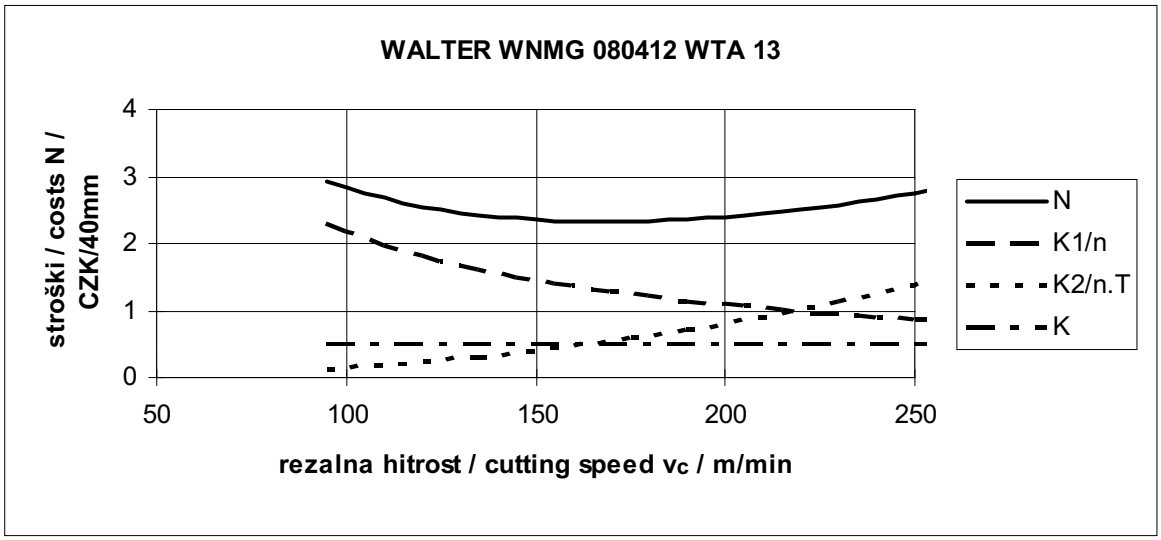

Sl. 10. *Grafična ponazoritev kriterija najmanjših stroškov obdelave*
Fig. 10. *Graphical expression of minimum machining costs criterion*

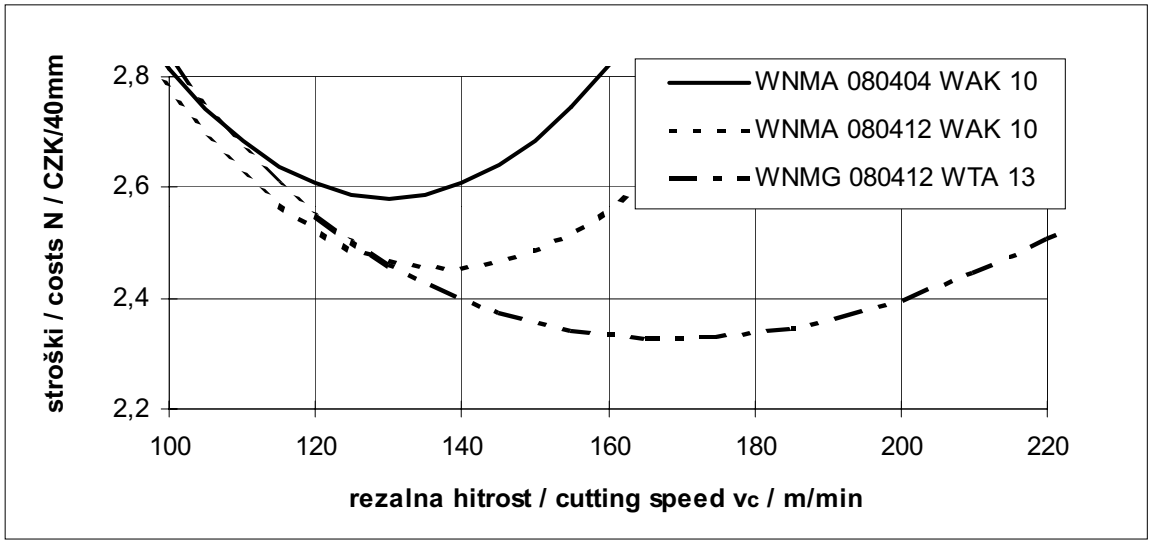

Sl. 11. *Grafična ponazoritev kriterija najmanjših stroškov obdelave*
Fig. 11. *Graphical expression of minimum machining costs criterion*

republike, so navedeni na sliki 11. S slike je očitno, da ima odvisnost skupnih stroškov od rezalne hitrosti obliko črke "U". Za stvarne razmere gospodarjenja torej vedno obstaja rezalna hitrost, pri kateri so skupni stroški za obdelavo najmanjši. Oblike krivulj za različne materiale orodij pa so različne. Iz oblike krivulje je prav tako očitno, da ima vsak odmik od optimalne rezalne hitrosti za posledico povečanje stroškov obdelave. Za obdelavo je torej najprimernejša uporaba modernih obdelovalnih strojev, ki omogočajo brezstopenjsko spremembo vrtljajev (rezalne hitrosti). Starejši stroji, ki so se do sedaj uporabljali v manjših delavnicah, te možnosti nimajo. Zato je treba v stroške za obdelavo vračunati tudi stroške zaradi neupoštevanja optimalne rezalne hitrosti.

To povečanje je odvisno od oblike krivulje odvisnosti skupnih stroškov od rezalne hitrosti. Iz grafične ponazoritve rezultatov preskusov je očitno, da bo pri ravni krivulji stroškov to povečanje manjše kakor pa pri strmi krivulji stroškov. Rezultati matematične analize tega problema za preučevane materiale orodja so navedeni v preglednici 8.

5 SKLEPI

V prispevku so objavljeni rezultati preskusov, ki so bili izvedeni z namenom, da bi določili uporabnost izbranih rezalnih materialov podjetja Walter za obdelavo navara, izdelanega s tehnologijo pulznega MIG/MAG varjenja žice C 508 v zaščitni atmosferi ogljikovega oksida.

V preskuse je bilo skupaj uvrščenih 6 tipov orodnih materialov. Po orientacijskih kratkoročnih preskusih so bili iz preskusov izločeni trije materiali. Preskusi dolgotrajne obstojnosti so bili izvedeni ob obdelavi navara z orodjem WAK 10 in WTA 13 v obliki IP tipa WNMA 080404 in WNMA 080412 oziroma WNMG 080412. Po obdelavi izmerjenih podatkov so bile izračunane enačbe odvisnosti obstojnosti T od rezalne hitrosti v_c. Na podlagi znanj teh odvisnosti je bila z uporabo računalniškega programa izvedena optimizacija rezalnih razmer za osnovne gospodarske kazalnike obrata in za cene, veljavne v Češki republiki. Rezultati vrednotenja izmerjenih vrednosti in optimizacije rezalnih razmer na osnovi kriterija najmanjših proizvodnih stroškov so navedeni v preglednici 9.

conditions of the Czech Republic are shown in Fig. 11. It is evident that the relationship between total costs and cutting speed has the shape of the letter U. For concrete economic conditions there always exists a cutting speed for which the total machining costs are at a minimum. However, the shape of the curve for different tool materials can vary. From the shape of the curve we can see, that any kind of elevation from the optimum cutting speed results in an increase in machining costs. Therefore, it is advantageous to use modern machine-tools with a stepless speed variation. Older machine-tools in use up to this time in smaller workshops do not have this possibility. Therefore, it is necessary to include the costs increase in the machining costs when the optimum cutting speed is not achieved.

This increase depends on the shape of the curve of the relationship between total costs and cutting speed. The graphical representation shows that for a flat curve this increase will be less than for a steep one. The mathematical analysis of this problem for the tested inserts is shown in Tab. 8.

5 CONCLUSIONS

In this paper we present test results on the usability of tool materials from the firm Walter for machining of the overlay made by pulsed carbon dioxide shielded surfacing technology using wire C 508.

Six types of tool material were tested. After the short-term orientation tests three tool materials were eliminated. The long-term tests of the overlay machining were made using the tool materials WAK 10 and WTA 13 in the form of inserts of the type WNMA 080404, WNMA 080412 and WNMG 080412. After processing the data we calculated the equations of the relationship between tool-life T and cutting speed v_c. On the basis of these equations, using a computer program, we calculated the optimum cutting conditions for the basic economic indexes of the workshop and the prices valid in the Czech Republic. The results of the evaluated measured values and the cutting-conditions optimization at the minimum machining costs criterion are shown in Tab. 9.

Preglednica 8. *Povečanje stroškov zaradi neupoštevanja optimalne rezalne hitrosti*
Table 8. *Costs increase resulting from a less(more)-than-optimum cutting speed*

IP / inserts	rezalna hitrost cutting speed v_{copt} / m.min^{-1}	vrtljaji revolutions n_{opt} / min^{-1}	vrtljaji revolutions n / min^{-1}	povečanja stroškov costs increase Δ_N / %
WNMA 080404 WAK 10	130,00	752,4	710	+ 0,5
			1 000	+ 19,3
WNMA 080412 WAK 10	138,10	799,2	710	+ 2,1
			1 000	+ 11,1
WNMG 080412 WTA 13	168,75	976,6	710	+ 8,5
			1 000	+ 0,1

Preglednica 9. *Rezultati preskusov*
Table 9. *Test results*

IP / insert	enačba obstojnosti T - rezalna hitrost v_C T - v_C equation	rezalna hitrost cutting speed v_{copt} m.min^{-1}	obstojnost orodja tool life T_{opt} min	stroški obdelave machining costs N_{min} CZK.40mm^{-1}
WNMA 080404 WAK 10	$T = 3{,}5798.10^{12} . v^{-5.1525}$	130,00	45,9	2,58
WNMA 080412 WAK 10	$T = 6{,}7542.10^{12} . v^{-5.2149}$	138,10	46,6	2,45
WNMG 080412 WTA 13	$T = 1{,}1169.10^{9} . v^{-3.4199}$	168,75	27,0	2,33

Pri preskusih je bila prav tako izmerjena hrapavost površine, dejansko parametra hrapavosti R_a in R_t. Iz vrednotenja izmerjenih vrednosti izhaja, da se s povečano obrabo (torej s povečanim časom delovanja stroja) oba parametra hrapavosti povečujeta. Hrapavost površine se je v vsem obdobju trajanja gibala v sprejemljivih mejah, le na koncu vsakega preskusa so se izmerjene vrednosti naglo povečale.

Na koncu lahko poudarimo, da je uporaba preskušenih orodnih materialov podjetja Walter, v obliki IP, za obdelavo navara žice C 508 primerna in ekonomsko utemeljena. Najboljši rezultati so bili doseženi z uporabo orodja WNMG 080412 WAT 13.

Along with the tests we measured the surface roughness and the parameters R_a and R_t. From the measured values it follows that with increasing wear (and so with increasing working time of the tool) both roughness parameters increase. During the tests the surface roughness was within acceptable limits, only at the end of each test did the measured values increase significantly.

We can conclude that the use of the tested tool materials from Walter in the form of inserts is suitable for overlay machining of an overlay made from C 508 wire. The best results were achieved with using the insert WNMG 080412 WTA 13.

ZAHVALA

Prispevek je nastal ob podpori Ministrstva za šolstvo, mladino in teleseno vzgojo Češke republike v okviru rešitve raziskovalnega načrta J03/98:41300016.

ACKNOWLEDGEMENTS

This paper has been supported by the Ministry of Education, Youth and Sports of the Czech Republic as part of research project J03/98:413100016.

6 LITERATURA
6 REFERENCES

[1] Brožek, M. (1995) Vybrané problémy navařování [Habilitační práce]. (Selected problems of surfacing. Inaugural dissertation). Praha, 148. - *CUA. Technical Fakulty*.
[2] Brožek, M. (1997) Obrábění návaru drátu C 508 nástroji ze slinutých karbidů různých firem. (Machining of overlay made by welding wire C 508 using sintered carbide tools of different firms). *Collection of papers of International Conference DIDMATTECH ´*97, Nitra, PF UK 1997, 115 - 118.
[3] Brožek, M. (2001) Optimalizace řezných podmínek při soustružení navařených vrstev. (Optimization of cutting conditions with turning of overlays). *Proceedings 1-st. International Congress of Precision Machining*. Ústí nad Labem, UJEP 2001, 95 - 100.
[4] Brožek, M. (2000) Soustružení návaru drátu C 508 nástroji firmy WIDIA. (Turning of overlays made by welding wire C 508 using WIDIA firm tools). *Strojírenská technologie*, V, Nr. 2, 25 - 33.
[5] Chasuj, A., O. Morigaki (1985) Naplavka i napylenie. (Surfacing technology). Moskva, *Mašinostroenie*, 240.
[6] Kamenarov, G., U. Pankow (1981) Über die Beeinflussung der Eigenschaften des Grundwerkstoffs bei der Instandsetzungsschweissung verguteter Einzelteile. (Affecting of basic materials properties at repair work of heat treated parts using surfacing). *Agrartechnik*, 31, Nr. 3, 120 - 121.
[7] Liemert, G., F. Drábek, J. Ondra, I. Vavřík (1974) Obrábění. (Machining). Praha, *SNTL* 1974, 352.
[8] Mádl, J., I. Kvasnička (1998) Optimalizace obráběcího procesu. (Optimization of machining process). Praha, *ČVUT* 1998, 168.
[9] Repair and maintenance welding handbook. ESAB AB, 120.
[10] Firm literature.

Naslov avtorja: prof. dr. Milan Brožek
Tehnična fakulteta
Češka univerza za kmetijstvo
Kamýcká 129
165 21 Praga 6 - Suchdol
Češka republika
brozek@tf.czu.cz

Authors' Address: Prof. Dr. Milan Brožek
Technical Faculty
Czech University of Agriculture
Kamýcká 129
165 21 Praha 6 - Suchdol
Czech Republic
brozek@tf.czu.cz

Prejeto:
Received: 6.5.2002

Sprejeto:
Accepted: 22.11.2002

Osebne vesti
Personal Events

Magisteriji, diplome

MAGISTERIJI

Na Fakulteti za strojništvo Univerze v Ljubljani je *dne 29. septembra 2002* **Franc Rotar** z uspehom zagovarjal svoje magistrsko delo z naslovom: "Razvoj generične strukture in programskih modulov elementarnega delovnega sistema".

S tem je navedeni kandidat dosegel akademsko stopnjo magistra tehničnih znanosti.

DIPLOMIRALI SO

Na Fakulteti za strojništvo Univerze v Ljubljani so pridobili naziv univerzitetni diplomirani inženir strojništva:

dne 24. septembra 2002: Tadej AUER, Matej PEGAN, Sergij PLEŠNAR, Danjela PRINČIČ, Rok SUŠNIK;

dne 27. septembra 2002: Aljaž ARNOLD, Rado BAJT, Andrej BIČEK, Danilo EKAR, Gašper GARANTINI, Goran KEZELE, Robert KOTNIK, Martin TERLEP, Andrej THALER, Silvester TOTH -POPE;

dne 30. septembra 2002: Sebastjan GREGORŠANEC, Marko OBID, Tadej POŽAR, Edvard SODNIK.

Na Fakulteti za strojništvo Univerze v Mariboru so pridobili naziv univerzitetni diplomirani inženir strojništva:

dne 2. septembra 2002: Vladan MLADENOVIĆ;

dne 26. septembra 2002: Franci JERENKO, Bojan RIZMAN, Andrej STARIČ.

*

Na Fakulteti za strojništvo Univerze v Ljubljani so pridobili naziv diplomirani inženir strojništva:

dne 11. septembra 2002: Dejan ARBI, Marjan GOVEKAR, Jernej JANŠKOVEC, Rudolf KRPIČ, Mihec KUZMAN, Matjaž RAKUN, Miran ŠUŠTERŠIČ, Bojana WEBER;

dne 12. septembra 2002: Branislav AVSEC, Florjan BEVC, Branko BIŠČAK, Simon OMAN, Rok STAVANJA;

dne 13. septembra 2002: Jernej FABIJAN, Janez FAJDIGA, Anton FORTUNAT, Gregor GOVEKAR, Matjaž KOVIČ, Dušan KRŠTINC, Matjaž LAPORNIK, Marko LEMUT, Gregor PODOBNIK, Aljoša ŠINKOVEC, Damir ŠKROBOT, Martin TRAMTE;

dne 16. septembra 2002: Matjaž COTAR, Janez KLJUN, Jurij KOS, Primož KRŽIČ, Slavko MARN, Zoran TURKALJ, Matej ZRIMŠEK;

dne 17. septembra 2002: Marijan CER, Bojan GANTAR, Janko MIKULETIČ, Matjaž RUPNIK, Branko ŠULER.

Na Fakulteti za strojništvo Univerze v Mariboru so pridobili naziv diplomirani inženir strojništva:

dne 12. septembra 2002: Roman DEŽELAK, Mitja DOBRAVC, Robert FAŠNIK, Jože IVANČIČ;

dne 25. septembra 2002: Boštjan GREGORC, Andrej JURIČ, Matej MEJAČ, Tonček PLEČKO, Marko PONGRAC, Drago SLANIČ, Jože TOPIČ;

dne 26. septembra 2002: Luka BERCKO, Boštjan CILENŠEK, Aleš DOLŽAN, Miroslav LOMBAR, Damir LUKEŽIĆ, Urban UVERA;

dne 27. septembra 2002: Stanko KRAJNC.

*

Na Fakulteti za strojništvo Univerze v Ljubljani so pridobili naziv inženir strojništva:

dne 11. septembra 2002: Uroš BIZJAK, Aleš HABICHT, Matej LOZAR;

dne 12. septembra 2002: Rok POPOVIĆ;

dne 13. septembra 2002: Bojan REPNIK;

dne 16. septembra 2002: Janez TOMAŽIN;

dne 17. septembra 2002: Branko ŠULER.

Na Fakulteti za strojništvo Univerze v Mariboru so pridobili naziv inženir strojništva:

dne 12. septembra 2002: Albin GREGORC, Mirsad HODA, Matjaž KNEZ, Simon KRAJNIK;

dne 25. septembra 2002: Robert BROZ, Miran DETIČEK, Robert DOLER, Jurica JAGARINEC, Albert KEKEC, Štefan KOLTAJ, Aleš PEČAK, Milan PETRAK, Bojan PUSTOSLEMŠEK, Andrej REBERNAK, Marjan SABO, Jasna ŠVAGAN, Nevenko VARŠIČ, Rajko VAVDI;

dne 26. septembra 2002: Oliver ANTONIĆ. Bojan CRNČEC, Jurij ERMAN, Branko FIJAVŽ, Vladimir FLORJAN, Rajko GORINŠEK, Primož KOPRIVNIKAR, Amela KRAJNC, Ludvik KRALJ, Zoran LUKEŽIĆ, Miodrag MILOŠEVIĆ, Avguštin RAJTAR, Edo TROBIŠ;

dne 27. septembra 2002: Tomaž VOVK;

dne 30. septembra 2002: Bernard PODVEZANEC.

Navodila avtorjem
Instructions for Authors

Članki morajo vsebovati:
- naslov, povzetek, besedilo članka in podnaslove slik v slovenskem in angleškem jeziku,
- dvojezične preglednice in slike (diagrami, risbe ali fotografije),
- seznam literature in
- podatke o avtorjih.

Strojniški vestnik izhaja od leta 1992 v dveh jezikih, tj. v slovenščini in angleščini, zato je obvezen prevod v angleščino. Obe besedili morata biti strokovno in jezikovno med seboj usklajeni. Članki naj bodo kratki in naj obsegajo približno 8 tipkanih strani. Izjemoma so strokovni članki, na željo avtorja, lahko tudi samo v slovenščini, vsebovati pa morajo angleški povzetek.

Vsebina članka

Članek naj bo napisan v naslednji obliki:
- Naslov, ki primerno opisuje vsebino članka.
- Povzetek, ki naj bo skrajšana oblika članka in naj ne presega 250 besed. Povzetek mora vsebovati osnove, jedro in cilje raziskave, uporabljeno metodologijo dela,povzetek rezulatov in osnovne sklepe.
- Uvod, v katerem naj bo pregled novejšega stanja in zadostne informacije za razumevanje ter pregled rezultatov dela, predstavljenih v članku.
- Teorija.
- Eksperimentalni del, ki naj vsebuje podatke o postavitvi preskusa in metode, uporabljene pri pridobitvi rezultatov.
- Rezultati, ki naj bodo jasno prikazani, po potrebi v obliki slik in preglednic.
- Razprava, v kateri naj bodo prikazane povezave in posplošitve, uporabljene za pridobitev rezultatov. Prikazana naj bo tudi pomembnost rezultatov in primerjava s poprej objavljenimi deli. (Zaradi narave posameznih raziskav so lahko rezultati in razprava, za jasnost in preprostejše bralčevo razumevanje, združeni v eno poglavje.)
- Sklepi, v katerih naj bo prikazan en ali več sklepov, ki izhajajo iz rezultatov in razprave.
- Literatura, ki mora biti v besedilu oštevilčena zaporedno in označena z oglatimi oklepaji [1] ter na koncu članka zbrana v seznamu literature. Vse opombe naj bodo označene z uporabo dvignjene številke[1].

Oblika članka

Besedilo naj bo pisano na listih formata A4, z dvojnim presledkom med vrstami in s 3 cm širokim robom, da je dovolj prostora za popravke lektorjev. Najbolje je, da pripravite besedilo v urejevalnilku Microsoft Word. Hkrati dostavite odtis članka na papirju, vključno z vsemi slikami in preglednicami ter identično kopijo v elektronski obliki.

Prosimo, da ne uporabljate urejevalnika LaTeX, saj program, s katerim pripravljamo Strojniški vestnik, ne uporablja njegovega formata. V urejevalniku LaTeX oblikujte grafe, preglednice in enačbe in jih stiskajte na kakovostnem laserskem tiskalniku, da jih bomo lahko presneli.

Enačbe naj bodo v besedilu postavljene v ločene vrstice in na desnem robu označene s tekočo številko v okroglih oklepajih

Enote in okrajšave

V besedilu, preglednicah in slikah uporabljajte le standardne označbe in okrajšave SI. Simbole fizikalnih veličin v besedilu pišite poševno (kurzivno), (npr. *v, T, n* itn.). Simbole enot, ki sestojijo iz črk, pa pokončno (npr. ms^{-1}, K, min, mm itn.).

Vse okrajšave naj bodo, ko se prvič pojavijo, napisane v celoti v slovenskem jeziku, npr. časovno spremenljiva geometrija (ČSG).

Papers submitted for publication should comprise:
- Title, Abstract, Main Body of Text and Figure Captions in Slovene and English,
- Bilingual Tables and Figures (graphs, drawings or photographs),
- List of references and
- Information about the authors.

Since 1992, the Journal of Mechanical Engineering has been published bilingually, in Slovenian and English. The two texts must be compatible both in terms of technical content and language. Papers should be as short as possible and should on average comprise 8 typed pages. In exceptional cases, at the request of the authors, speciality papers may be written only in Slovene, but must include an English abstract.

The format of the paper

The paper should be written in the following format:
- A Title, which adequately describes the content of the paper.
- An Abstract, which should be viewed as a miniversion of the paper and should not exceed 250 words. The Abstract should state the principal objectives and the scope of the investigation, the methodology employed, summarize the results and state the principal conclusions.
- An Introduction, which should provide a review of recent literature and sufficient background information to allow the results of the paper to be understood and evaluated.
- A Theory
- An Experimental section, which should provide details of the experimental set-up and the methods used for obtaining the results.
- A Results section, which should clearly and concisely present the data using figures and tables where appropriate.
- A Discussion section, which should describe the relationships and generalisations shown by the results and discuss the significance of the results making comparisons with previously published work. (Because of the nature of some studies it may be appropriate to combine the Results and Discussion sections into a single section to improve the clarity and make it easier for the reader.)
- Conclusions, which should present one or more conclusions that have been drawn from the results and subsequent discussion.
- References, which must be numbered consecutively in the text using square brackets [1] and collected together in a reference list at the end of the paper. Any footnotes should be indicated by the use of a superscript[1].

The layout of the text

Texts should be written in A4 format, with double spacing and margins of 3 cm to provide editors with space to write in their corrections. Microsoft Word for Windows is the preferred format for submission. One hard copy, including all figures, tables and illustrations and an identical electronic version of the manuscript must be submitted simultaneously.

Please do not use a LaTeX text editor, since this is not compatible with the publishing procedure of the Journal of Mechanical Engineering. Graphs, tables and equations in LaTeX may be supplied in good quality hard-copy format, so that they can be copied for inclusion in the Journal.

Equations should be on a separate line in the main body of the text and marked on the right-hand side of the page with numbers in round brackets.

Units and abbreviations

Only standard SI symbols and abbreviations should be used in the text, tables and figures. Symbols for physical quantities in the text should be written in Italics (e.g. *v, T, n,* etc.). Symbols for units that consist of letters should be in plain text (e.g. ms^{-1}, K, min, mm, etc.).

All abbreviations should be spelt out in full on first appearance, e.g., variable time geometry (VTG).

Slike

Slike morajo biti zaporedno oštevilčene in označene, v besedilu in podnaslovu, kot sl. 1, sl. 2 itn. Posnete naj bodo v kateremkoli od razširjenih formatov, npr. BMP, JPG, GIF. Za pripravo diagramov in risb priporočamo CDR format (CorelDraw), saj so slike v njem vektorske in jih lahko pri končni obdelavi preprosto povečujemo ali pomanjšujemo.

Pri označevanju osi v diagramih, kadar je le mogoče, uporabite označbe veličin (npr. *t, v, m* itn.), da ni potrebno dvojezično označevanje. V diagramih z več krivuljami, mora biti vsaka krivulja označena. Pomen oznake mora biti pojasnjen v podnapisu slike.

Vse označbe na slikah morajo biti dvojezične.

Za vse slike po fotografskih posnetkih je treba priložiti izvirne fotografije ali kakovostno narejen posnetek. V izjemnih primerih so lahko slike tudi barvne.

Preglednice

Preglednice morajo biti zaporedno oštevilčene in označene, v besedilu in podnaslovu, kot preglednica 1, preglednica 2 itn. V preglednicah ne uporabljajte izpisanih imen veličin, ampak samo ustrezne simbole, da se izognemo dvojezični podvojitvi imen. K fizikalnim veličinam, npr. *t* (pisano poševno), pripišite enote (pisano pokončno) v novo vrsto brez oklepajev.

Vsi podnaslovi preglednic morajo biti dvojezični.

Seznam literature

Vsa literatura mora biti navedena v seznamu na koncu članka v prikazani obliki po vrsti za revije, zbornike in knjige:

[1] Tarng, Y.S., Y.S. Wang (1994) A new adaptive controler for constant turning force. *Int J Adv Manuf Technol* 9(1994) London, pp. 211-216.

[2] Čuš, F., J. Balič (1996) Rationale Gestaltung der organisatorischen Abläufe im Werkzeugwesen. *Proceedings of International Conference on Computer Integration Manufacturing,* Zakopane, 14.-17. maj 1996.

[3] Oertli, P.C. (1977) Praktische Wirtschaftskybernetik. *Carl Hanser Verlag,* München.

Podatki o avtorjih

Članku priložite tudi podatke o avtorjih: imena, nazive, popolne poštne naslove, številke telefona in faksa ter naslove elektronske pošte.

Sprejem člankov in avtorske pravice

Uredništvo Strojniškega vestnika si pridržuje pravico do odločanja o sprejemu članka za objavo, strokovno oceno recenzentov in morebitnem predlogu za krajšanje ali izpopolnitev ter terminološke in jezikovne korekture.

Avtor mora predložiti pisno izjavo, da je besedilo njegovo izvirno delo in ni bilo v dani obliki še nikjer objavljeno. Z objavo preidejo avtorske pravice na Strojniški vestnik. Pri morebitnih kasnejših objavah mora biti SV naveden kot vir.

Rokopisi člankov ostanejo v arhivu SV.

Vsa nadaljnja pojasnila daje:

Uredništvo
STROJNIŠKEGA VESTNIKA
p.p. 197/IV
1001 Ljubljana
Telefon: (01) 4771-757
Telefaks: (01) 2518-567
E-mail: strojniski.vestnik@fs.uni-lj.si

Figures

Figures must be cited in consecutive numerical order in the text and referred to in both the text and the caption as Fig. 1, Fig. 2, etc. Figures may be saved in any common format, e.g. BMP, GIF, JPG. However, the use of CDR format (CorelDraw) is recommended for graphs and line drawings, since vector images can be easily reduced or enlarged during final processing of the paper.

When labelling axes, physical quantities, e.g. *t, v, m,* etc. should be used whenever possible to minimise the need to label the axes in two languages. Multi-curve graphs should have individual curves marked with a symbol, the meaning of the symbol should be explained in the figure caption.

All figure captions must be bilingual.

Good quality black-and-white photographs or scanned images should be supplied for illustrations. In certain circumstances, colour figures may be considered.

Tables

Tables must be cited in consecutive numerical order in the text and referred to in both the text and the caption as Table 1, Table 2, etc. The use of names for quantities in tables should be avoided if possible: corresponding symbols are preferred to minimise the need to use both Slovenian and English names. In addition to the physical quantity, e.g. *t* (in Italics), units (normal text), should be added in new line without brackets.

All table captions must be bilingual.

The list of references

References should be collected at the end of the paper in the following styles for journals, proceedings and books, respectively:

[1] Tarng, Y.S., Y.S. Wang (1994) A new adaptive controler for constant turning force. *Int J Adv Manuf Technol* 9(1994) London, pp. 211-216.

[2] Čuš, F., J. Balič (1996) Rationale Gestaltung der organisatorischen Abläufe im Werkzeugwesen. *Proceedings of International Conference on Computer Integration Manufacturing,* Zakopane, 14.-17. maj 1996.

[3] Oertli, P.C. (1977) Praktische Wirtschaftskybernetik. *Carl Hanser Verlag,* München.

Author information

The following information about the authors should be enclosed with the paper: names, complete postal addresses, telephone and fax numbers and E-mail addresses.

Acceptance of papers and copyright

The Editorial Committee of the Journal of Mechanical Engineering reserves the right to decide whether a paper is acceptable for publication, obtain professional reviews for submitted papers, and if necessary, require changes to the content, length or language.

Authors must also enclose a written statement that the paper is original unpublished work, and not under consideration for publication elsewhere. On publication, copyright for the paper shall pass to the Journal of Mechanical Engineering. The JME must be stated as a source in all later publications.

Papers will be kept in the archives of the JME.

You can obtain further information from:

Editorial Board of the
JOURNAL OF MECHANICAL ENGINEERING
P.O.Box 197/IV
1001 Ljubljana, Slovenia
Telephone: +386 (0)1 4771-757
Fax: +386 (0)1 2518-567
E-mail: strojniski.vestnik@fs.uni-lj.si